UNIVERSITÀ DEGLI STUDI DELL'AQUILA

DIPARTIMENTO DI SCIENZE FISICHE E CHIMICHE

TESI DI LAUREA MAGISTRALE IN FISICA SPAZIALE

A probabilistic approach to the Drag-Based Model for the forecasting of Interplanetary CMEs arrivals

RELATORI:
DOTT. ERMANNO PIETROPAOLO
Università degli studi dell'Aquila

DOTT. DARIO DEL MORO
Università degli studi di Roma ''Tor Vergata''

CANDIDATO:
GIANLUCA NAPOLETANO
MATR. 234126

Anno Accademico 2015/2016

Coronal Mass Ejections

Coronal Mass Ejections

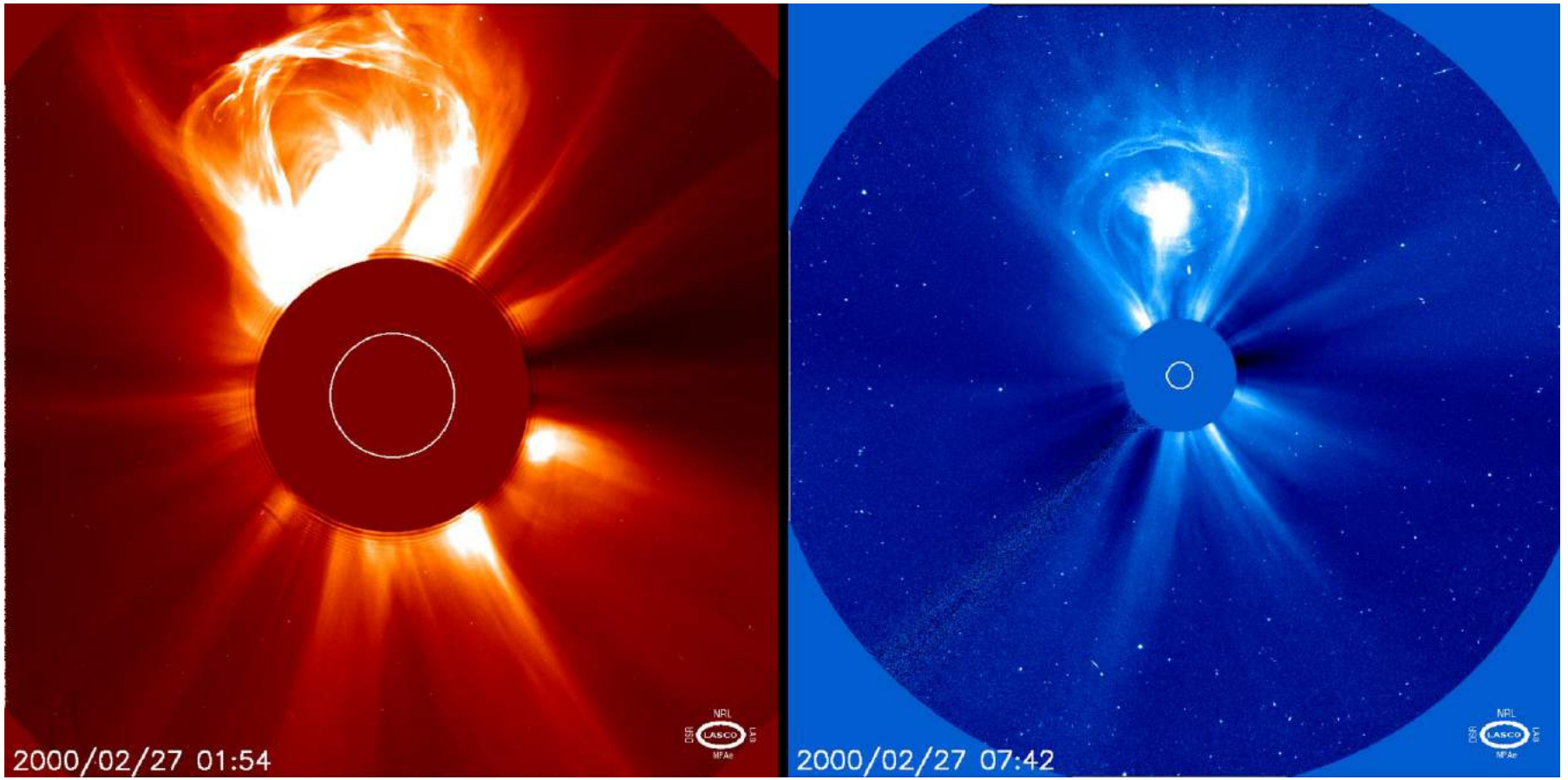

2000/02/27 CME event observed by LASCO coronagraph on board SOHO.
Source: https://sohowww.nascom.nasa.gov

Coronal Mass Ejections

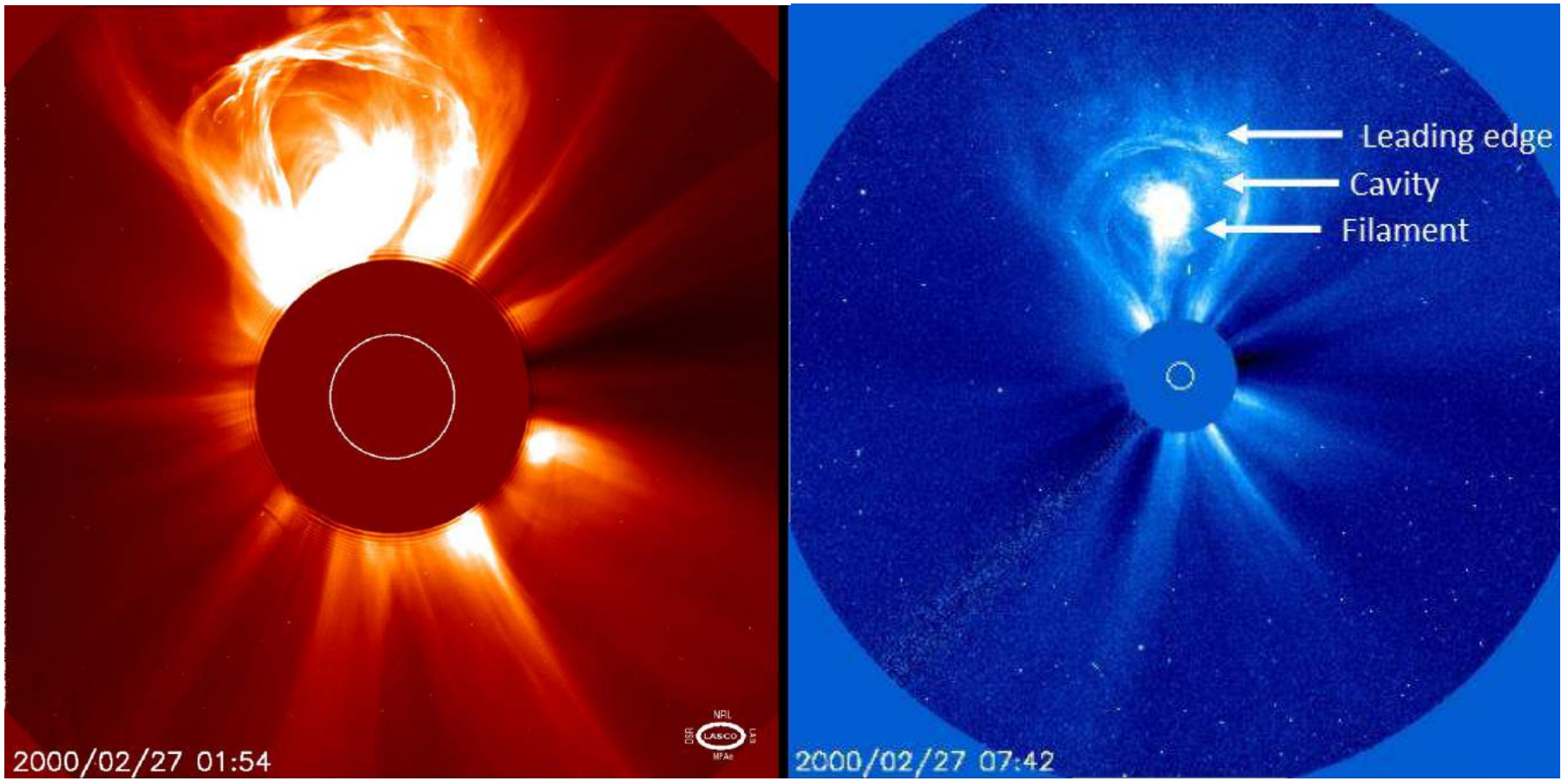

2000/02/27 CME event observed by LASCO coronagraph on board SOHO.
Source: https://sohowww.nascom.nasa.gov

Coronal Mass Ejections

Earth effects

Coronal Mass Ejections

Earth effects

- Interference of telecommunication to and from satellites;
- Increase in radiation exposure to high-altitude and/or high latitude aircraft fliers and astronauts;
- Increase in atmospheric drag on orbiting spacecraft, thereby reducing orbit lifetime;
- Interference in spacecraft circuitry;
- Damage to spacecraft hardware (e.g. solar cells);
- Interference/damage to ground-based micro and nanocircuitry;
- Unexpected current generation in power lines, resulting in power station damage.

Forecasting methods of CMEs arrivals

Forecasting methods of CMEs arrivals

- Empirical/Statistical

Forecasting methods of CMEs arrivals

- Empirical/Statistical

- MHD simulations

Forecasting methods of CMEs arrivals

- Empirical/Statistical
- MHD simulations
- Simplified dynamical models

The Drag-Based Model

The Drag-Based Model

Foundations of the Drag-Based Model

- Gravity and magnetic field only play a role during formation and launch of CMEs (heliocentric distances within 20 solar radii) (**Chen 1996**)
- ICMEs which are faster than the ambient solar wind are decelerated, whereas those slower than the solar wind are accelerated by the ambient flow (**Gopalswamy et. al 2000**);
- The forces acting on the ICME in interplanetary medium must lead to an equalisation of the ICME and solar wind velocities (**Cargill 2004**);

The Drag-Based Model

Foundations of the Drag-Based Model

- Gravity and magnetic field only play a role during formation and launch of CMEs (heliocentric distances within 20 solar radii) (**Chen 1996**)
- ICMEs which are faster than the ambient solar wind are decelerated, whereas those slower than the solar wind are accelerated by the ambient flow (**Gopalswamy et. al 2000**);
- The forces acting on the ICME in interplanetary medium must lead to an equalisation of the ICME and solar wind velocities (**Cargill 2004**);

Assumptions

- ICME evolution is entirely governed by fluid dynamics (i.e. the interplanetary magnetic field plays no role);
- ICME dynamics always act to achieve kinematic equilibrium with the solar wind;
- This model describes the propagation of the leading edge (not the shock).

The Drag-Based Model

Foundations of the Drag-Based Model

- Shapes of CMEs appear to be consistent with a nearly perfect circular cross section;

(**Schwenn et al. 2005**).

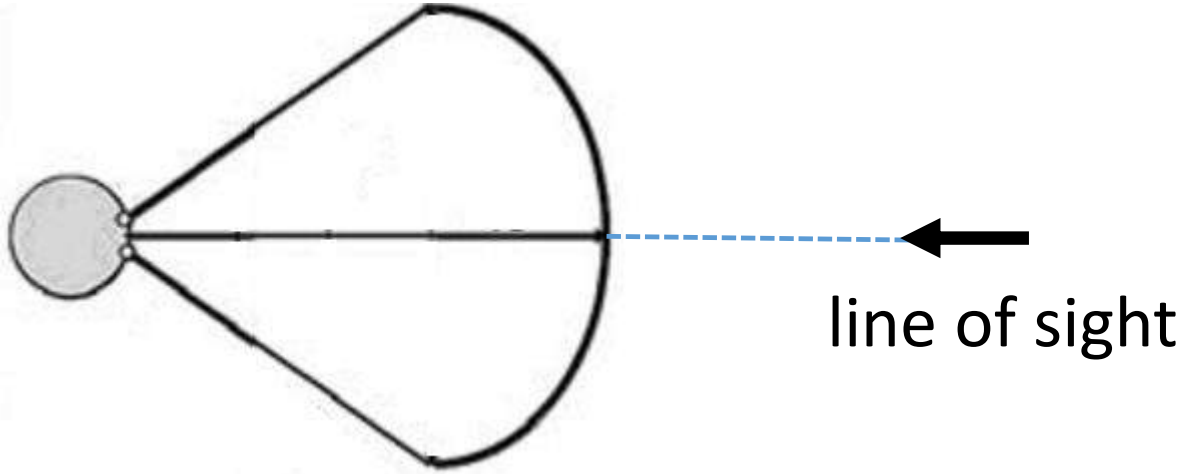

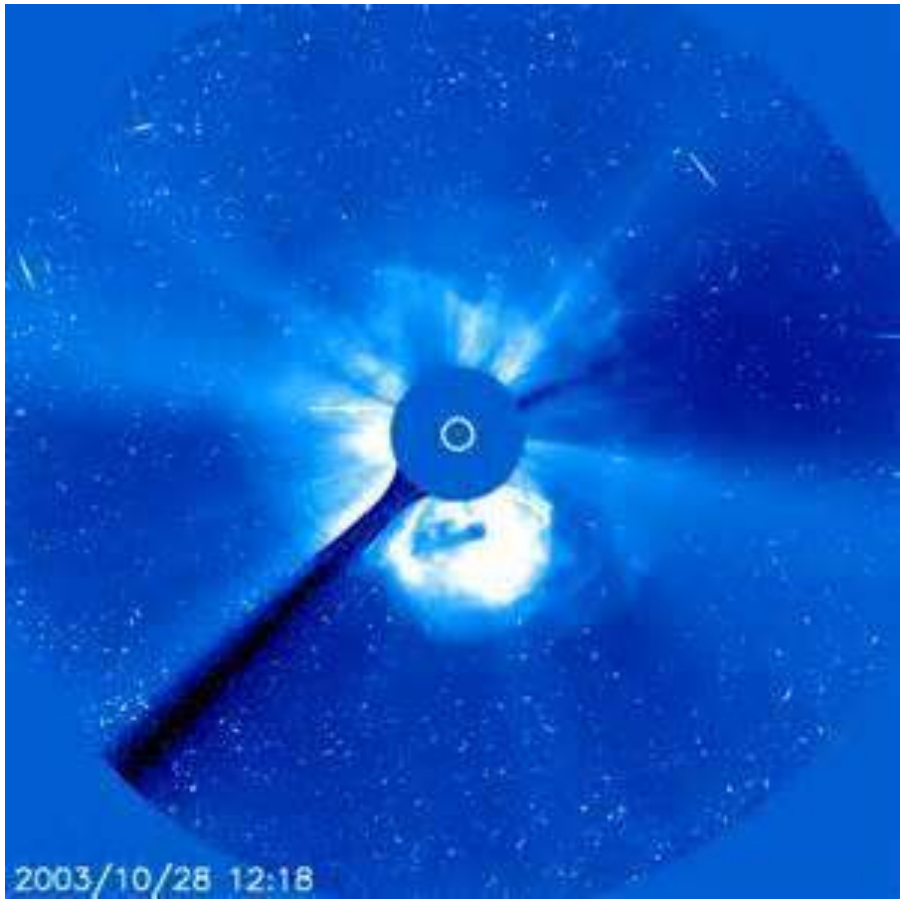

The Drag-Based Model

Foundations of the Drag-Based Model

- Shapes of CMEs appear to be consistent with a nearly perfect circular cross section;

(**Schwenn et al. 2005**).

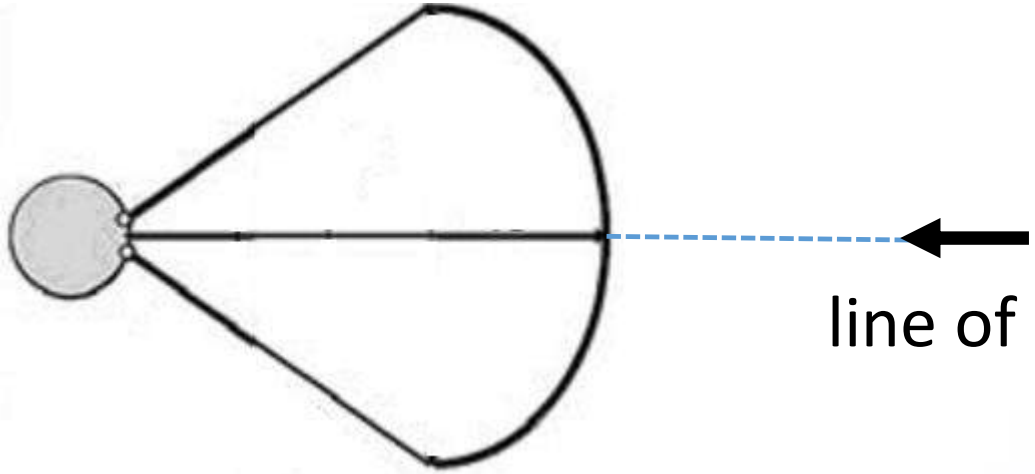

line of sight

ICME cross section A

The Drag-Based Model

Foundations of the Drag-Based Model

- Self expansion: cone angles and shapes of CMEs are usually well maintained (**Schwenn et al. 2005**).

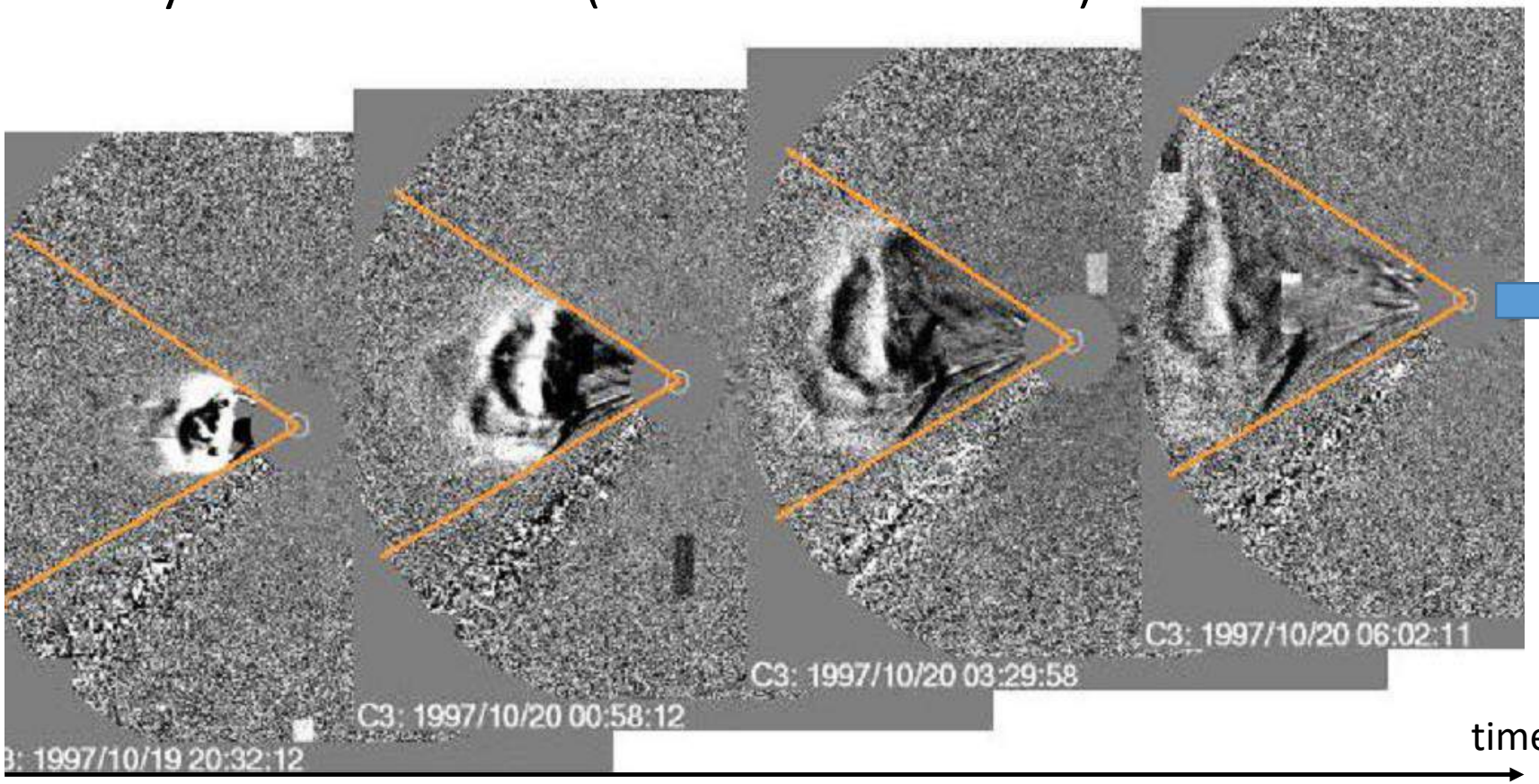

- Radial propagation of CME elements

- Cross section

$$A \propto r^2$$

The Drag-Based Model

Aerodynamic Drag ($R > 20R_\odot$)

$$\vec{F}_D = -\rho_W A C_D (\vec{v} - \vec{w})|\vec{v} - \vec{w}|$$

$$M\frac{d^2\vec{v}}{dt^2} = \vec{F}_D$$

$\vec{v}$	ICME speed
A	ICME cross section
C_D	drag coefficient
ρ_W	solar wind density
$\vec{w}$	solar wind speed
M	ICME mass

The Drag-Based Model

Aerodynamic Drag ($R > 20R_{\odot}$)

Leblanc model for the solar wind density from Sun to 1 AU (**Leblanc et al. 1996**)

$$\rho_w = \frac{A}{r^6} + \frac{B}{r^4} + \frac{C}{r^2}$$

$$\frac{\partial}{\partial r}(r^2 w \rho_w) = 0$$

$$w(r) \propto \frac{1}{r^2 \rho_w(r)}$$

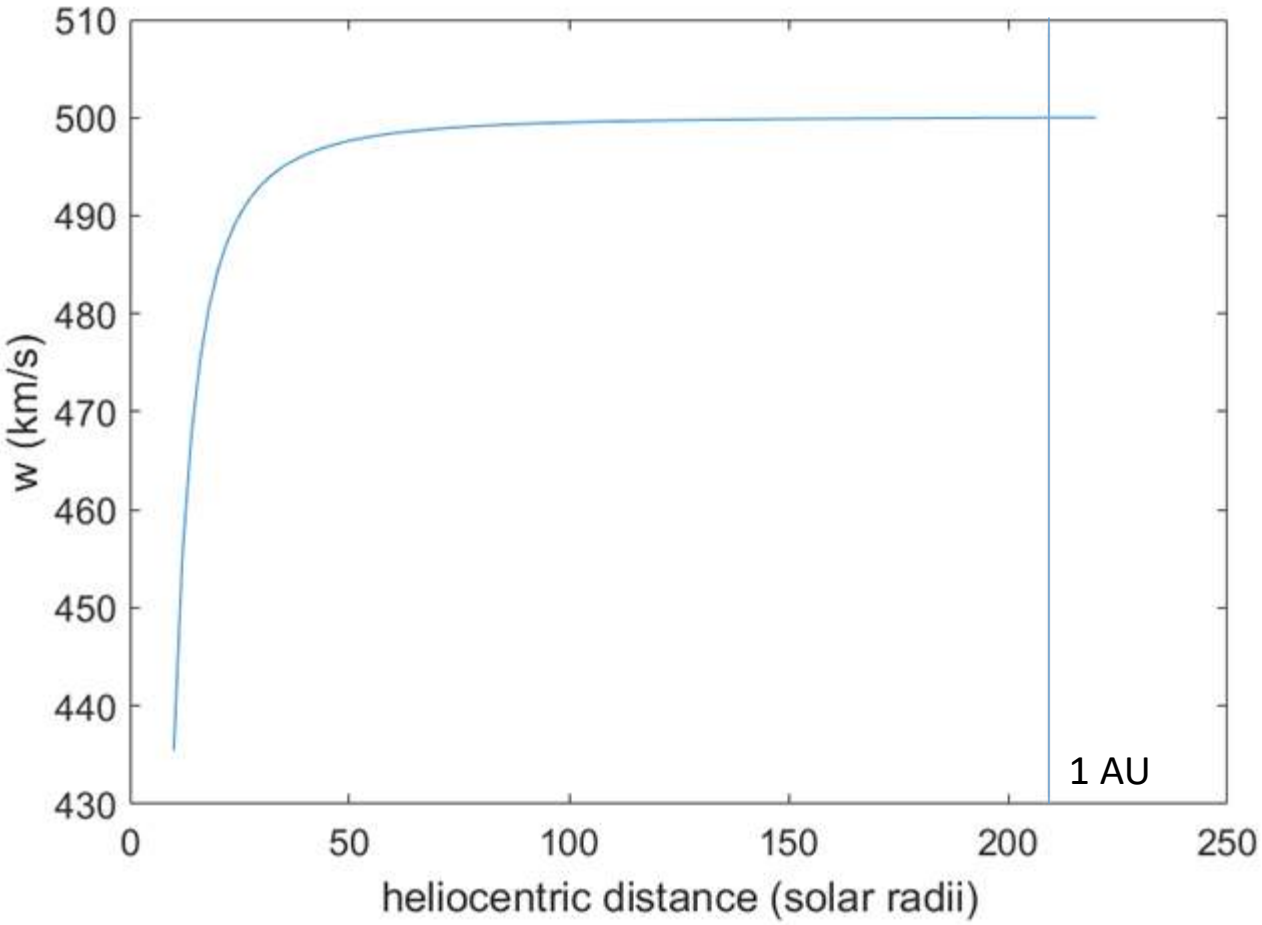

The Drag-Based Model

Aerodynamic Drag

radial equation $$\frac{d^2r}{dt^2} = -\gamma\left(\frac{dr}{dt} - w\right)\left|\frac{dr}{dt} - w\right|$$

drag parameter $$\gamma = \frac{C_D A}{V\left(\frac{\rho}{\rho_W} + \frac{1}{2}\right)} \simeq \frac{\rho_W A}{M}$$ approximation of dense ICMEs (**Cargill 1996**)

$$\gamma \simeq 0.2 \div 2 \times 10^{-7}\ \mathrm{km}^{-1}$$ constant during ICME propagation

The Drag-Based Model

With constant solar wind speed and drag parameter

The Drag-Based Model

With constant solar wind speed and drag parameter

$$r(t) = \pm\frac{1}{\gamma}\ln\left[1 \pm \gamma(v_0 - w)t\right] + wt + r_0$$

$$v(t) = \frac{v_0 - w}{1 \pm \gamma(v_0 - w)t} + w$$

$r_0 = r(t = 0) \simeq 20R_\odot$

$v_0 = v(t = 0)$

$\pm$ acceleration/deceleration regime

The Drag-Based Model

Constant solar wind speed and drag parameter

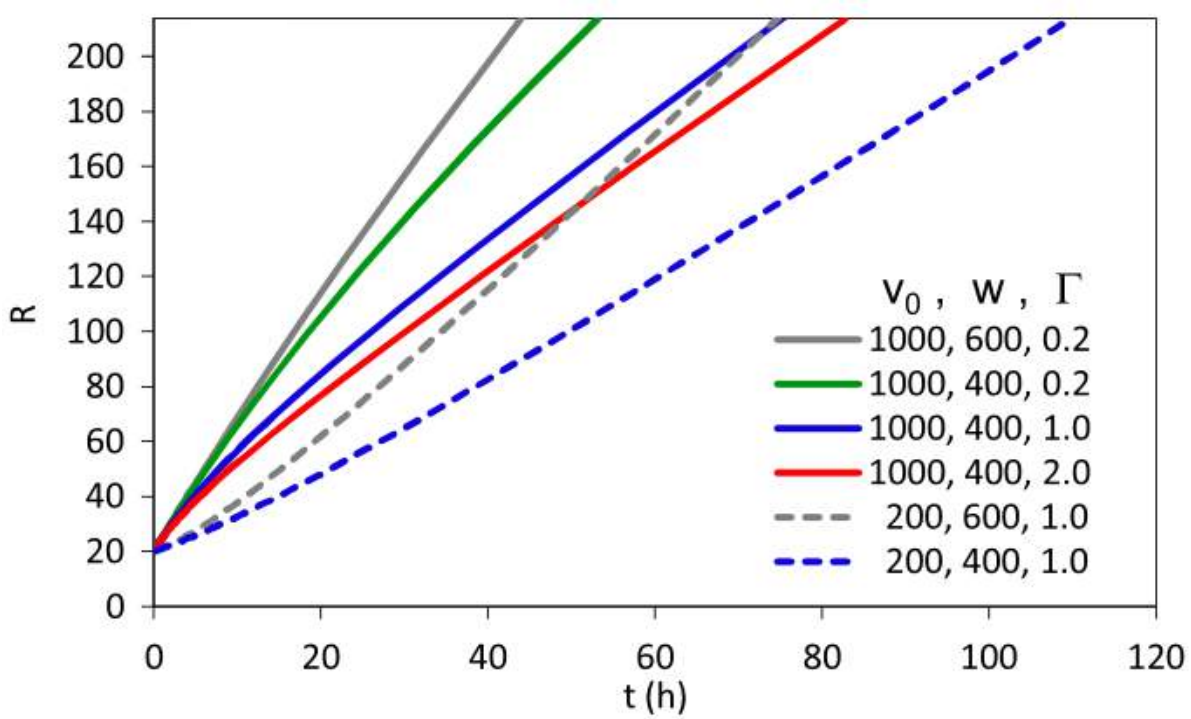

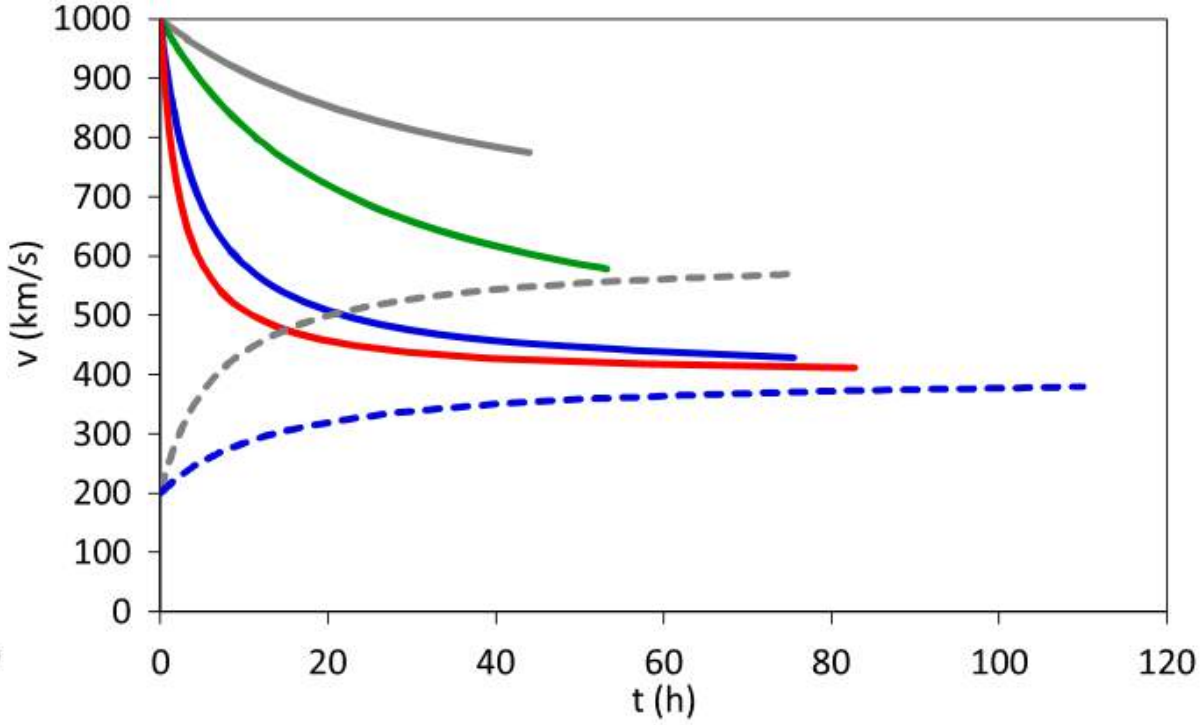

$\Gamma = \gamma \times 10^7$

R in solar radii

Advanced Drag-Based Model

Advanced Drag-Based Model

Cone model (**Fisher & Munro 1984, Vrsnak & Zic 2005**)

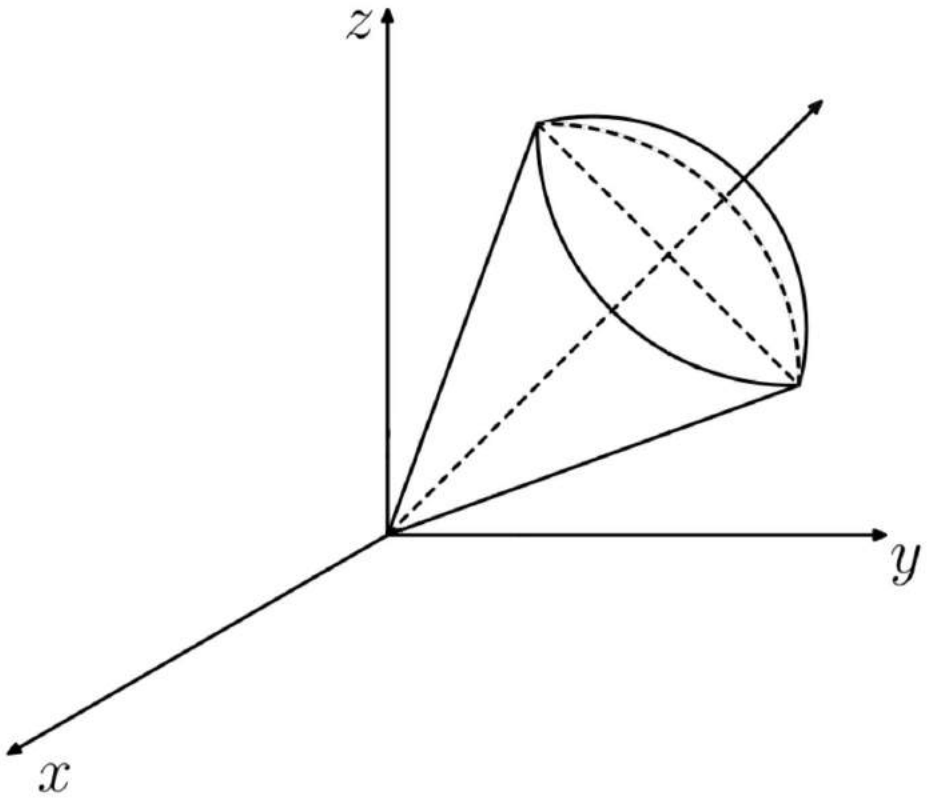

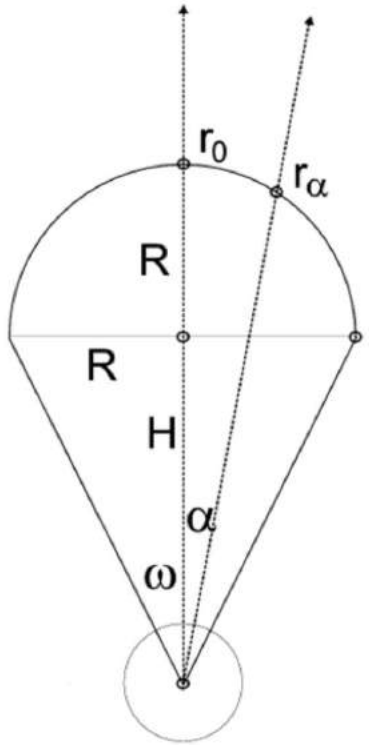

ω half angular width

α target angle

$$r_\alpha = r_0 \frac{\cos\alpha + \sqrt{\tan^2\omega - \sin^2\alpha}}{1 + \tan\omega}$$

$$v_\alpha = v_0 \frac{\cos\alpha + \sqrt{\tan^2\omega - \sin^2\alpha}}{1 + \tan\omega}$$

Advanced Drag-Based Model

Cone model (**Fisher & Munro 1984, Vrsnak & Zic 2005**)

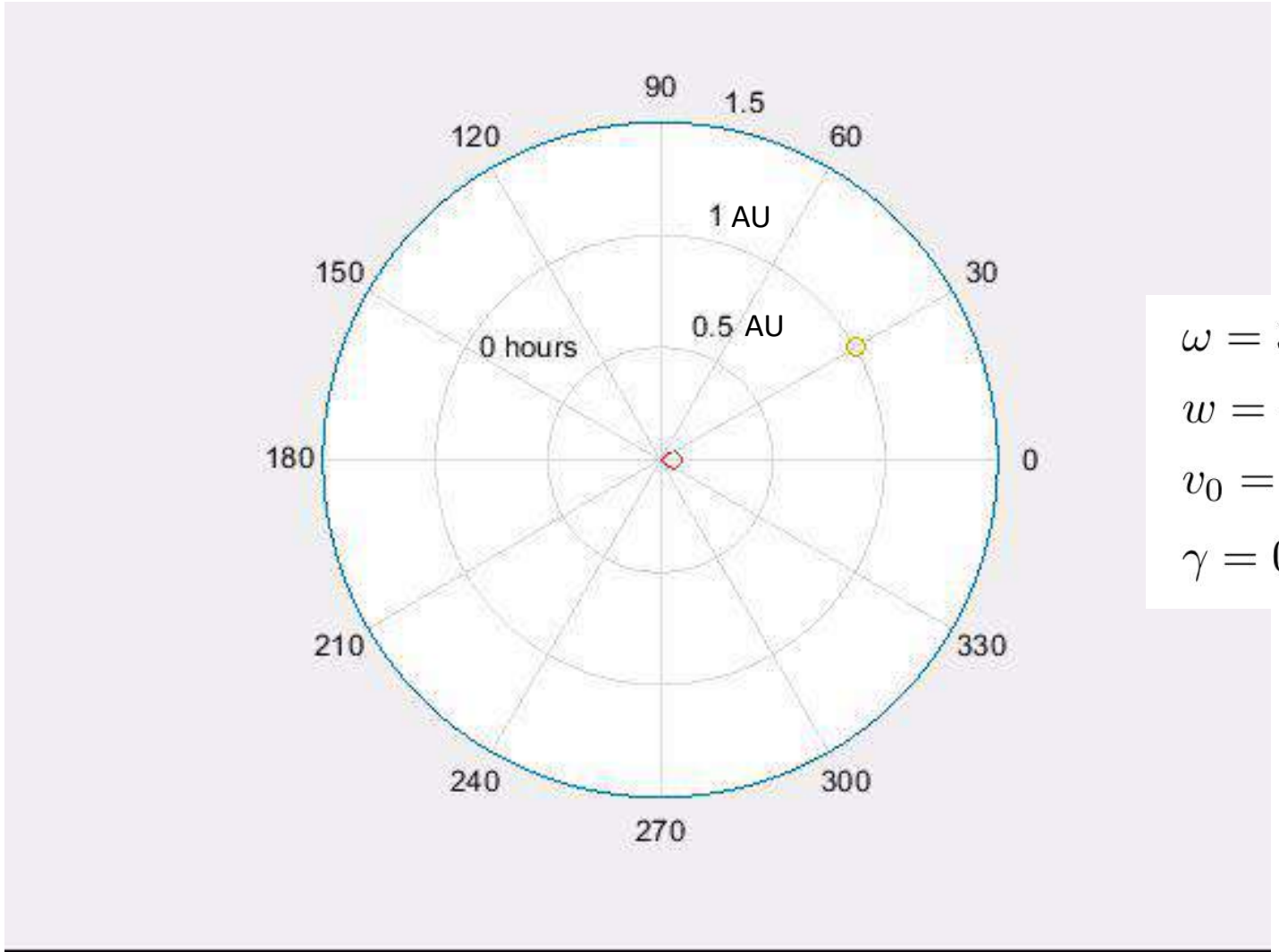

$$\omega = 35^\circ$$
$$w = 450\mathrm{km/s}$$
$$v_0 = 1000\mathrm{km/s}$$
$$\gamma = 0.2 \times 10^{-7}\ \mathrm{km}^{-1}$$

Test of the Advanced Drag-Based Model

Test of the Advanced Drag-Based Model

Data sample

Tong Shi et al. 2015

- r_0 , v_0 , t_O (shock or magnetic effect in WIND data) for 14 events;
- known errors on determination of leading edge position and speed from coronagraphic images.
- known CME morphology (Cone Model) thanks to reconstruction of ICME shape obtained by means of multiple point of view observations (STEREO spacecrafts);
- **unknown drag parameter and solar wind values**

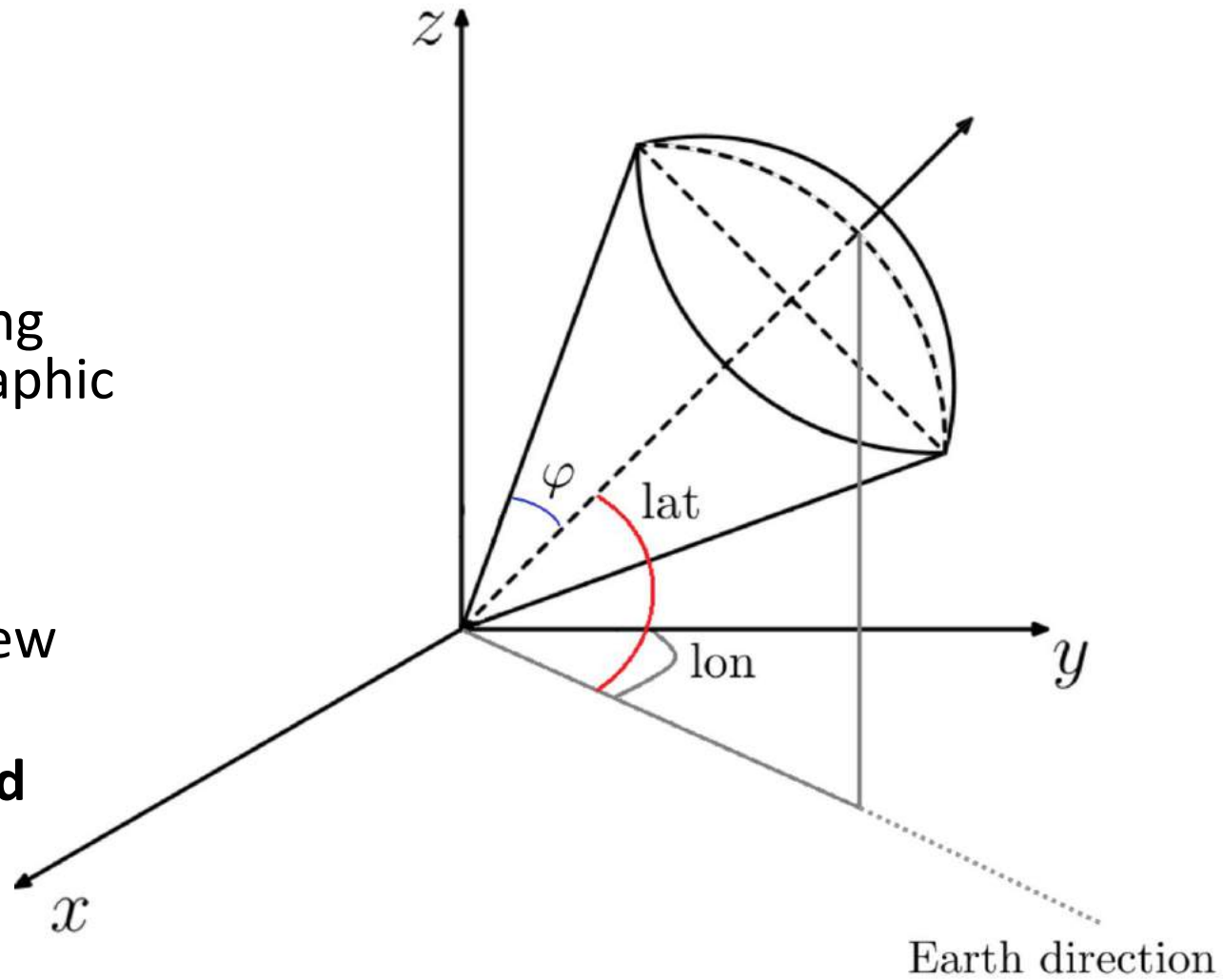

Probabilistic Advanced Drag-Based Model

$(r_\alpha, v_\alpha, w, \gamma)$

Probabilistic Advanced Drag-Based Model

$(r_\alpha, v_\alpha, w, \gamma)$ → Distribution of initial conditions and parameters

Probabilistic Advanced Drag-Based Model

$(r_\alpha, v_\alpha, w, \gamma)$ ⟶ Distribution of initial conditions and parameters

drag parameter distribution obtained by inversion of DBM equations by employing a sample of 91 CME events. (**Vrsnak et al. 2012**)

$$\gamma = f(r_0, v_0, v_{1AU}, t_O) \longrightarrow$$

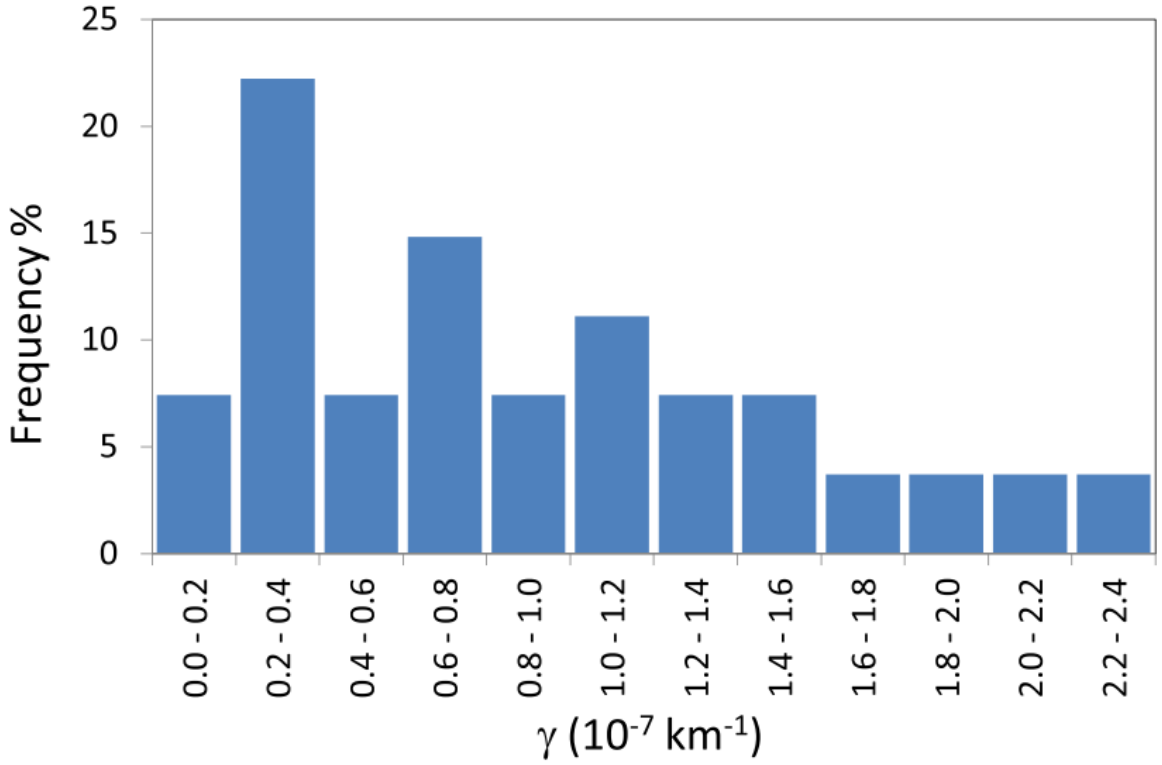

Probabilistic Advanced Drag-Based Model

Distribution of initial conditions and parameters

Lognormal distribution of drag parameter

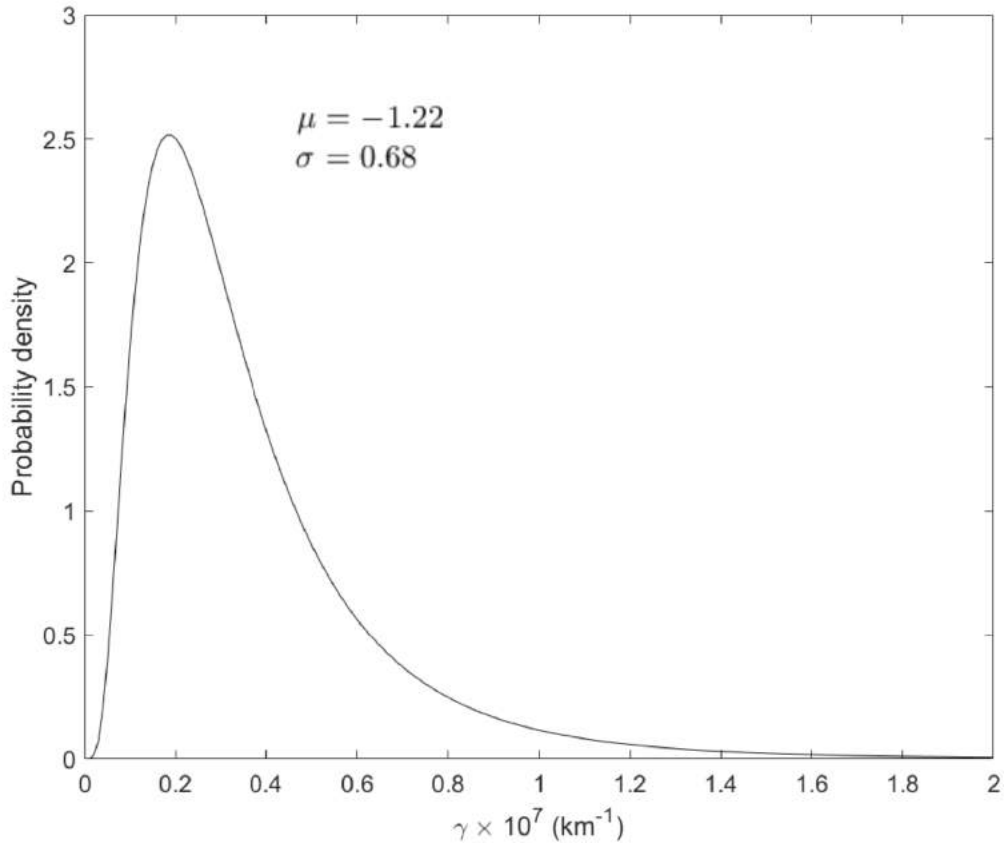

Probabilistic Advanced Drag-Based Model

Distribution of initial conditions and parameters

Lognormal distribution of drag parameter

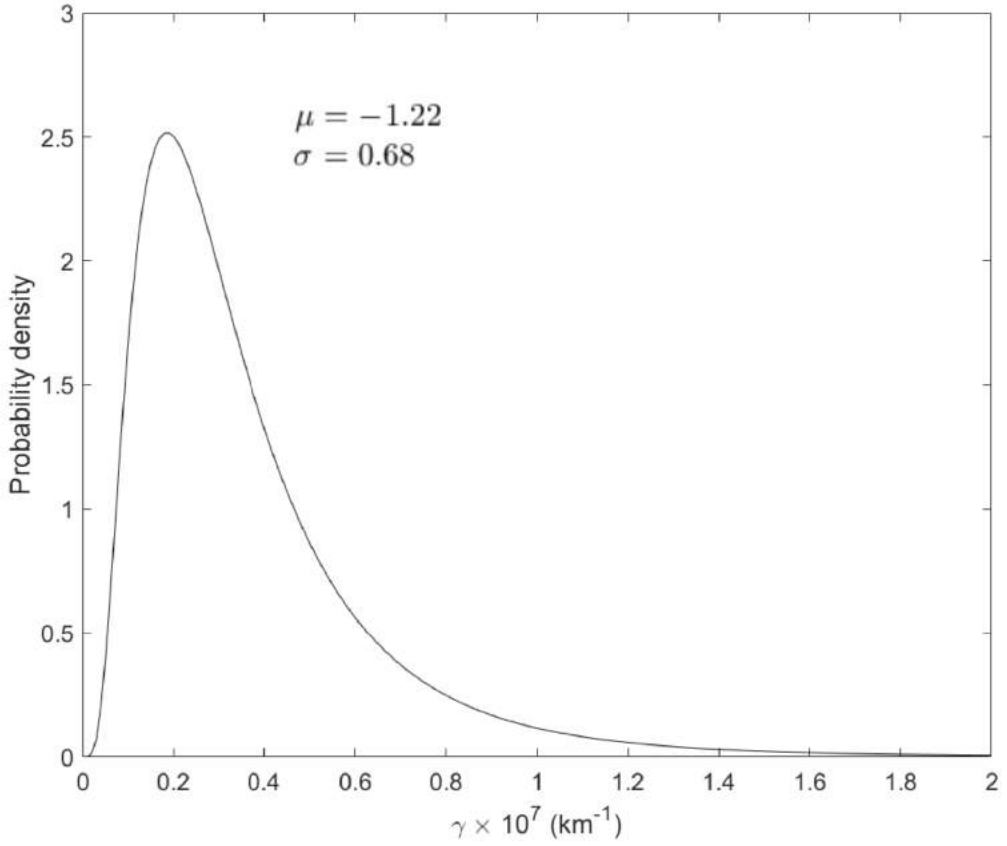

Gaussian distribution of solar wind speed

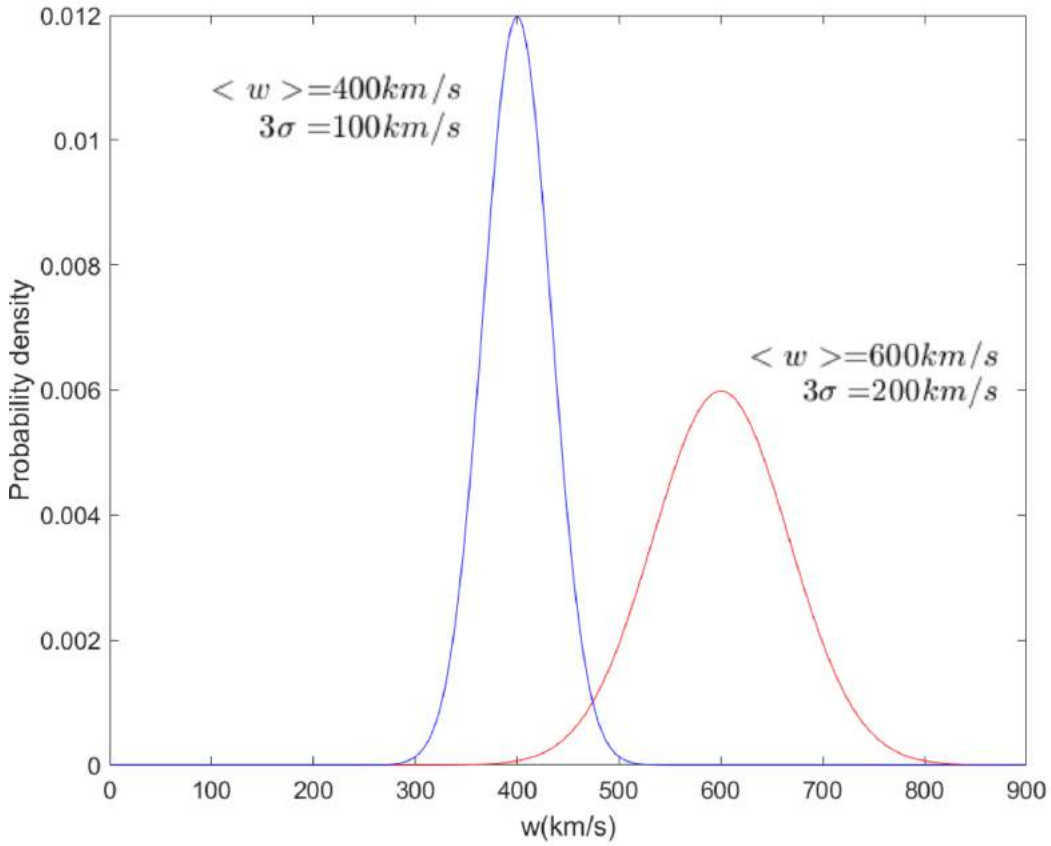

Probabilistic Advanced Drag-Based Model

$(r_\alpha, v_\alpha, w, \gamma)$ randomly chosen from:

- Gaussian distribution of leading edge position;
- Gaussian distribution of speed;
- Lognormal distribution of drag parameter;
- Gaussian distribution of solar wind speed (Fast or Slow).

Probabilistic Advanced Drag-Based Model

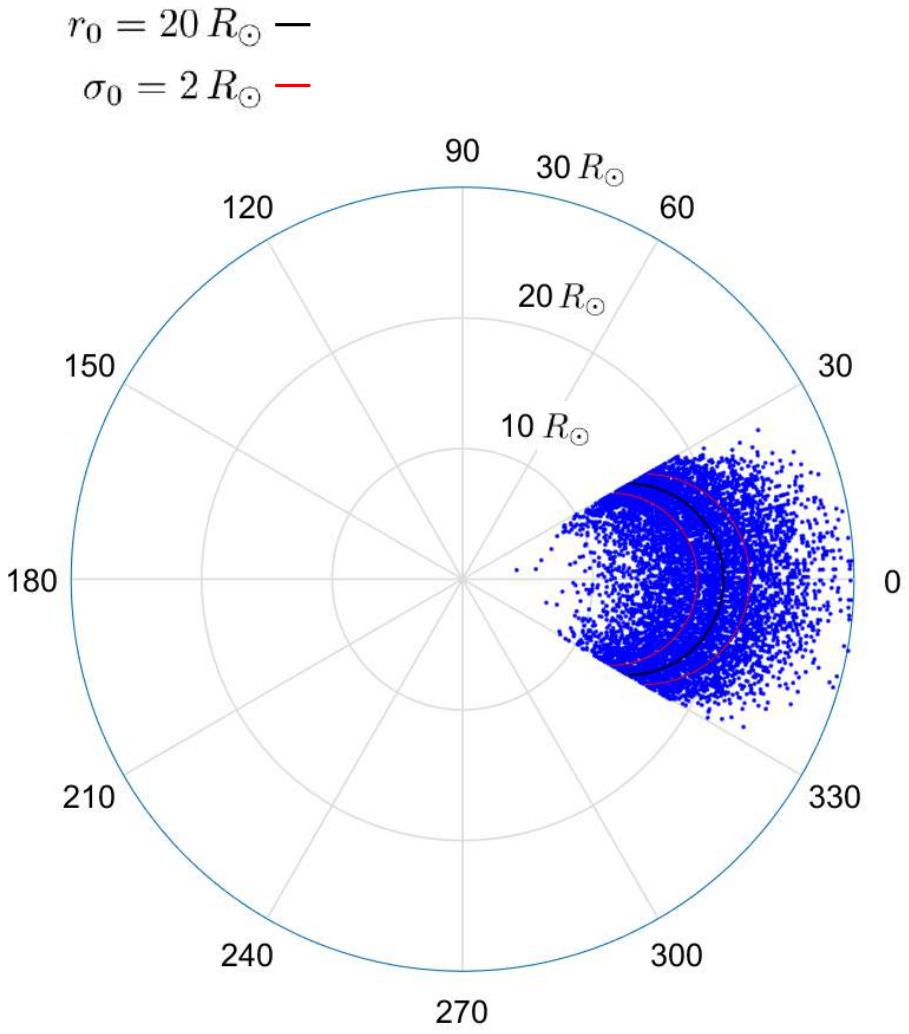

$(r_\alpha, v_\alpha, w, \gamma)$ randomly chosen from:

- Gaussian distribution of leading edge position;
- Gaussian distribution of speed;
- Lognormal distribution of drag parameter;
- Gaussian distribution of solar wind speed (Fast or Slow).

Probabilistic Advanced Drag-Based Model

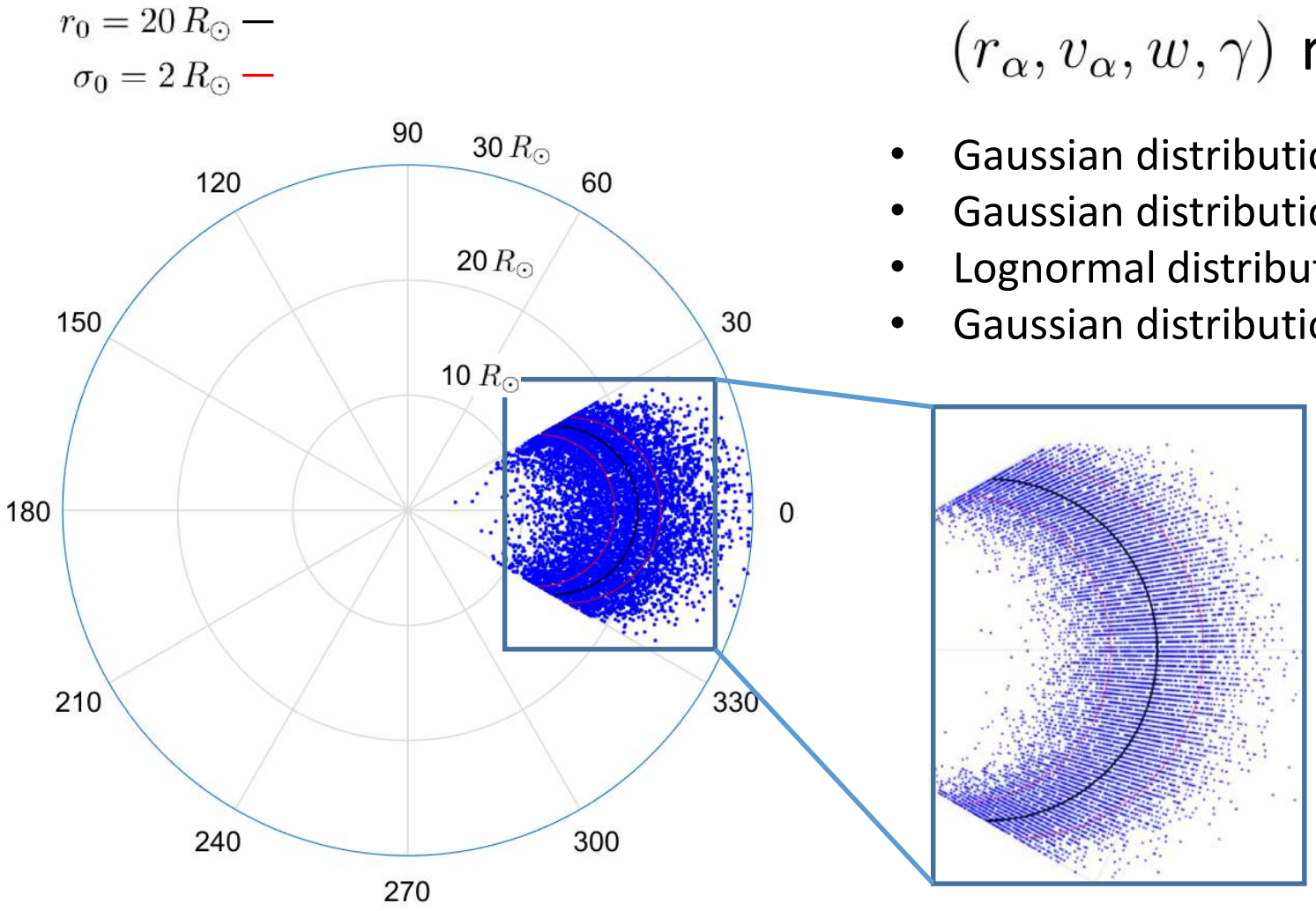

$(r_\alpha, v_\alpha, w, \gamma)$ randomly chosen from:

- Gaussian distribution of leading edge position;
- Gaussian distribution of speed;
- Lognormal distribution of drag parameter;
- Gaussian distribution of solar wind speed (Fast or Slow).

Probabilistic Advanced Drag-Based Model

$r_0 = 20\,R_\odot$ —
$\sigma_0 = 2\,R_\odot$ —

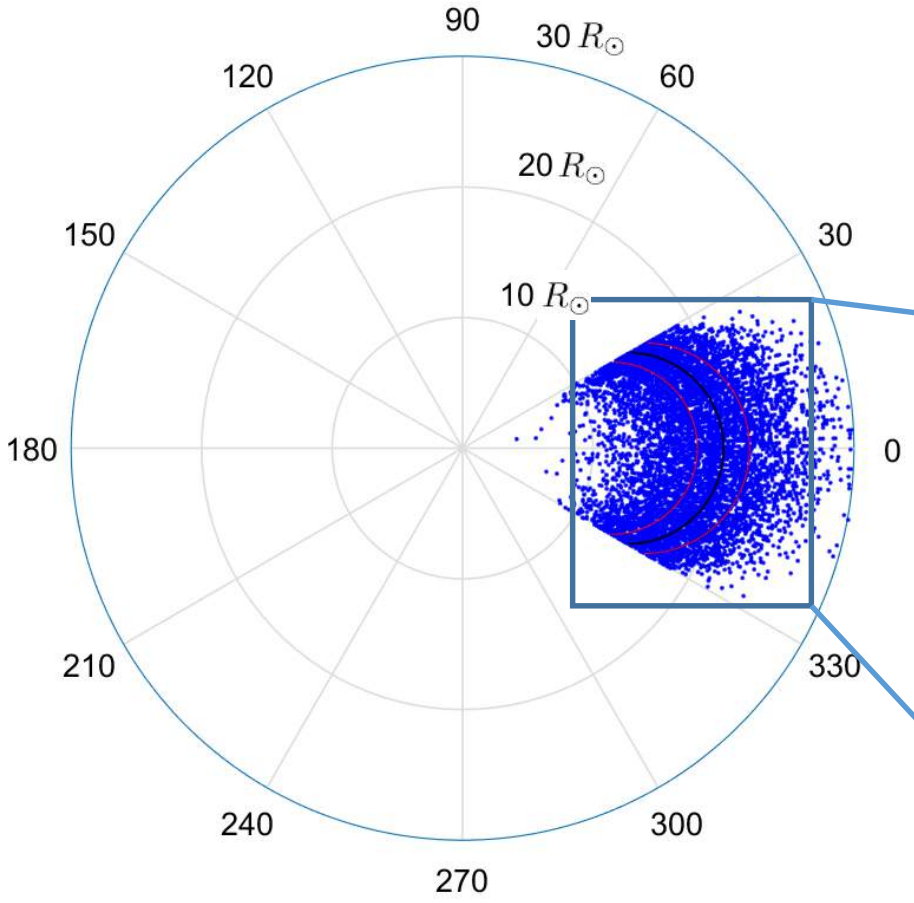

$(r_\alpha, v_\alpha, w, \gamma)$ randomly chosen from:

- Gaussian distribution of leading edge position;
- Gaussian distribution of speed;
- Lognormal distribution of drag parameter;
- Gaussian distribution of solar wind speed (Fast or Slow).

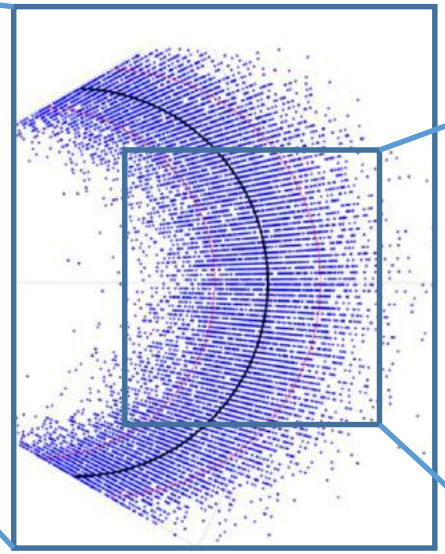

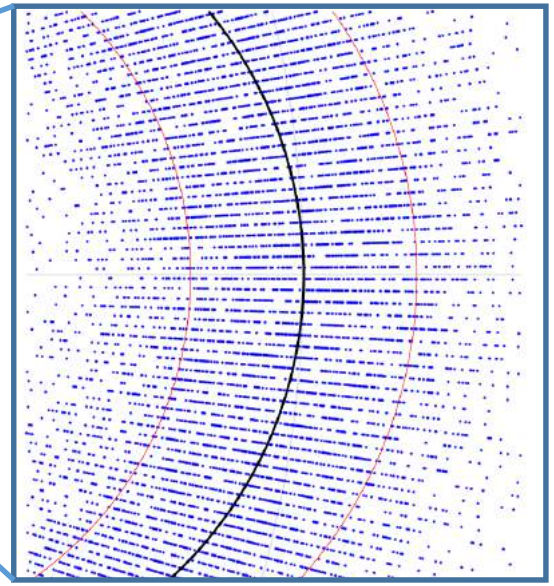

Probabilistic Advanced Drag-Based Model

Time distribution → $t_C =< t_C > \pm \sigma_t$

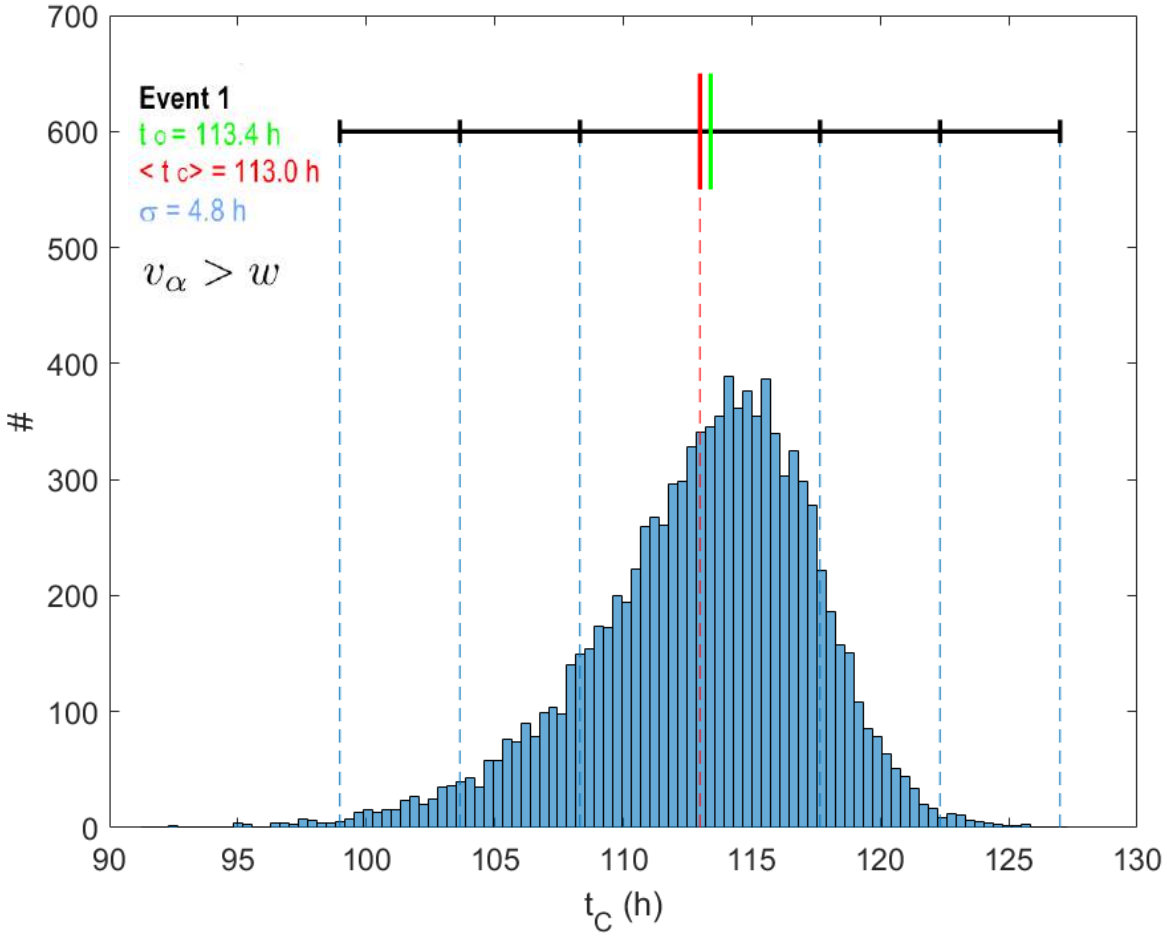

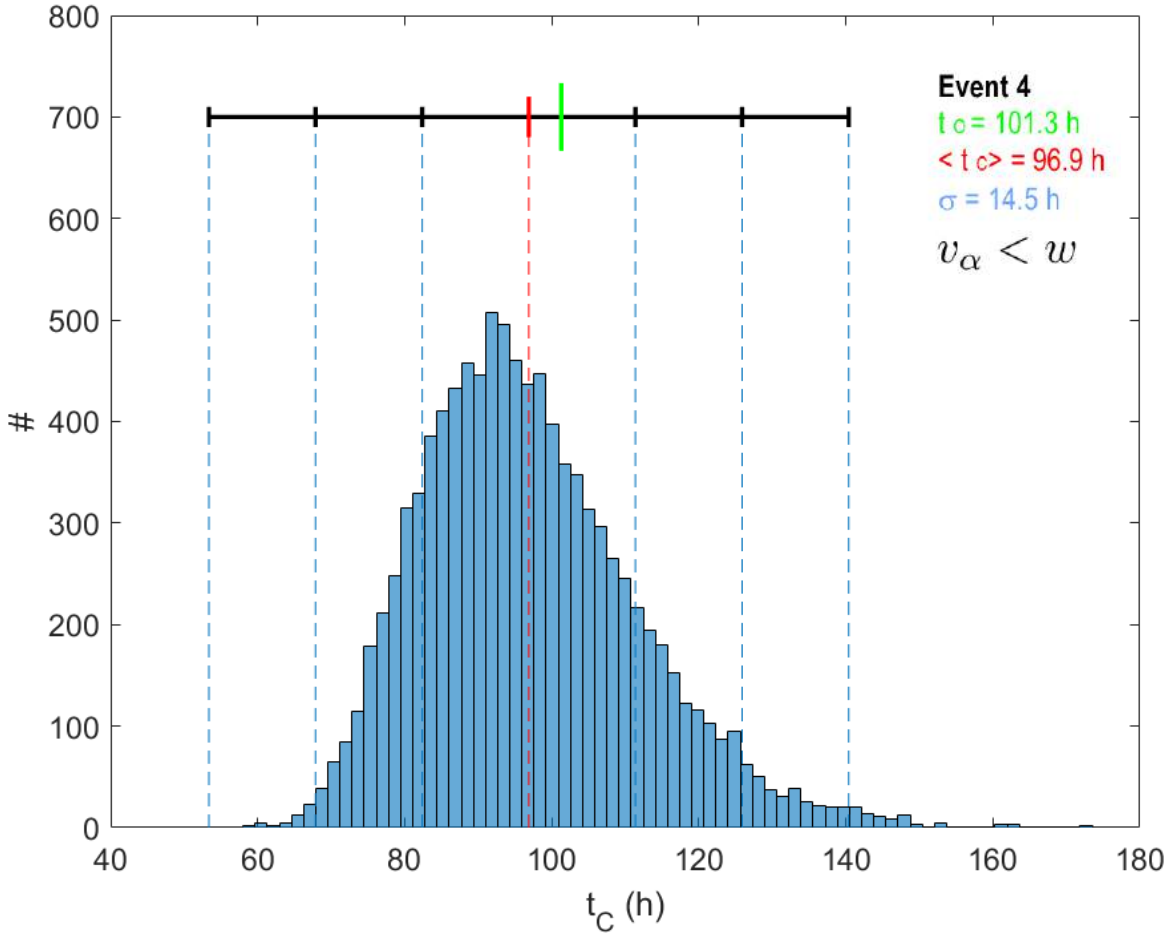

Probabilistic Advanced Drag-Based Model

calculated vs observed times (1σ error bar)

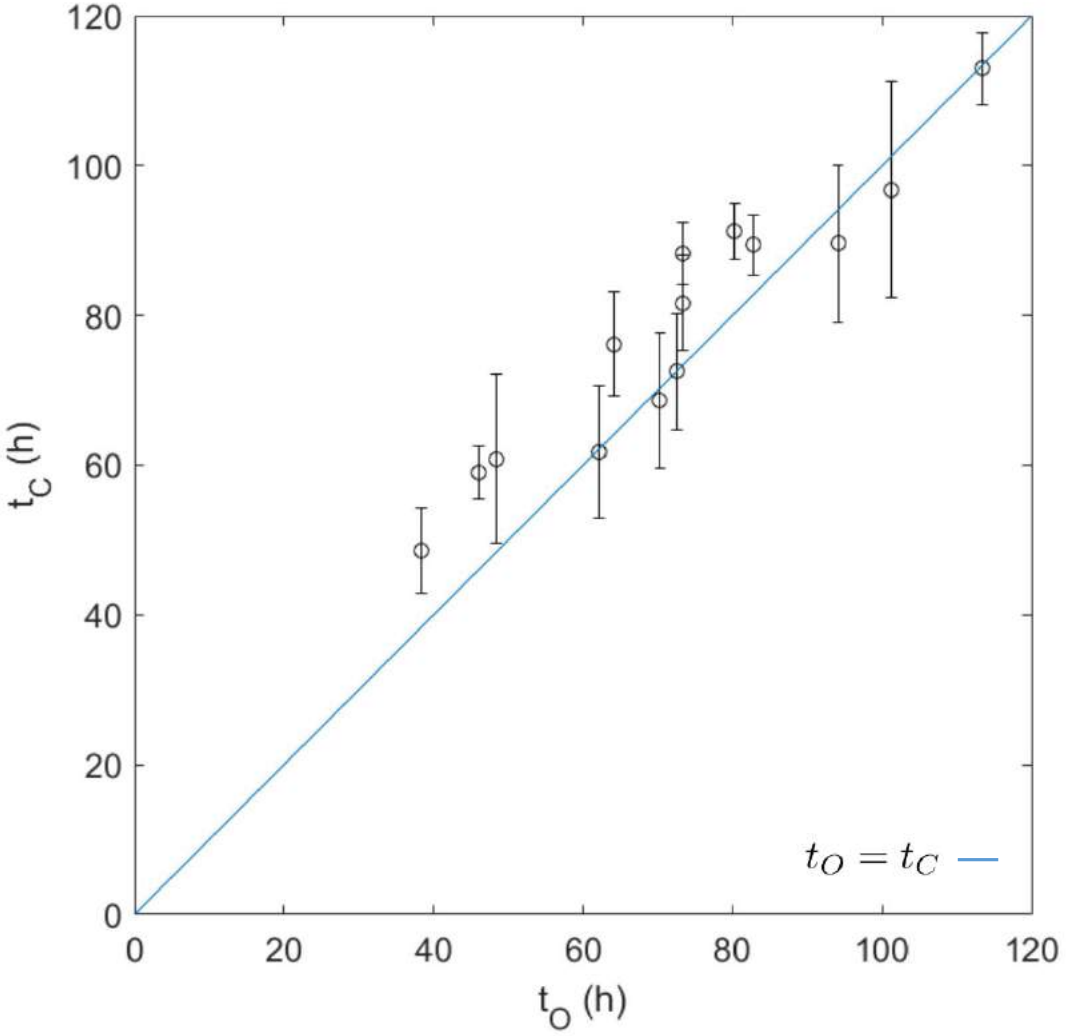

Probabilistic Advanced Drag-Based Model

calculated vs observed times (1σ error bar)

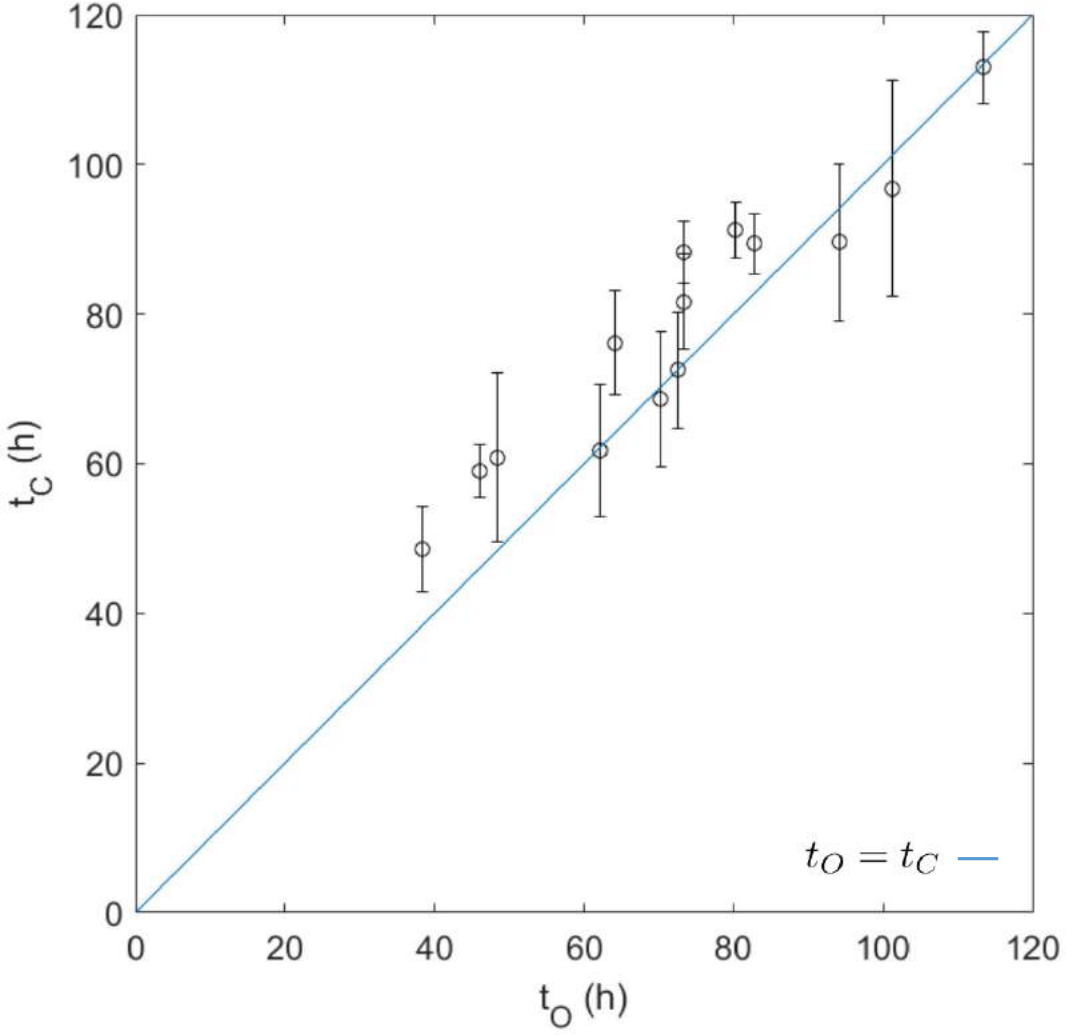

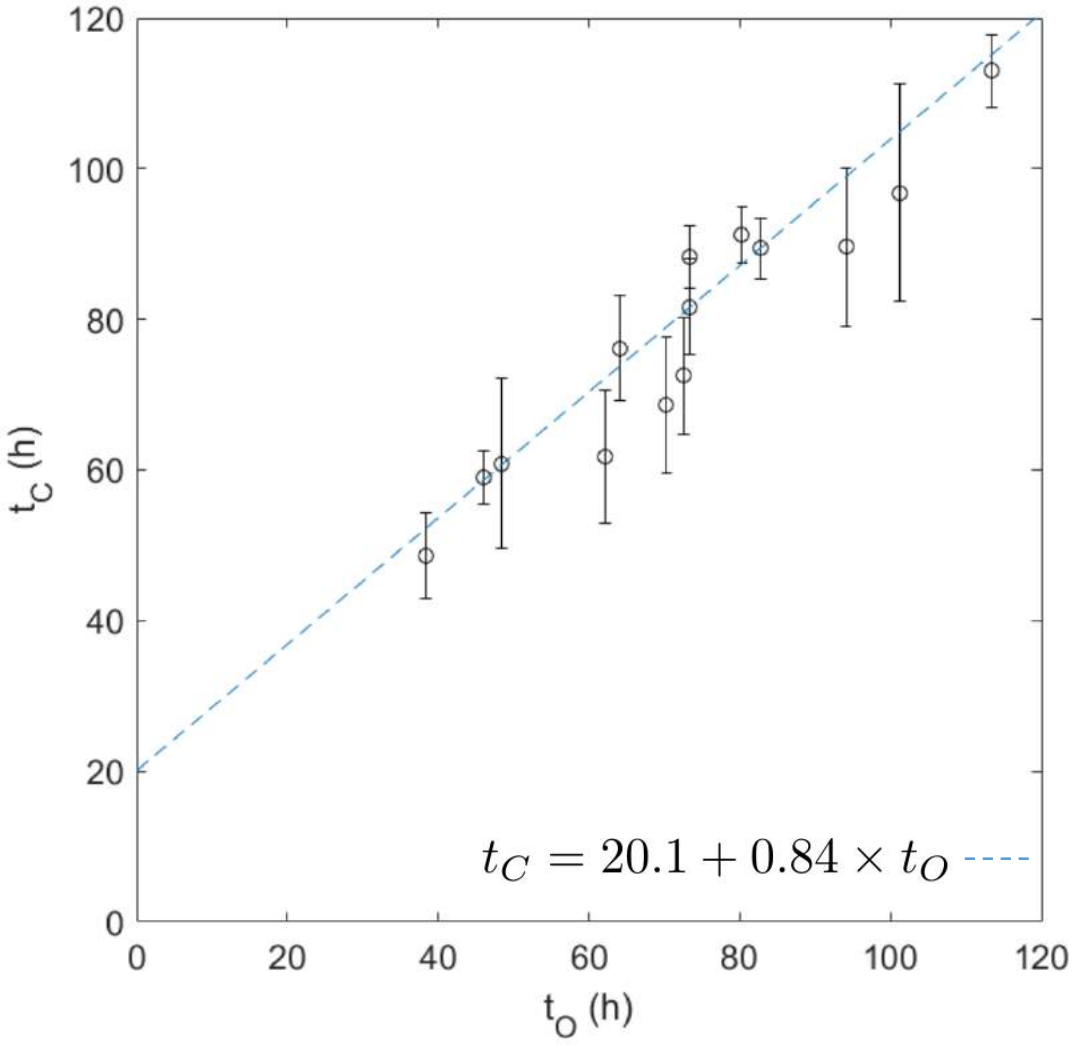

Probabilistic Advanced Drag-Based Model

Time of arrival of shock for 10 events

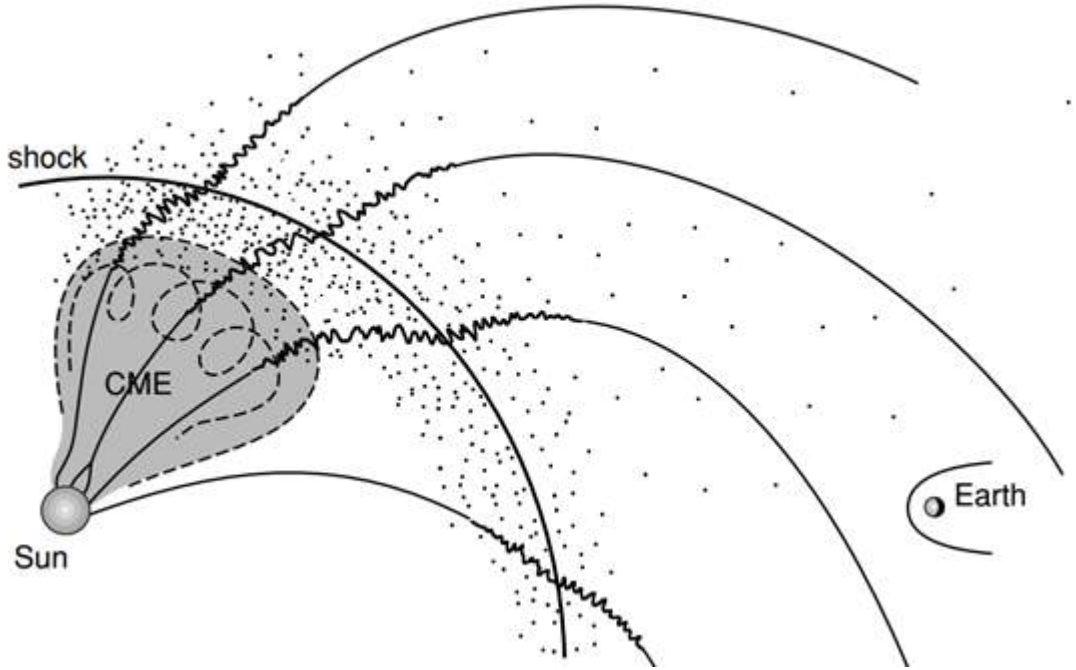

(**Mikic & Lee 2006**)

Probabilistic Advanced Drag-Based Model

Time of arrival of shock for 10 events

For 7 out of 10 shock events $t_C > t_O$

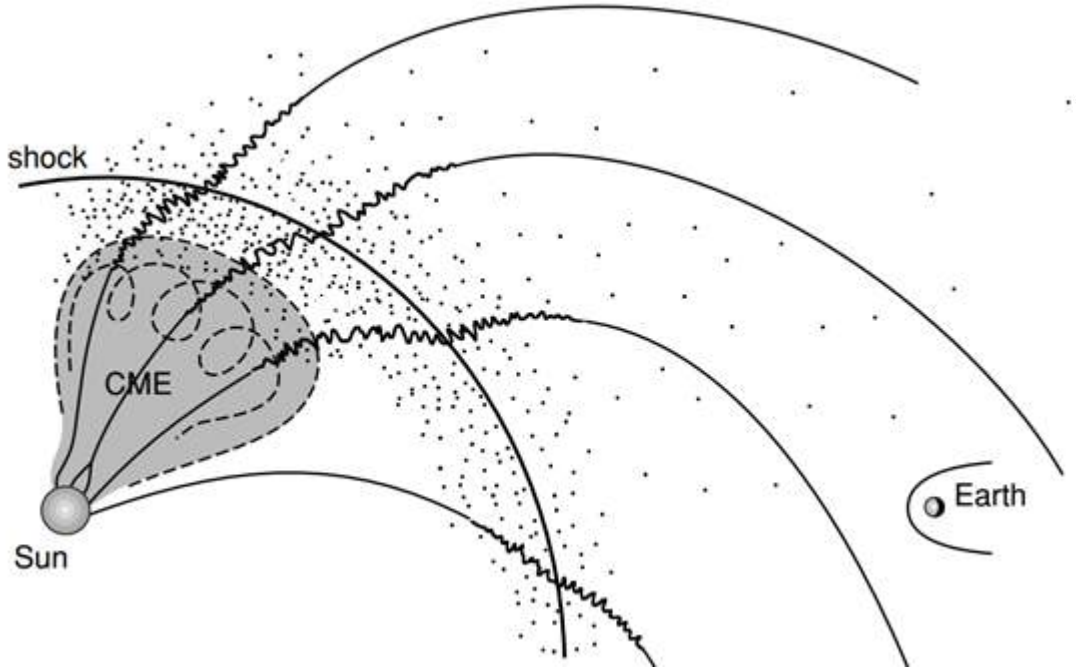

(**Mikic & Lee 2006**)

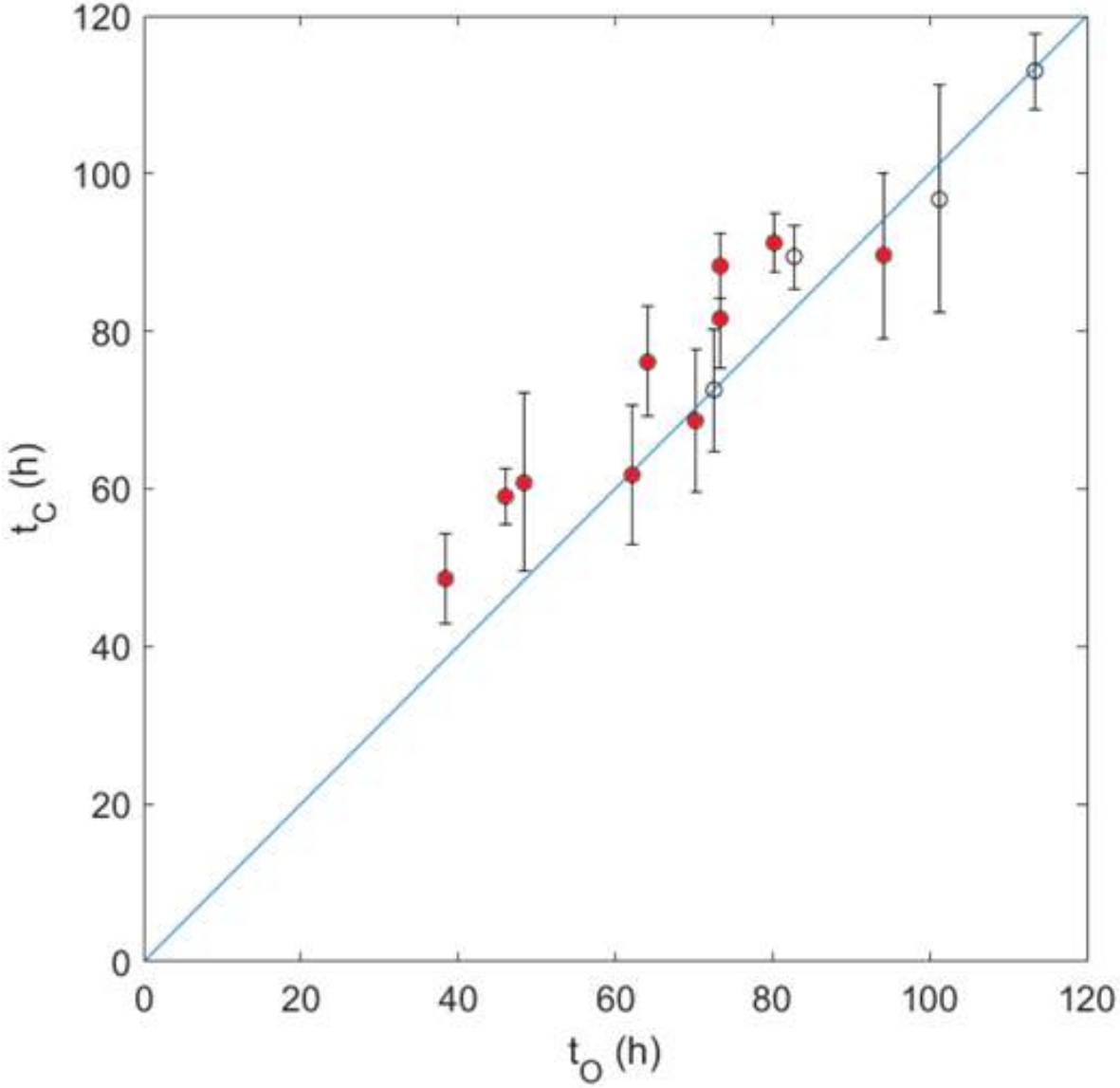

Probabilistic Advanced Drag-Based Model

Time difference between shock detection and magnetic effect (149 events from Schwenn's sample)

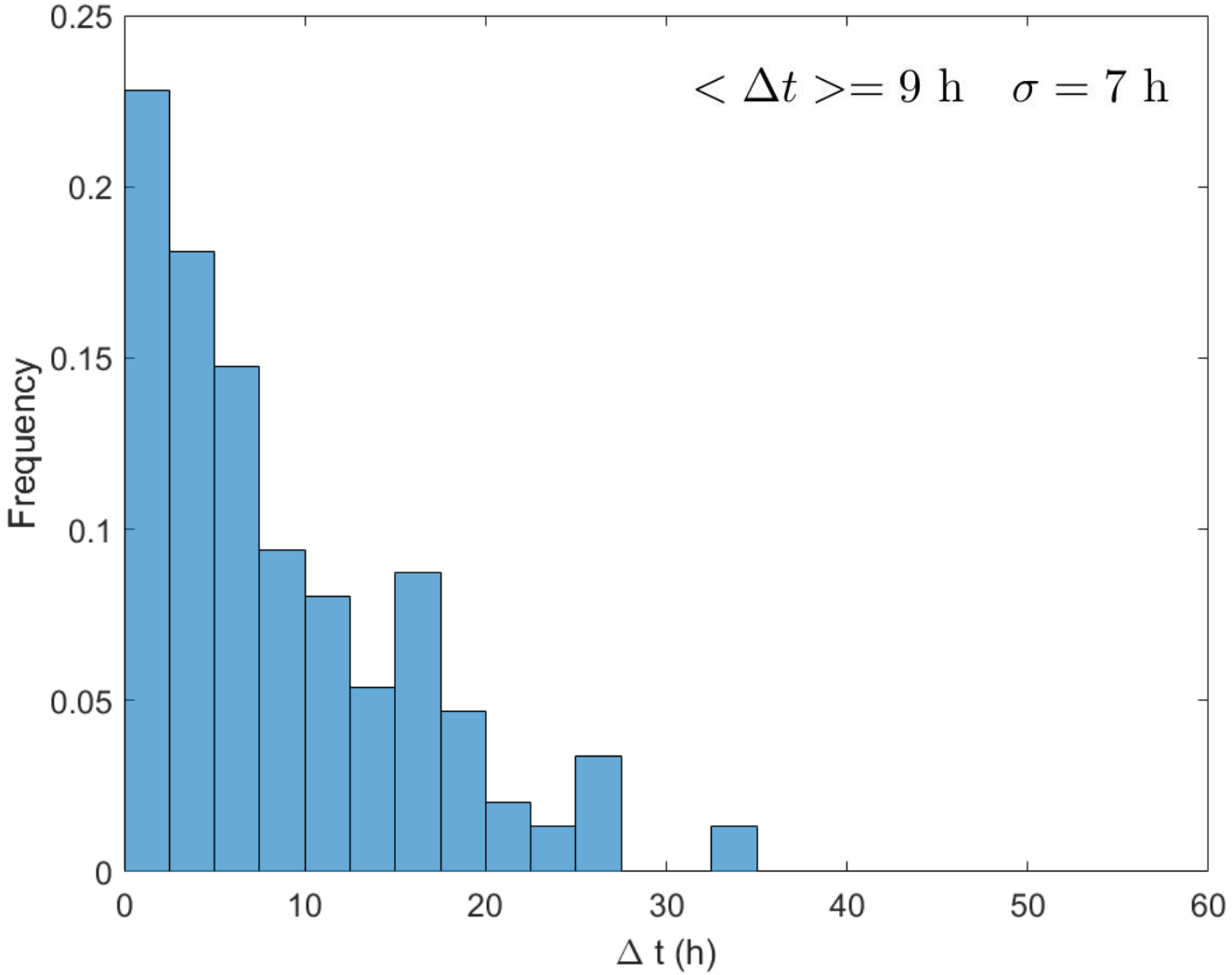

Probabilistic Advanced Drag-Based Model

Time difference between shock detection and magnetic effect (149 events from Schwenn's sample)

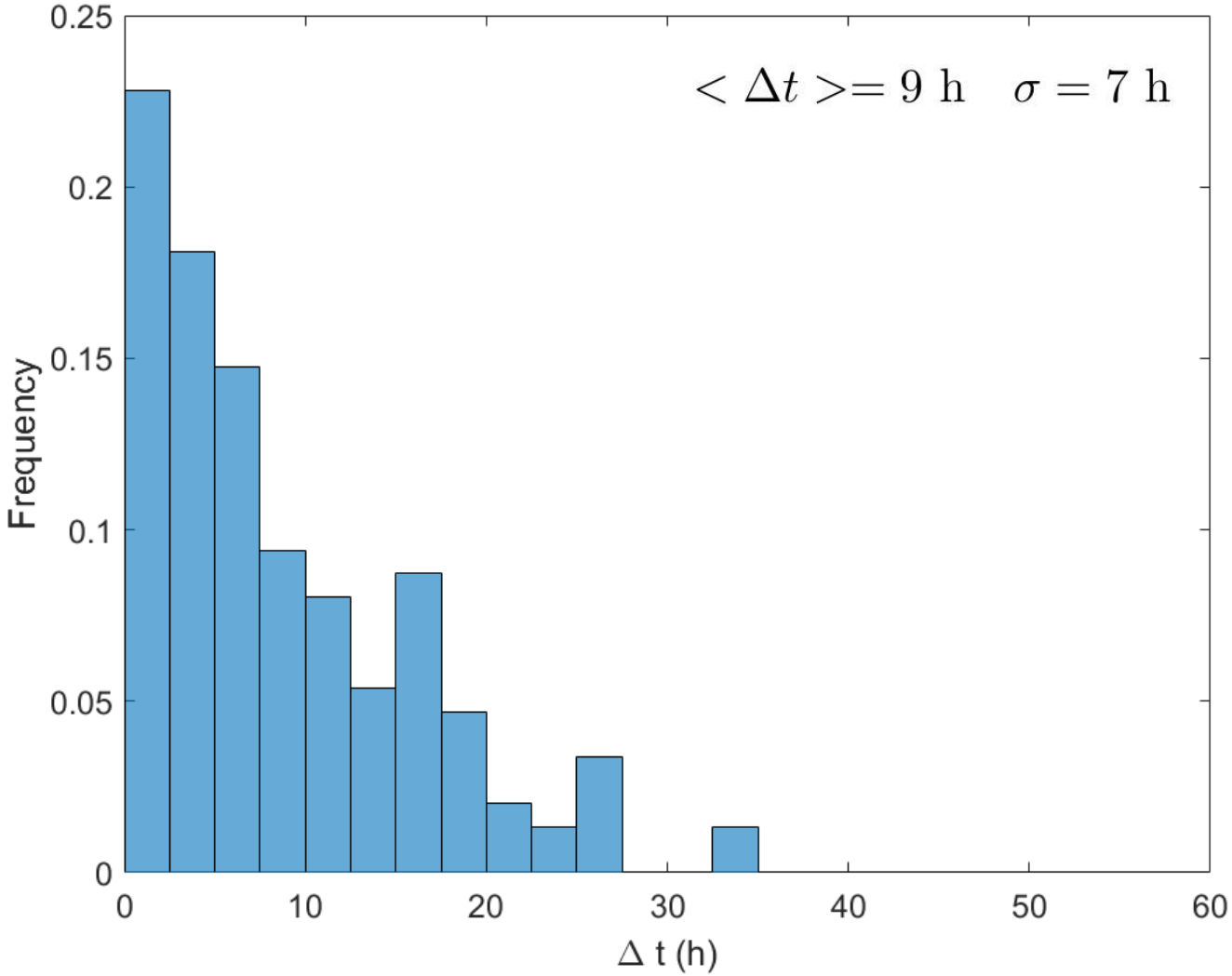

$$t_O = t_O^s + < \Delta t >$$

Probabilistic Advanced Drag-Based Model

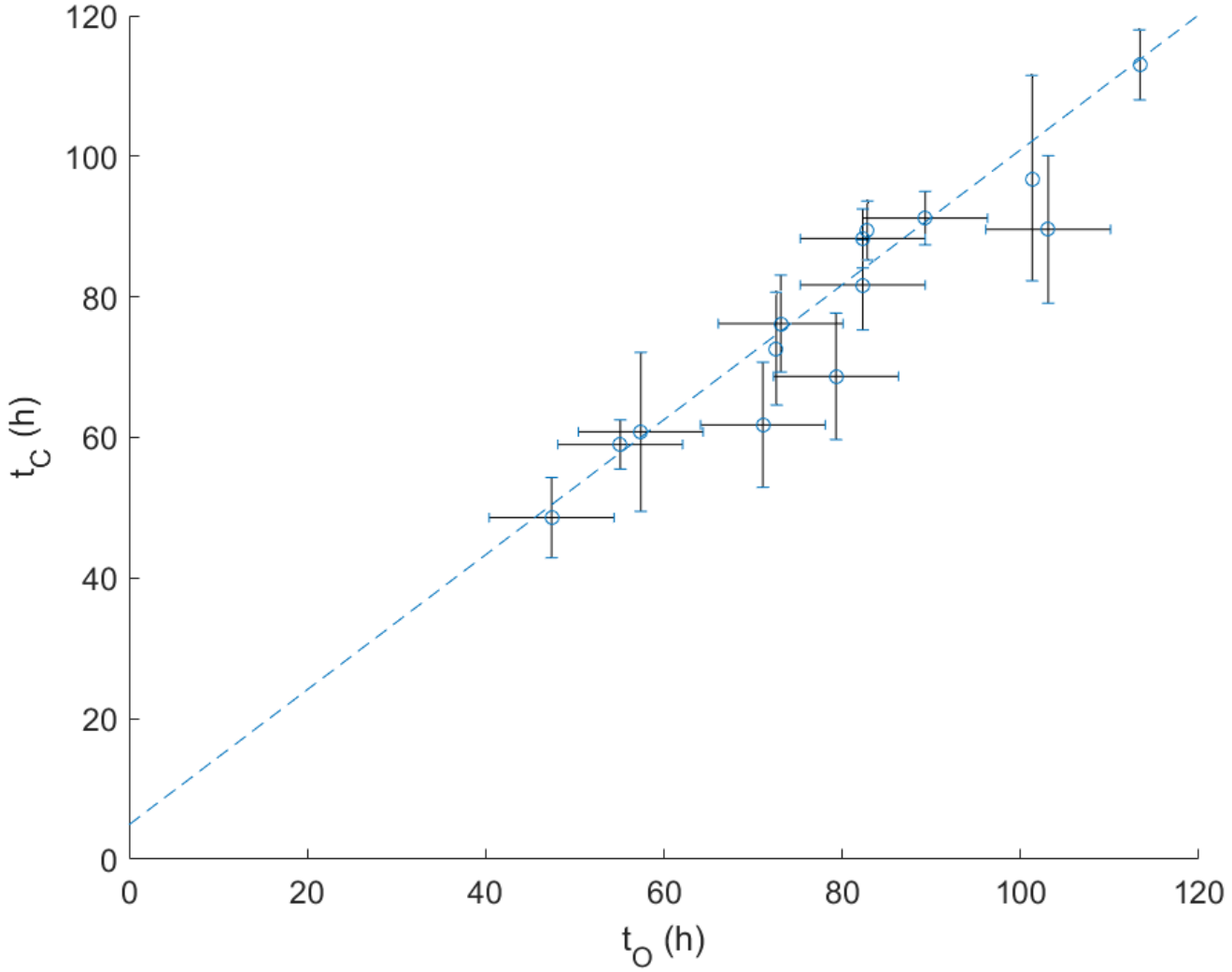

$$t_C = 4.9 + 0.96 \times t_O$$
$$\sigma_a = 9.3 \text{ h}$$
$$\sigma_b = 0.11$$
$$\rho_{ab} = -0.97$$

Conclusions

- The Drag-Based Model effectively describes ICME propagation in interplanetary space;
- Importance of ICME morphological features for forecasting;
- Probabilistic approach is able to give uncertainty on single prediction in short computational times.

Conclusions

- The Drag-Based Model effectively describes ICME propagation in interplanetary space;
- Importance of ICME morphological features for forecasting;
- Probabilistic approach is able to give uncertainty on single prediction in short computational times.

Future works

- Analysis employing a larger data sample;
- Re-examination of initial conditions and parameter distributions;
- Extension of the model by inclusion of the effect of interplanetary magnetic field and shock on ICME propagation.

Thank you for your attention

Coronal Mass Ejections

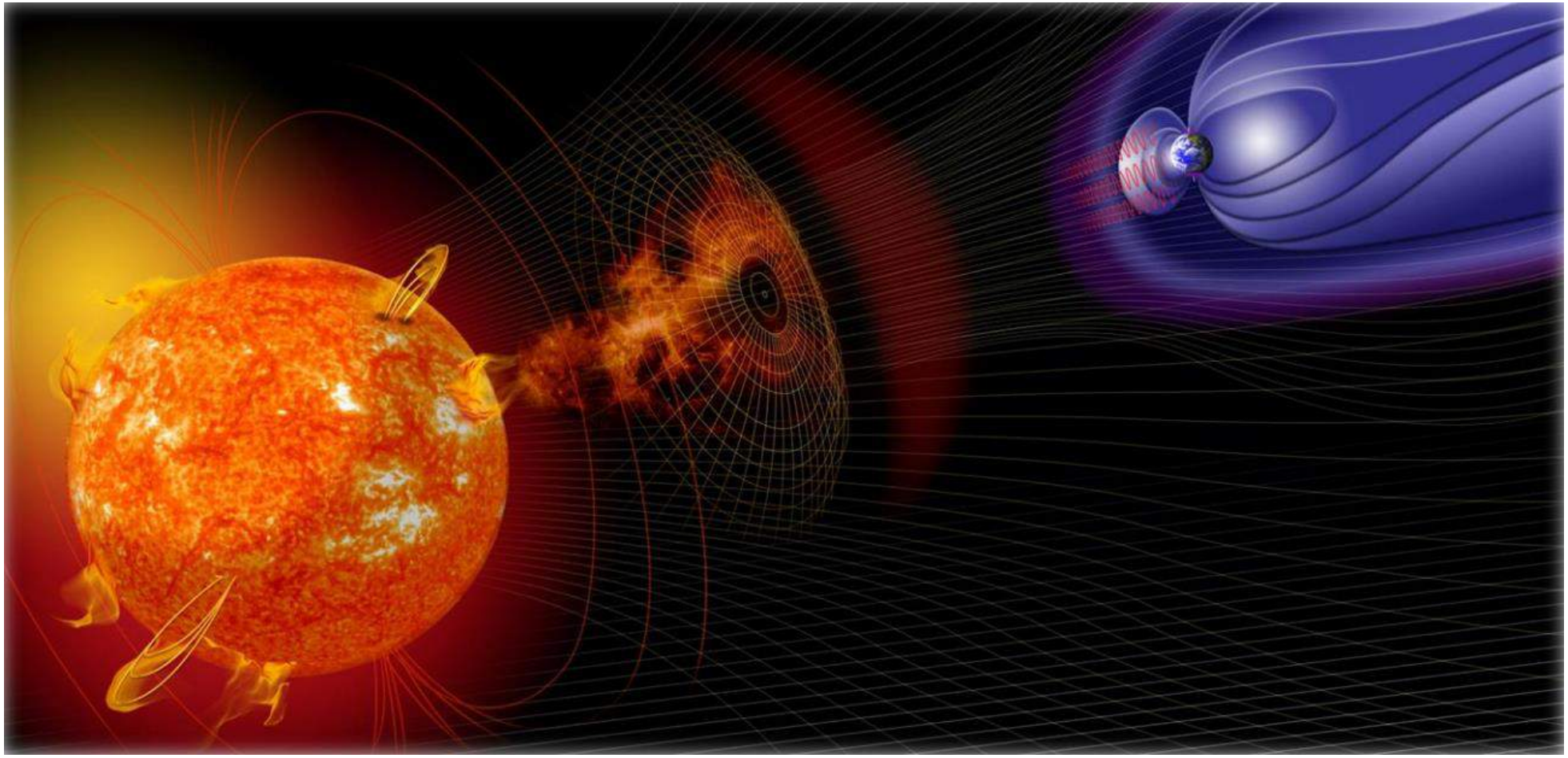

Coronal Mass Ejections

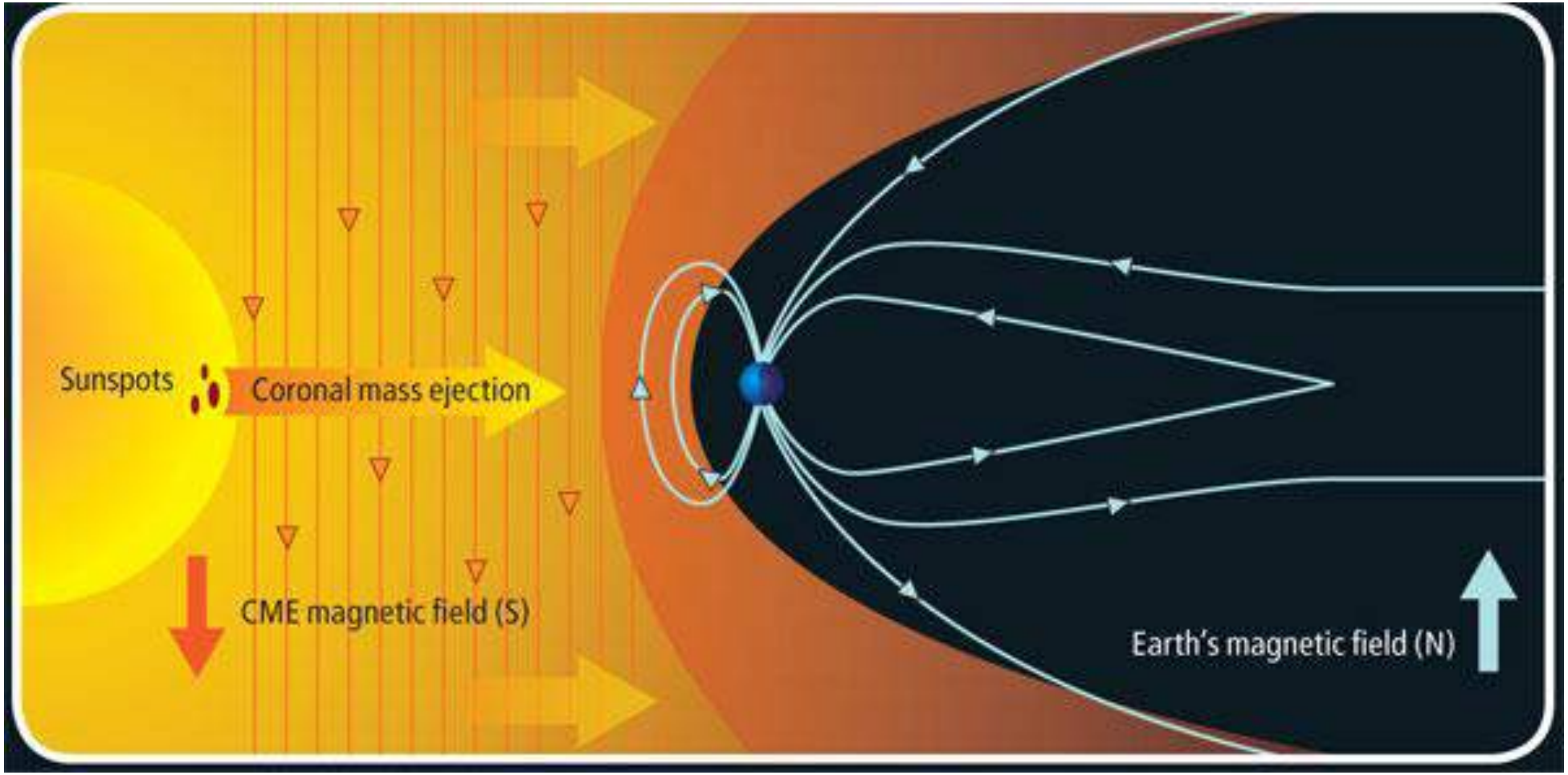

Acknowledgements

Extra Slides

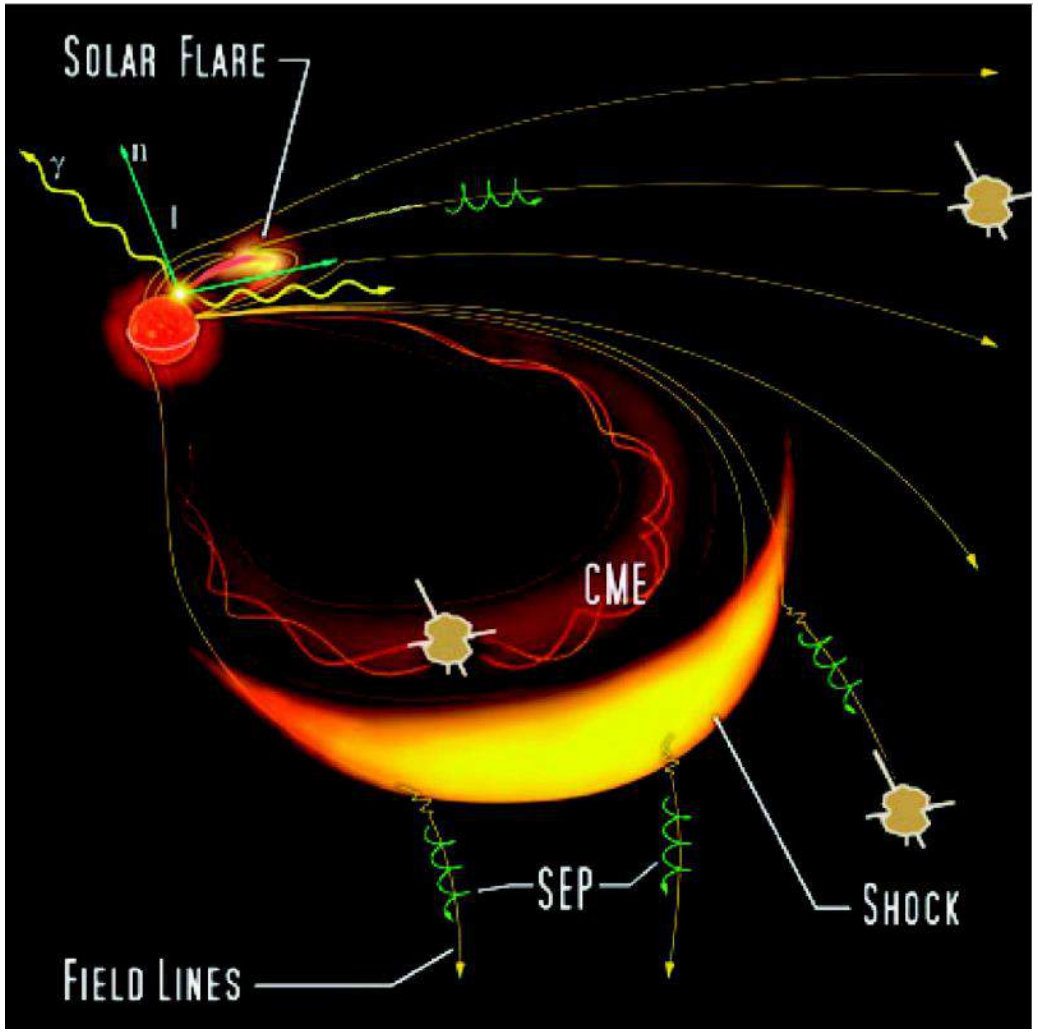

Forecasting methods of CMEs arrivals

Empirical/Statistical

Forecasting methods of CMEs arrivals

Empirical/Statistical

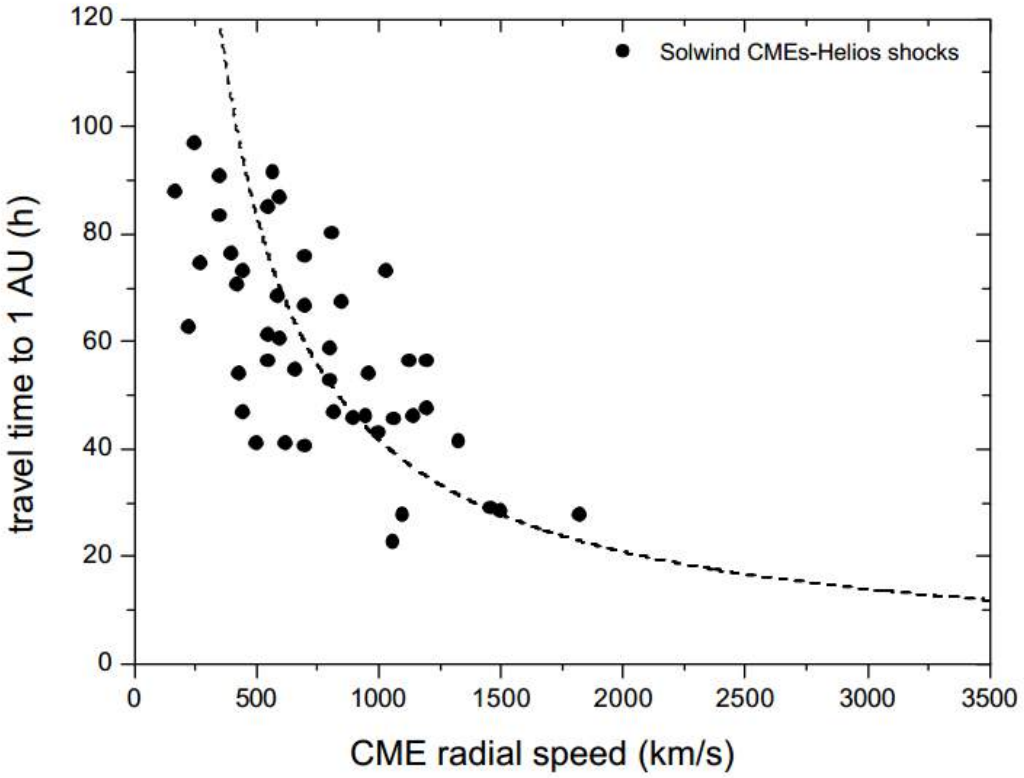

$$T_{tr} = 203 - 20.77 * ln(V_{exp})$$

(**Schwenn et al. 2005**)

Forecasting methods of CMEs arrivals

Empirical/Statistical

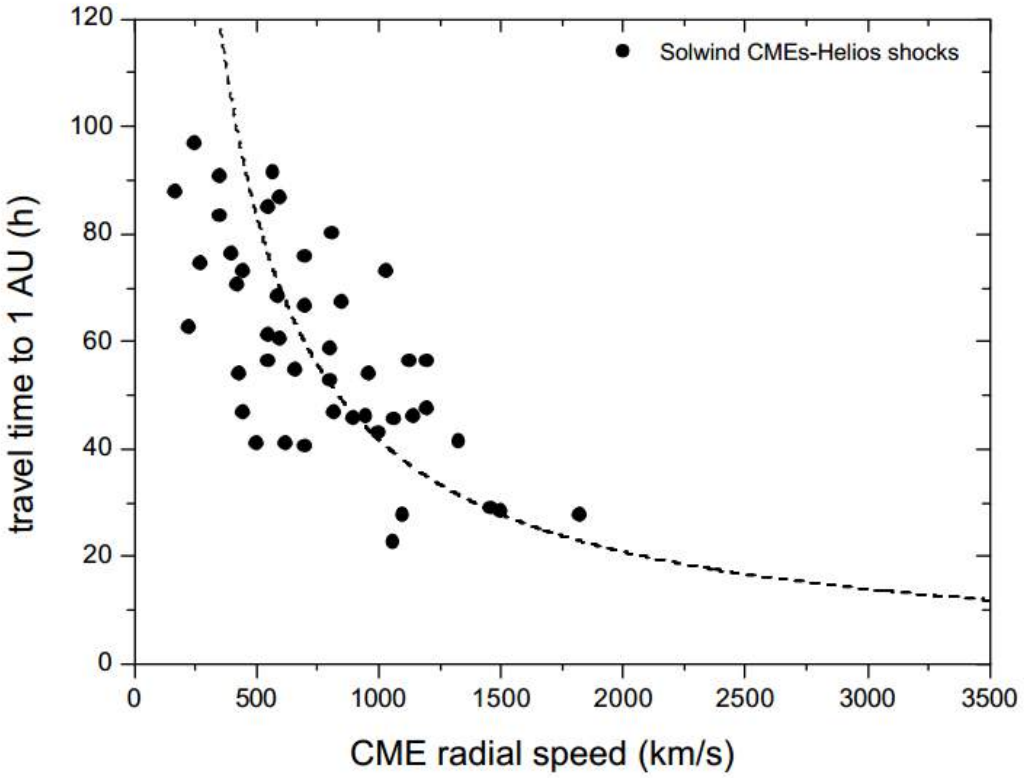

$$T_{tr} = 203 - 20.77 * ln(V_{exp})$$

(**Schwenn et al. 2005**)

MHD simulations

Forecasting methods of ICMEs arrivals

Empirical/Statistical

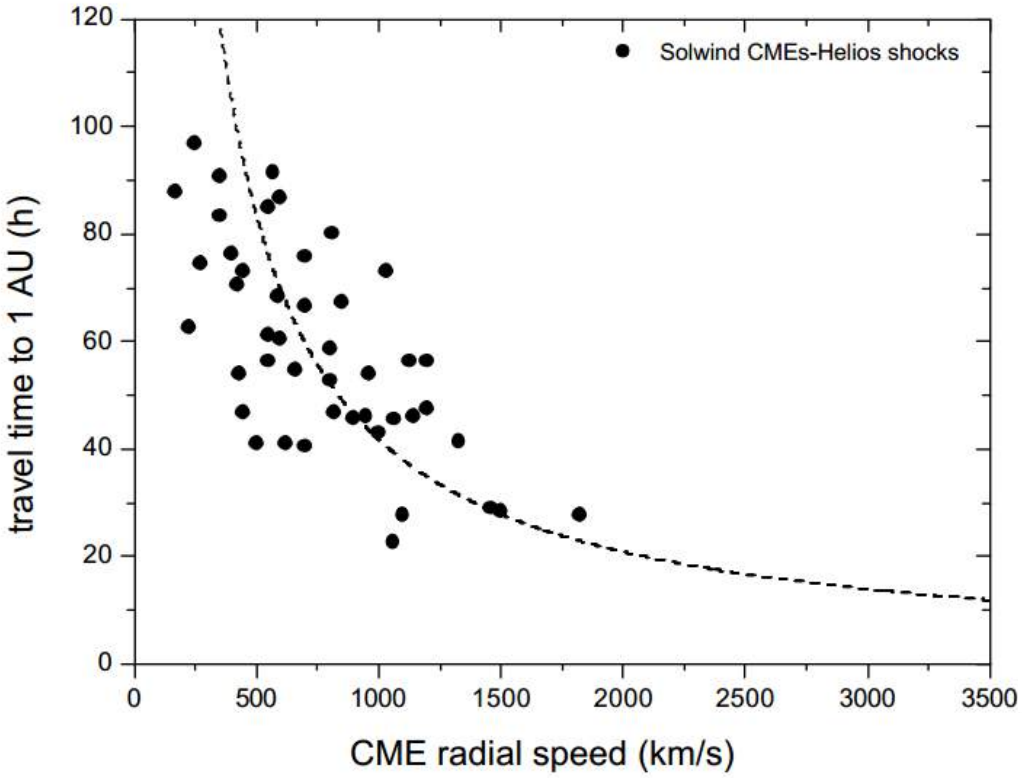

$$T_{tr} = 203 - 20.77 * ln(V_{exp})$$

(**Schwenn et al. 2005**)

MHD simulations

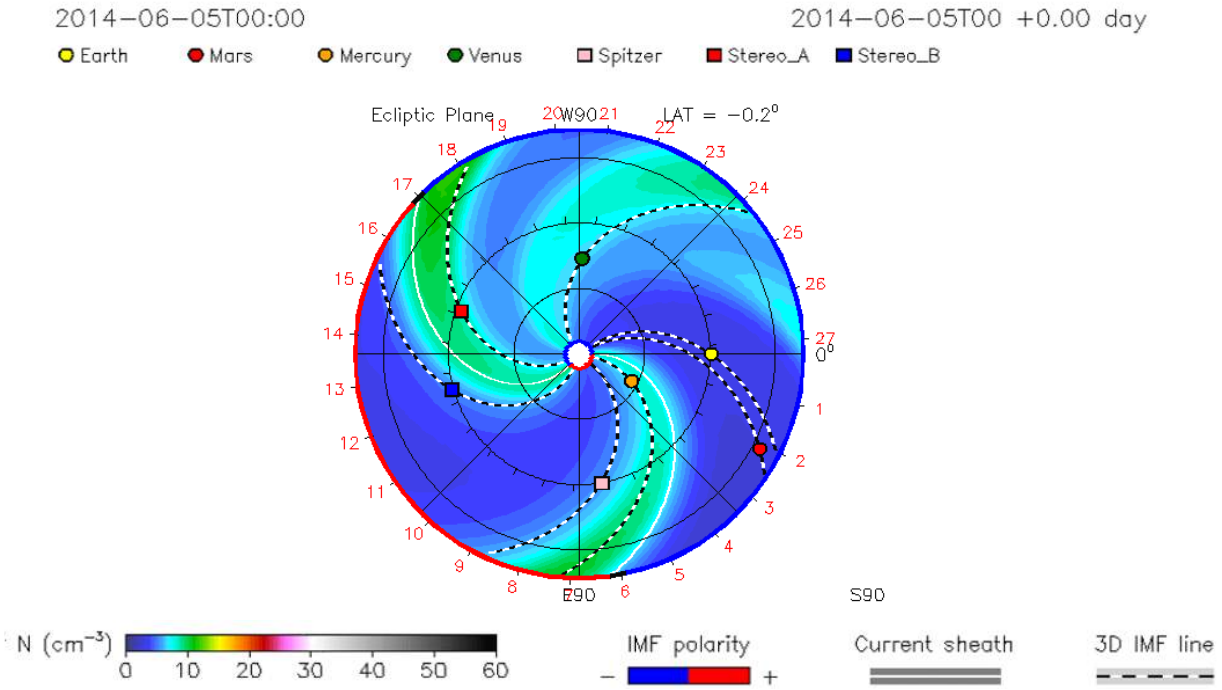

Wang-Sheeley-Arge ENLIL model

Forecasting methods of ICMEs arrivals

Empirical/Statistical

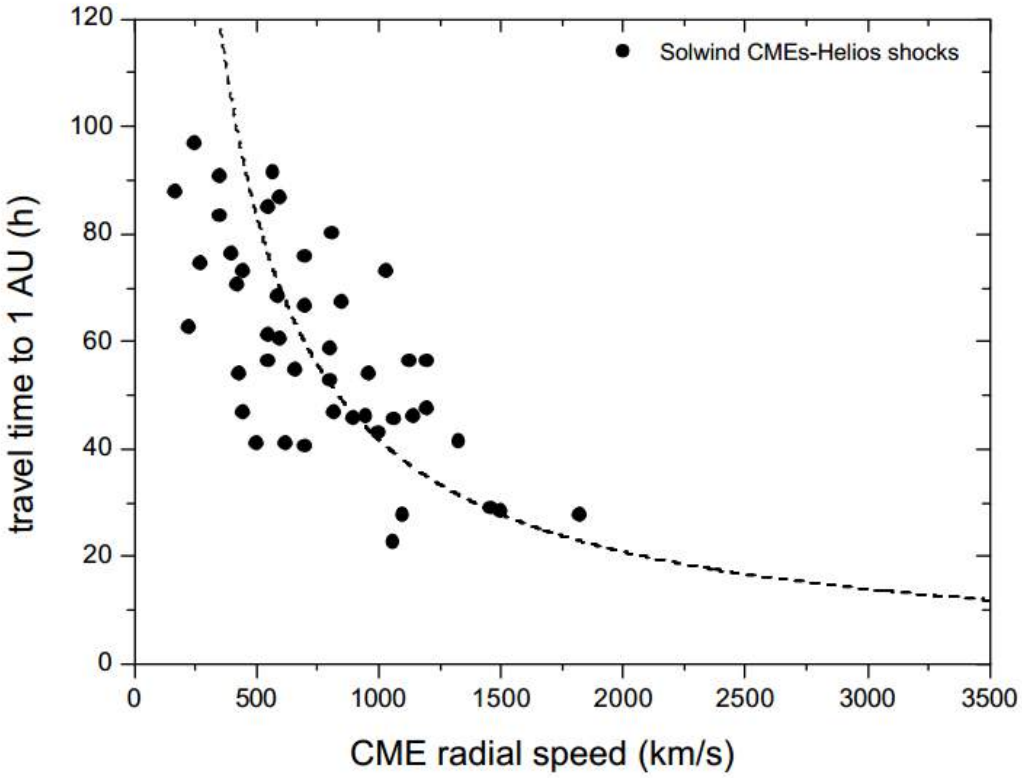

$$T_{tr} = 203 - 20.77 * ln(V_{exp})$$

(**Schwenn et al. 2005**)

MHD simulations

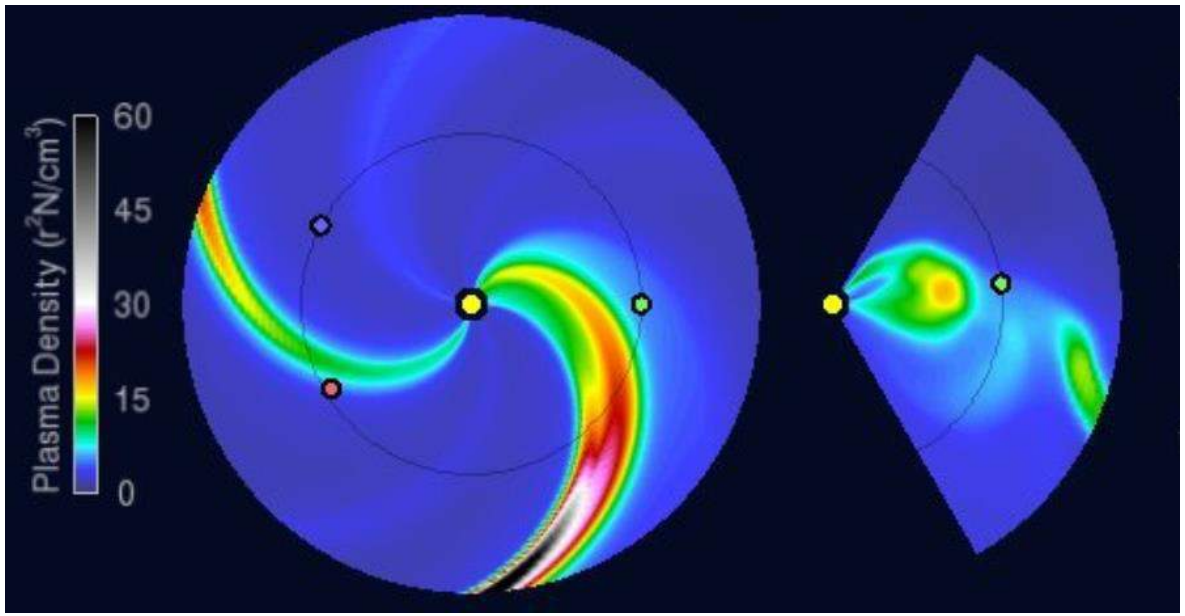

Wang-Sheeley-Arge ENLIL model

Extra Slides

Table 1. List of the CME Events Studied and the Results for Shock Arrival Time Errors[a]

Event	Date	Start (LASCO)	POS Speed at 20 R_s (LASCO) (km/s)	Observed Transit Time (hours)	V_r Cone Model (km/s)	Δt_{err} ENLIL (hours)	Δt_{err} Reference Model (V_{ref} = 850 km/s) (hours)	Δt_{err} ESA (hours)
1	9 Aug. 2000	1630	720	49	960	4	−1	1
2	29 Mar. 2001	1030	957	38	913	7	10	16
3	6 Apr. 2001	1930	1215	39	1570	−6	9	−12
4	9 Oct. 2001	1130	811	52	1297*	−5	−4	−16
5	17 Nov. 2001	0530	1350	60	934*	−9	−12	−6
6	18 Mar. 2002	0330	971	58	971	−11	−10	−7
7	15 Apr. 2002	0400	731	52	736	−1	−6	10
8	17 Apr. 2002	0830	1198	48	1134	−3	0	−8
9	16 Aug. 2002	1230	1447	53	1249*	−10	−5	−15
10	24 Aug. 2002	0130	1992	57	915	−5	−9	4
11	28 Oct. 2003	1130	2268	19	2752*	1	29	−3
12	29 Oct. 2003	2100	1519	20	2048*	6	28	1
13	25 Jul. 2004	1500	1359	31	1289	9	17	2
14	13 Dec. 2006	0300	1573	35	2170	−5	13	−16
Average absolute						5.9	10.9	8.4

[a]Start (LASCO) means UT of the corresponding date, when the CME is first seen in LASCO C2 coronograph image. POS means plane of sky projection. V_r is the radial velocity, obtained using the cone model method of *Xie et al.* [2004]. Here Δt_{err} means arrival time error. The error in negative if the observed shock arrival was later than model predicted and is positive in the opposite case. Values with asterisks are taken from the paper by *Xie et al.* [2006].

Extra Slides

Foundations of the Drag-Based Model

- Acceleration mechanism dependent on the solar wind speed;

(**Gopalswamy et. al 2000**)

6. Conclusions

We studied a set of 28 IP ejecta associated with white light CMEs observed by the SOHO/LASCO coronagraphs to quantify the influence of solar wind on the propagation of CMEs. We considered only the kinematic properties and ignored internal evolution of CMEs as they propagated from the Sun to 1 AU. We postulated a global, effective acceleration representing the solar wind-CME interaction and found a simple relation between the acceleration and the initial speed of the CMEs. We found a critical velocity of ~ 400 km s^{-1} which delineates fast and slow CMEs; slow CMEs are accelerated and fast CMEs are decelerated. We identified this critical velocity to be the average velocity of the solar wind measured during our study period. The empirical relationship between this effective acceleration and the initial speed of CMEs may be used as a tool for predicting the arrival time of CMEs at 1 AU.

Extra Slides

Foundations of the Drag-Based Model

- Tendency of the ICME velocity to the solar wind speed;

(**Manoharan 2006**)

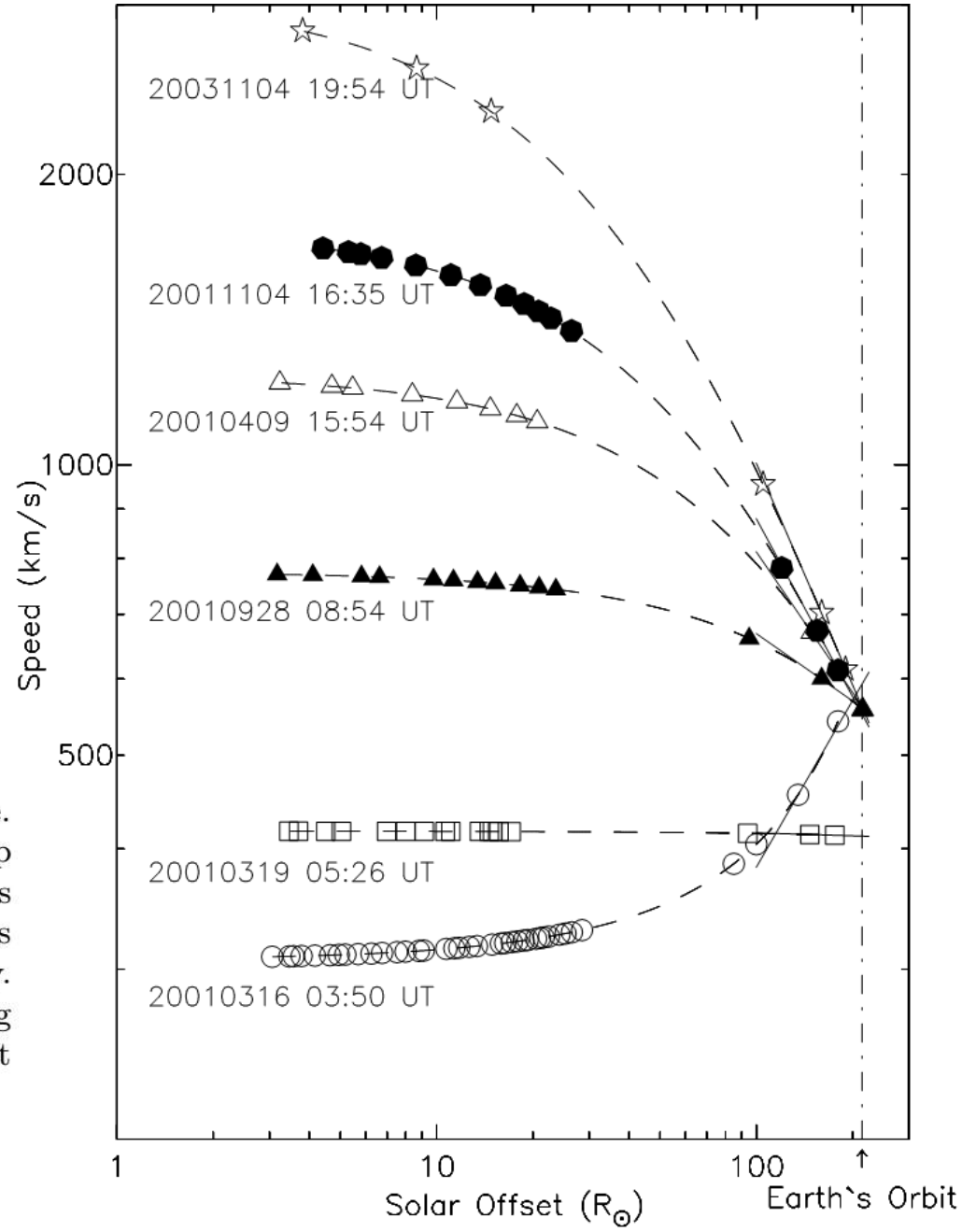

Figure 5. Representative speed-distance, *V(R)*, profiles plotted on log-log scale. Average initial speed of the CME increases from bottom ($\sim$ 300 kms^{-1}) to top ($\sim$ 2500 kms^{-1}). The date and the start time of each CME are shown. These profiles converge toward the ambient solar wind speed at the Earth's orbit. The data points at $R \leq 30\ R_\odot$ and $R \geq 80\ R_\odot$ are from LASCO and IPS measurements, respectively. The *straight-line* fit to the data points at $R \geq 100\ R_\odot$ gives the slope, α, according to $V \sim R^{-\alpha}$ (refer to Section 4.2). The *vertical line* indicates the Earth's orbit ($R \approx 215\ R_\odot$).

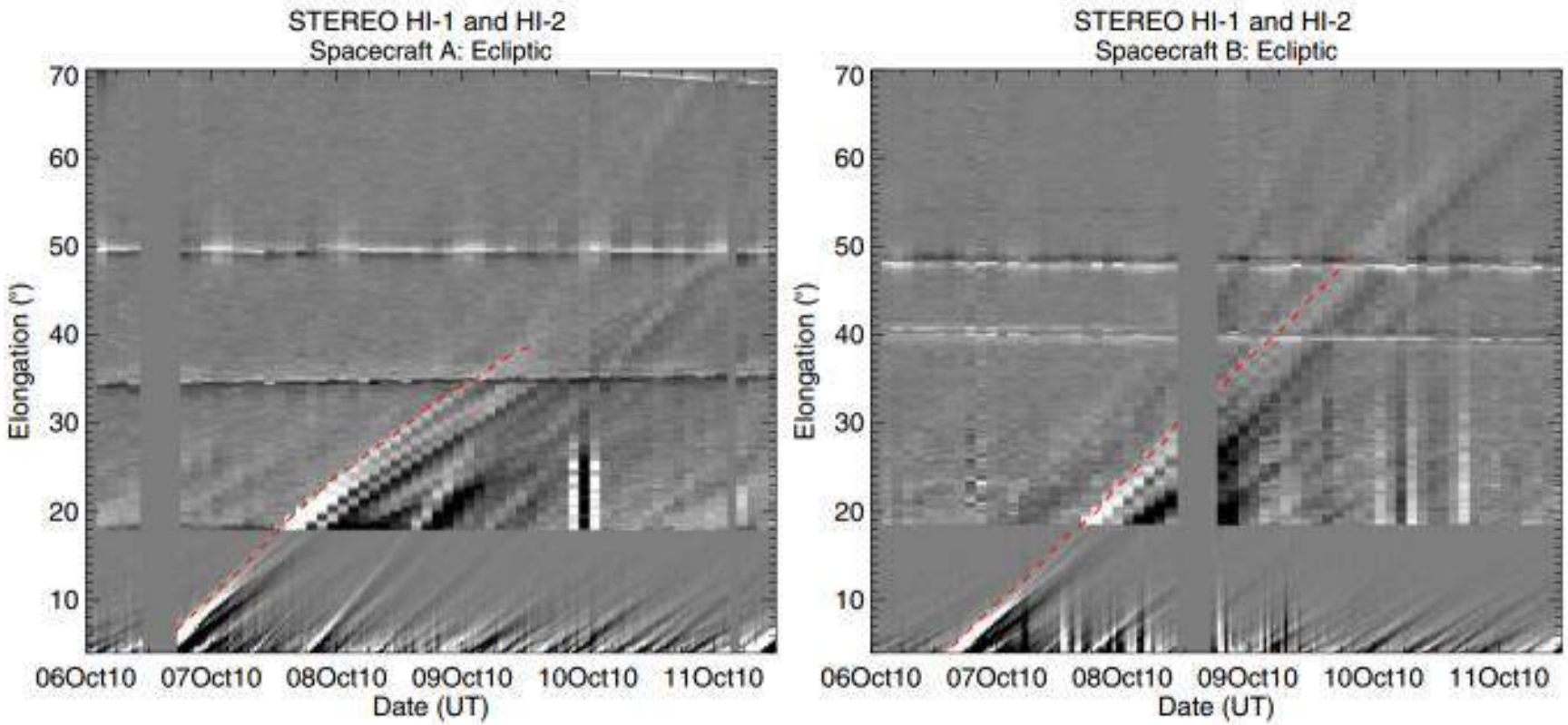

Figure 1.4: Ecliptic J-maps covering the passage of the 2010 October 6 CME, from the viewpoints of both STEREO-A (left) and STEREO-B (right) constructed from running differences images from HI1 and HI2, for the time interval extending from UT 2010 October 6 00:00 UT to October 11 12:00. The dashed red line tracks the leading edge of the CME front, while the Earth is identified with the line of constant elongation of 49.5° in the left panel and with 48.2° in the right panel. From [5].

Extra Slides

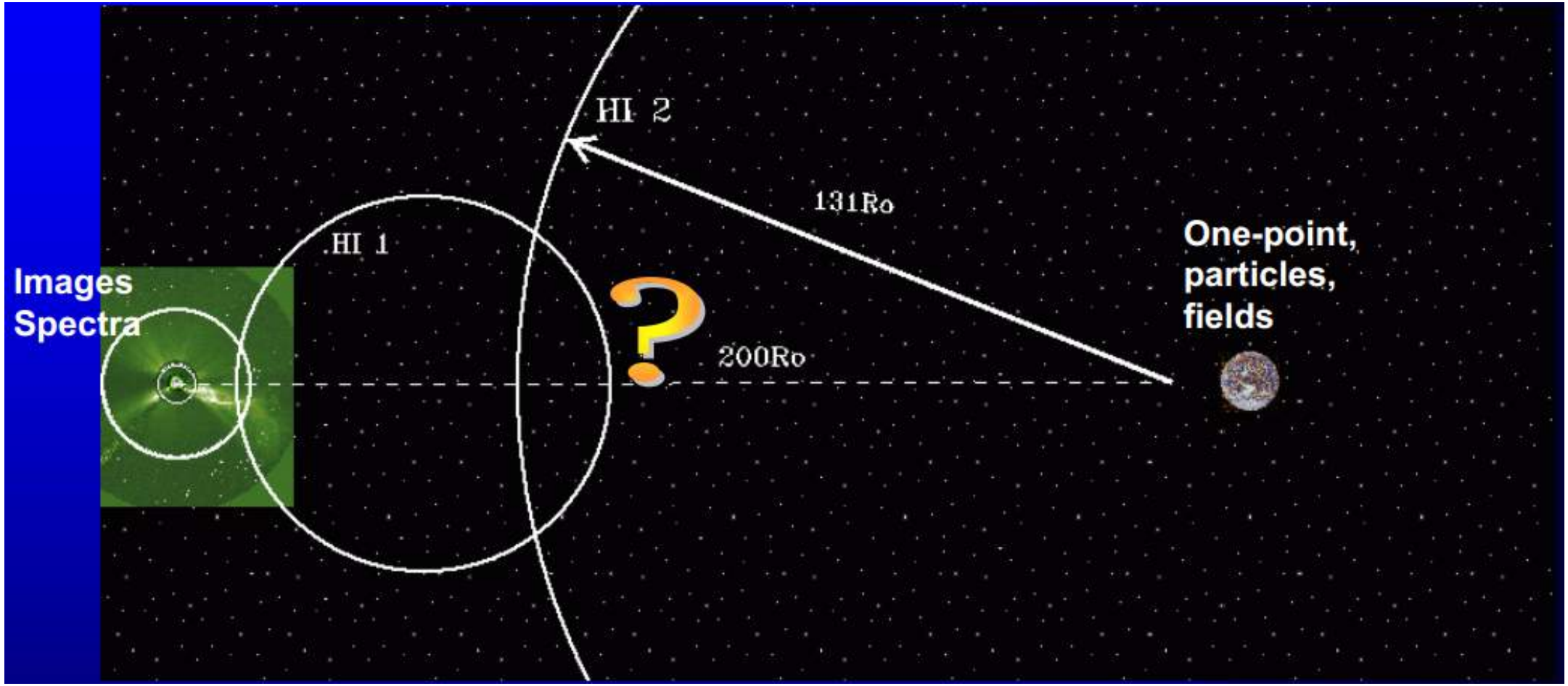

Extra Slides

Foundations of the Drag-Based Model

- Tendency of the ICME velocity to the solar wind speed;

(**Cargill 2004**)

AU. However, a significant difficulty is that estimates of ICME arrival time at 1 AU based on the CME speed at the Sun are too early by a considerable amount. While CMEs seen with coronagraphs have velocities ranging anywhere between 100 and 2000 km s^{-1} (e.g., Hundhausen, 1999; St Cyr *et al.*, 2000), the corresponding ICMEs typically have velocities that differ by only 100–200 km s^{-1} from the solar wind speed. Thus the forces acting on the ICME in the interplanetary medium must lead to an 'equalisation' of the ICME and solar wind velocities.

The dynamics of an ICME is determined by (a) the outward or inward Lorentz force, (b) the inward gravitational force and (c) forces due to the interaction of

Solar Physics **221:** 135–149, 2004.

Extra Slides

(**Crooker & Horbury 2005**)

Foundations of the Drag-Based Model

- Radial propagation alone and maintenance of a coherent structure lead to a flattening of the CME (pancaking);

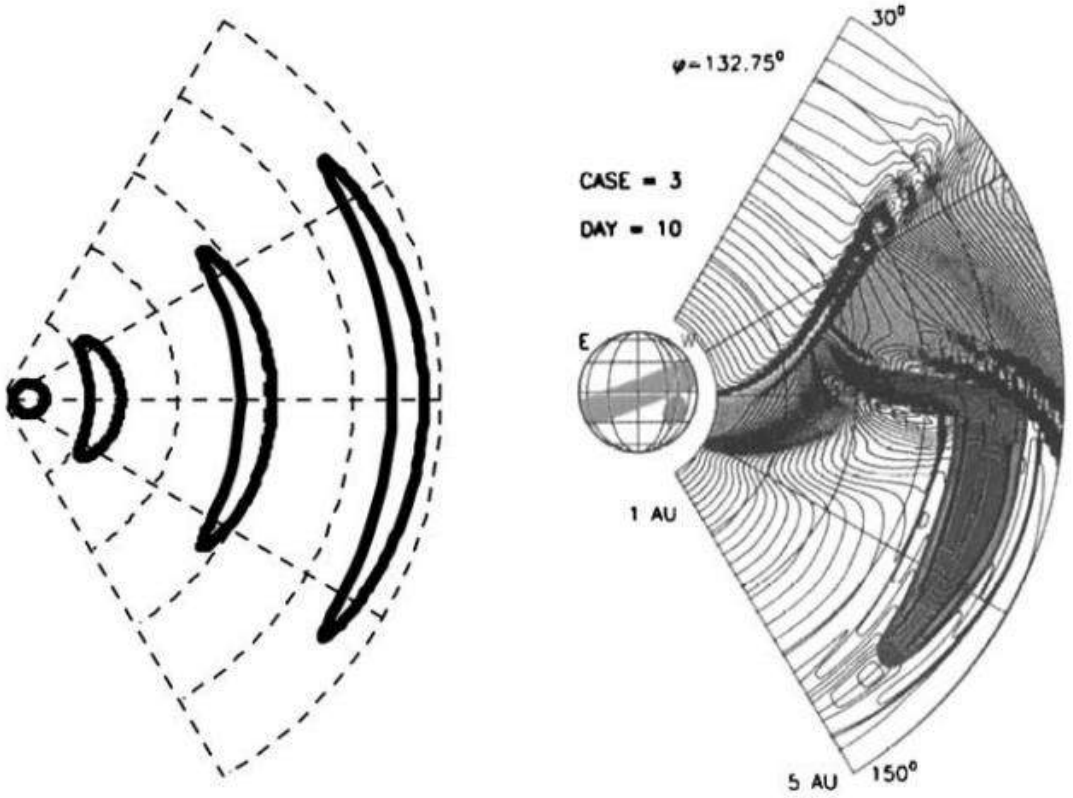

Figure 5. (a) Schematic of the kinematic effects of the radial expansion of ICMEs, leading to a "pancake" shape. (b) Results of a 3D simulation of an ICME propagating through a structured solar wind: the ICME is greatly distorted by its interaction with slow solar wind at low latitudes (after Odstrčil and Pizzo, 1999b).

The Drag-Based Model

Foundations of the Drag-Based Model

- Shapes of CMEs appear to be consistent with a nearly perfect circular cross section;

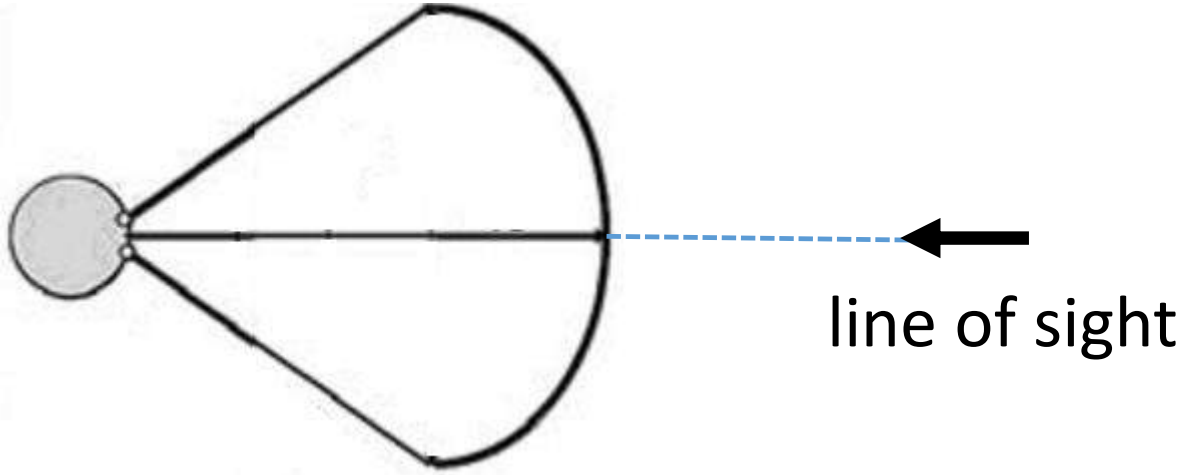

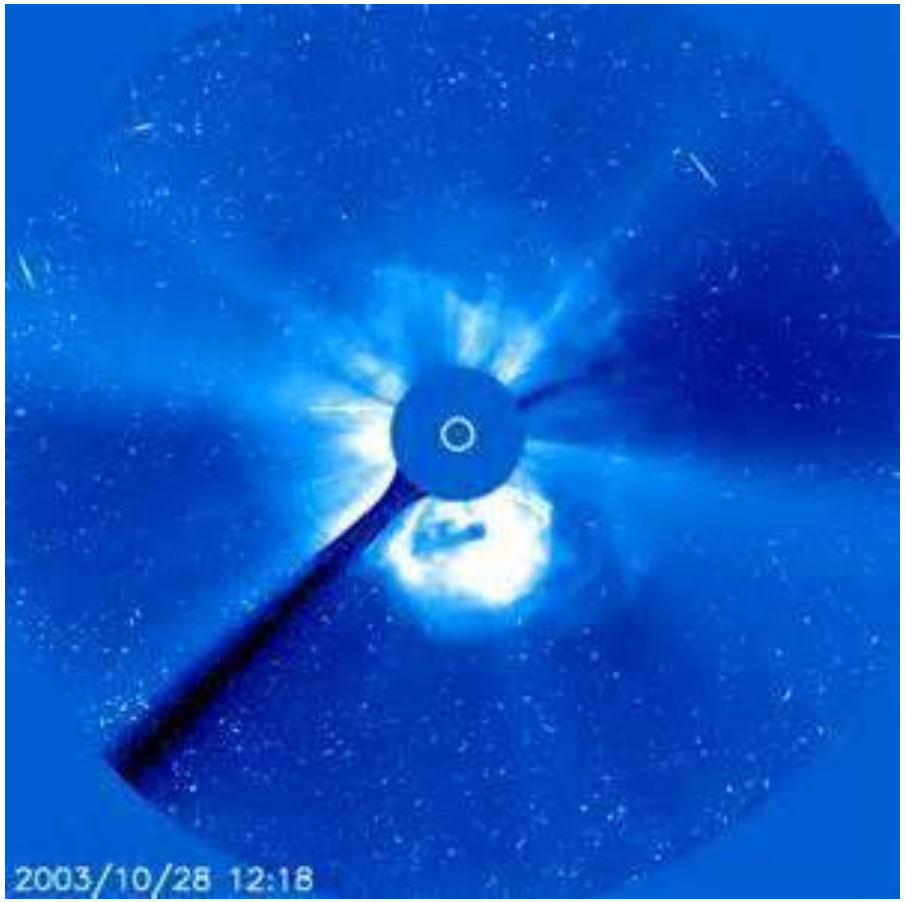

The Drag-Based Model

Foundations of the Drag-Based Model

- Shapes of CMEs appear to be consistent with a nearly perfect circular cross section;

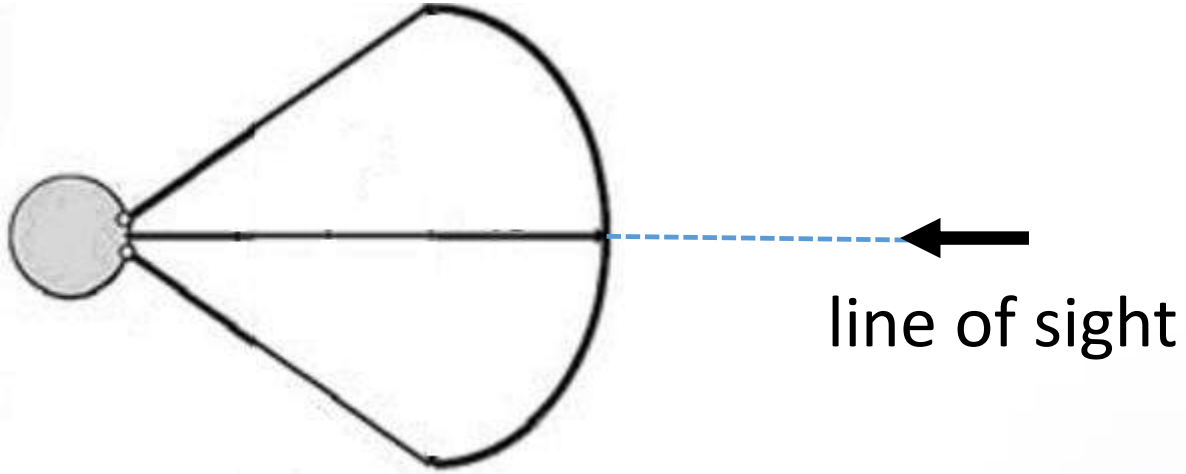

line of sight

ICME cross section A

Extra Slides

- Circular cross section

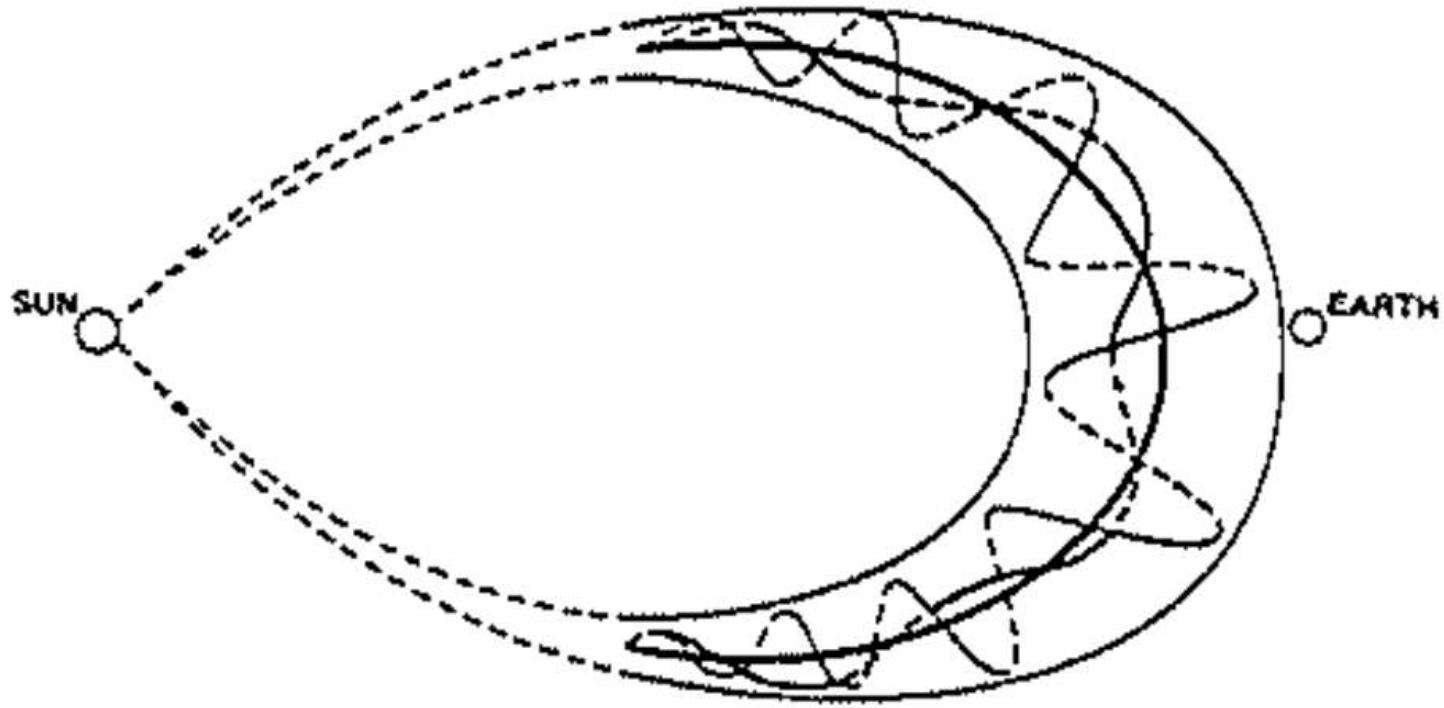

Extra Slides

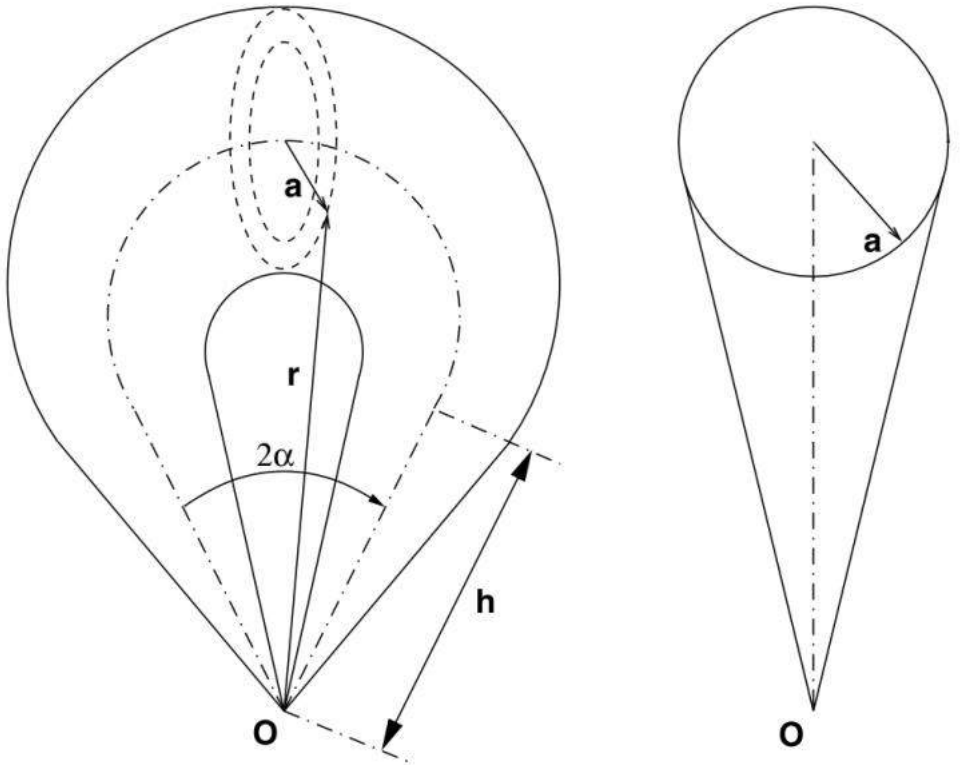

Figure 2.4: Geometry of the GCS Model (front and side section) developed by Thernisien, Howard and Vourlidas. From [12].

Extra Slides

- GCS model

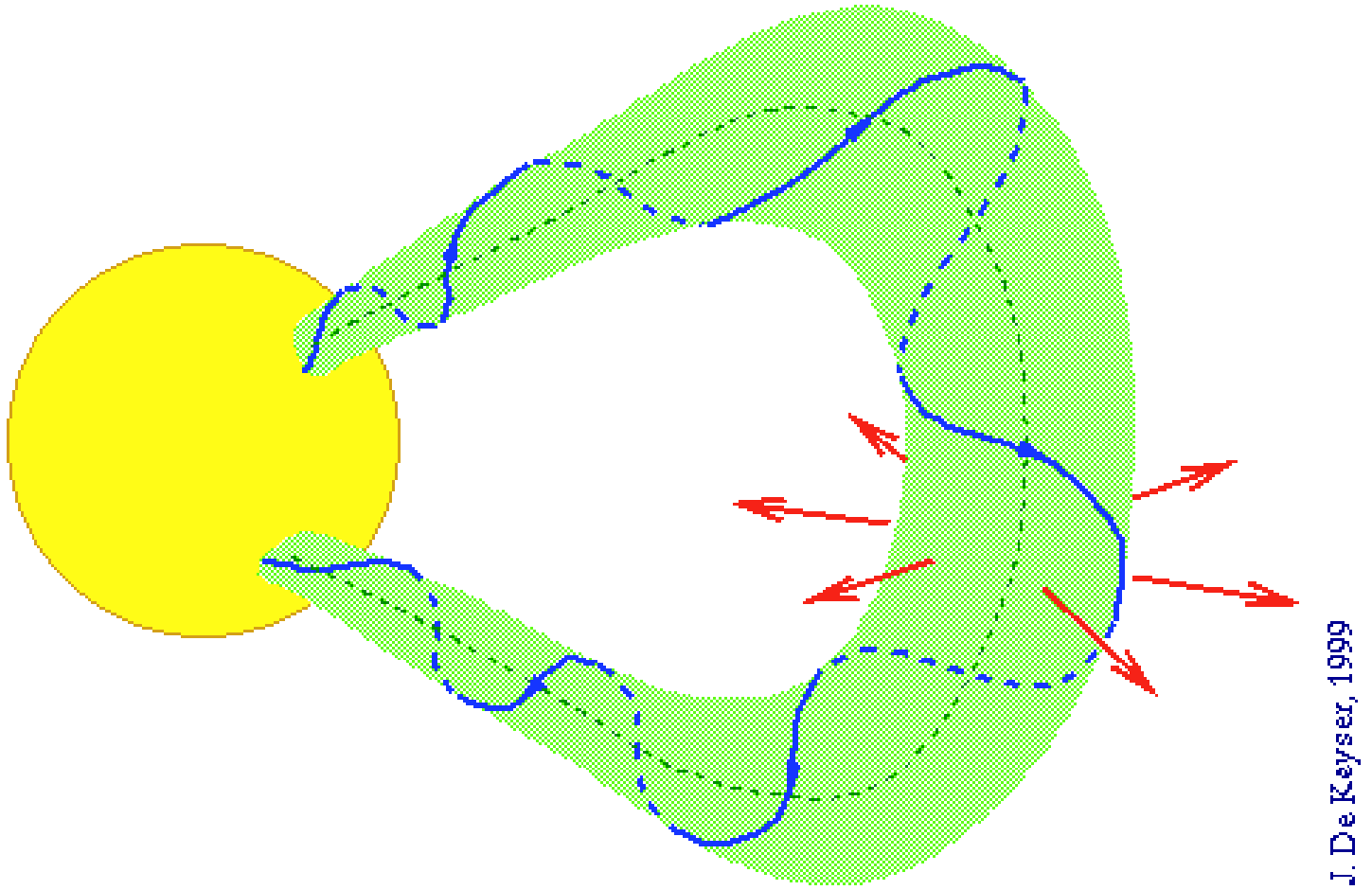

Extra Slides

- GCS model

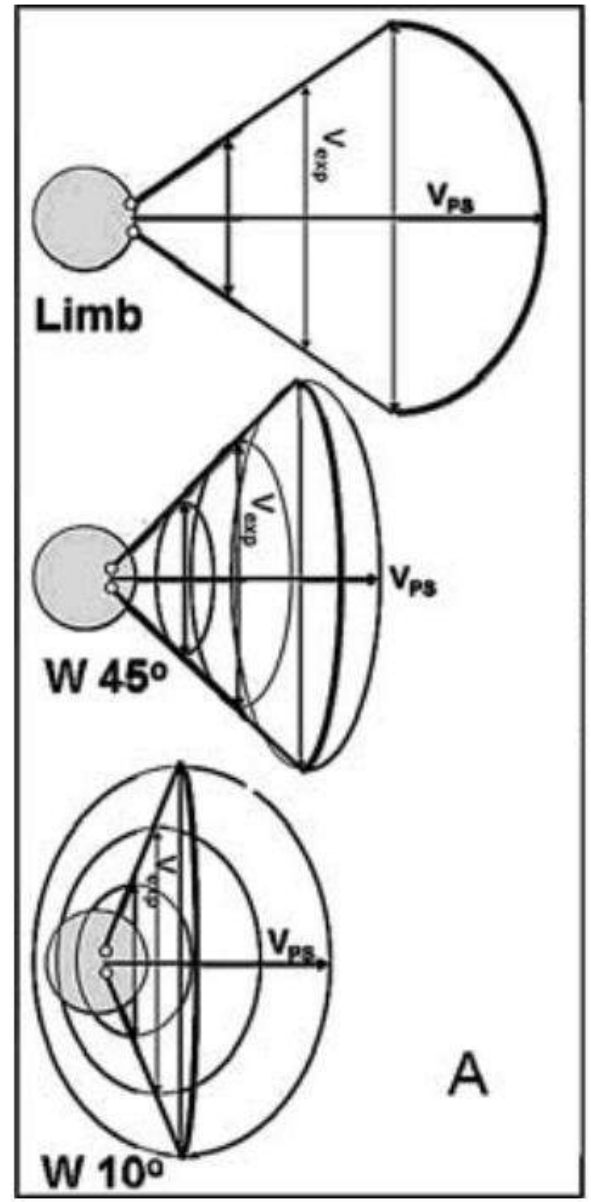

Probabilistic Advanced Drag-Based Model

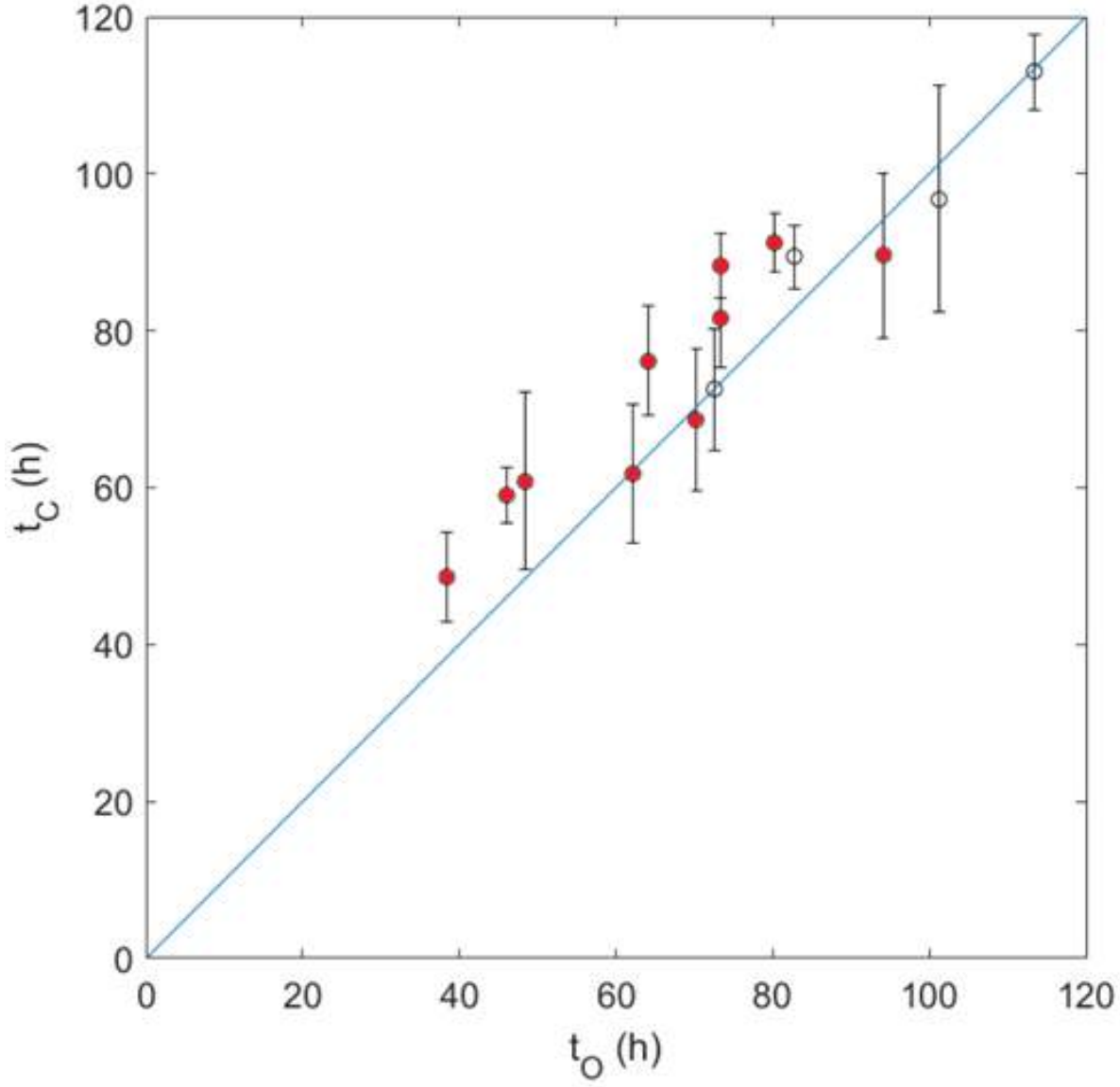

For 7 out of 10 shock events (red dots)

$t_C > t_O$

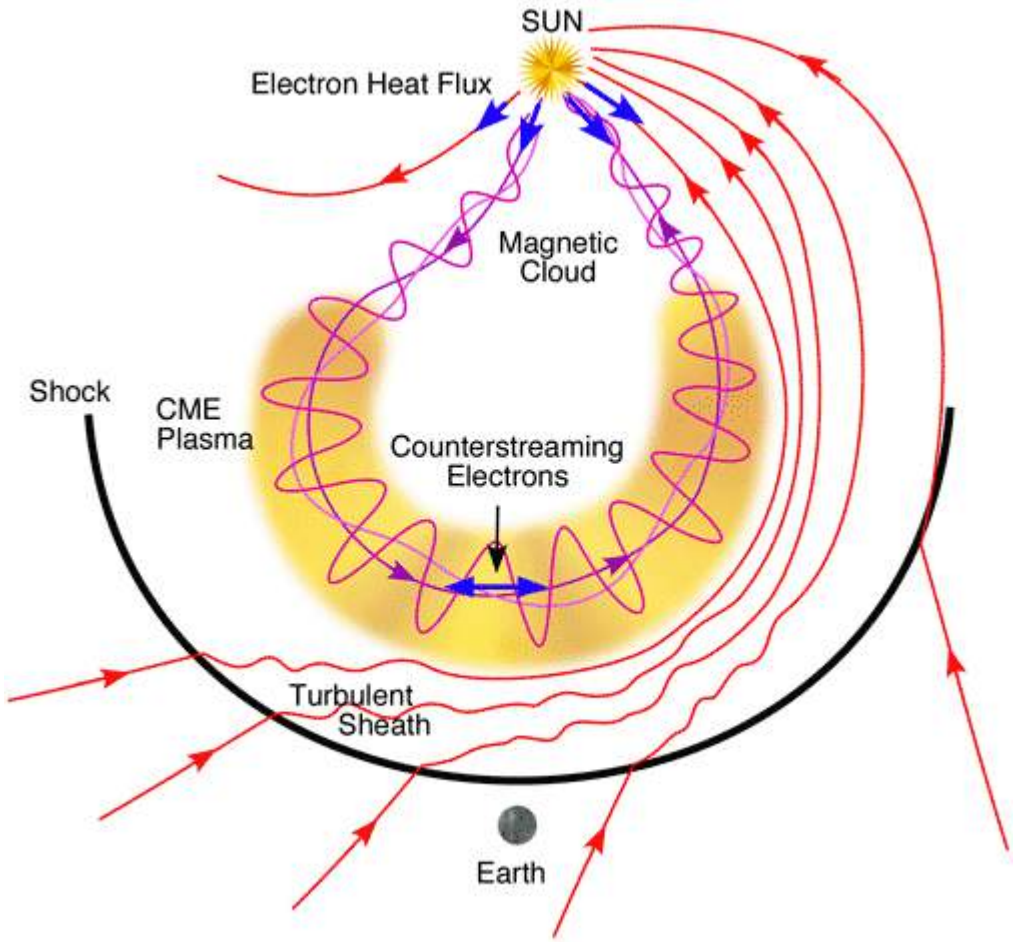

The Drag-Based Model

Aerodynamic Drag ($R > 20R_\odot$)

$$\vec{F}_D = -\rho_W A C_D (\vec{v} - \vec{w})|\vec{v} - \vec{w}|$$

$$M_* \frac{d^2\vec{v}}{dt^2} = \vec{F}_D$$

$\vec{v}$	ICME speed
A	ICME cross section
C_D	drag coefficient
ρ_W	solar wind density
$\vec{w}$	solar wind speed
M_*	ICME mass + virtual mass

The Drag-Based Model

Aerodynamic Drag ($R > 20R_\odot$)

$$\vec{F}_D = -\rho_W A C_D (\vec{v} - \vec{w})|\vec{v} - \vec{w}|$$

$\vec{v}$	ICME speed
A	ICME cross section
C_D	drag coefficient
ρ_W	solar wind density
$\vec{w}$	solar wind speed

Leblanc model for the solar wind density from Sun to 1 AU (Leblanc et al. 1996)

$$n_w(R) = \frac{8.0 \times 10^7}{R^6} + \frac{4.1 \times 10^6}{R^4} + \frac{3.3 \times 10^5}{R^2}$$

R in solar radii, n_w in cm^{-3}

$$\frac{\partial}{\partial r}(r^2 w \rho_w) = 0$$

$$w(r) \propto \frac{1}{r^2 \rho_w(r)}$$

Extra Slides

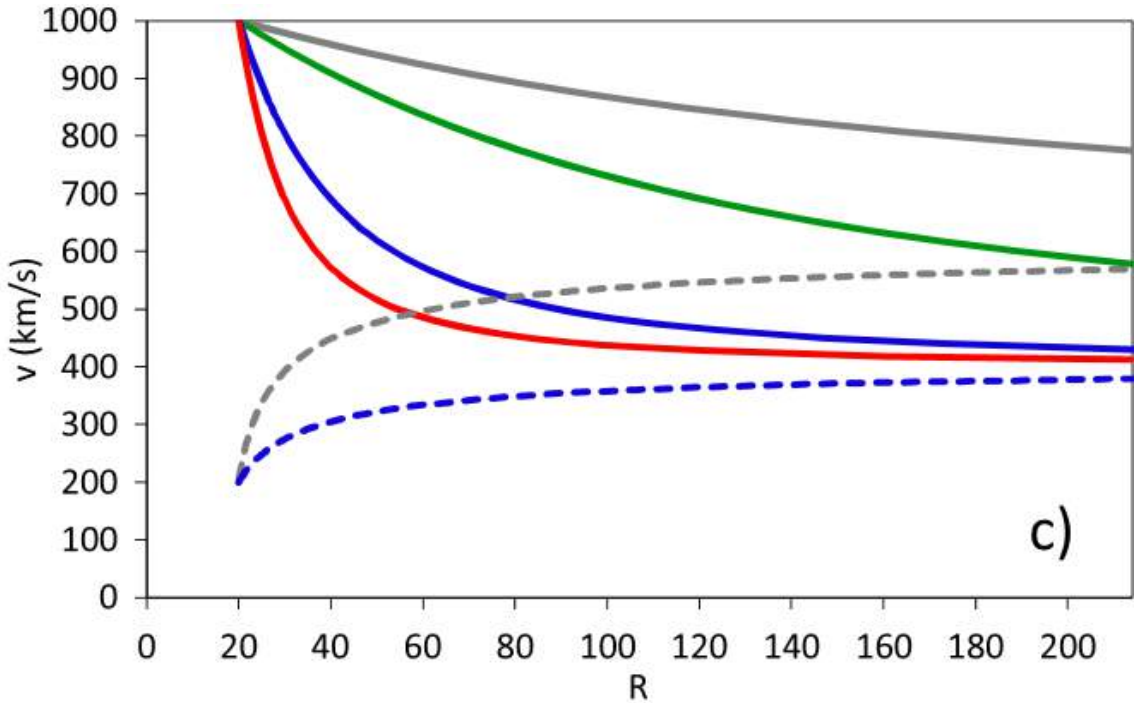

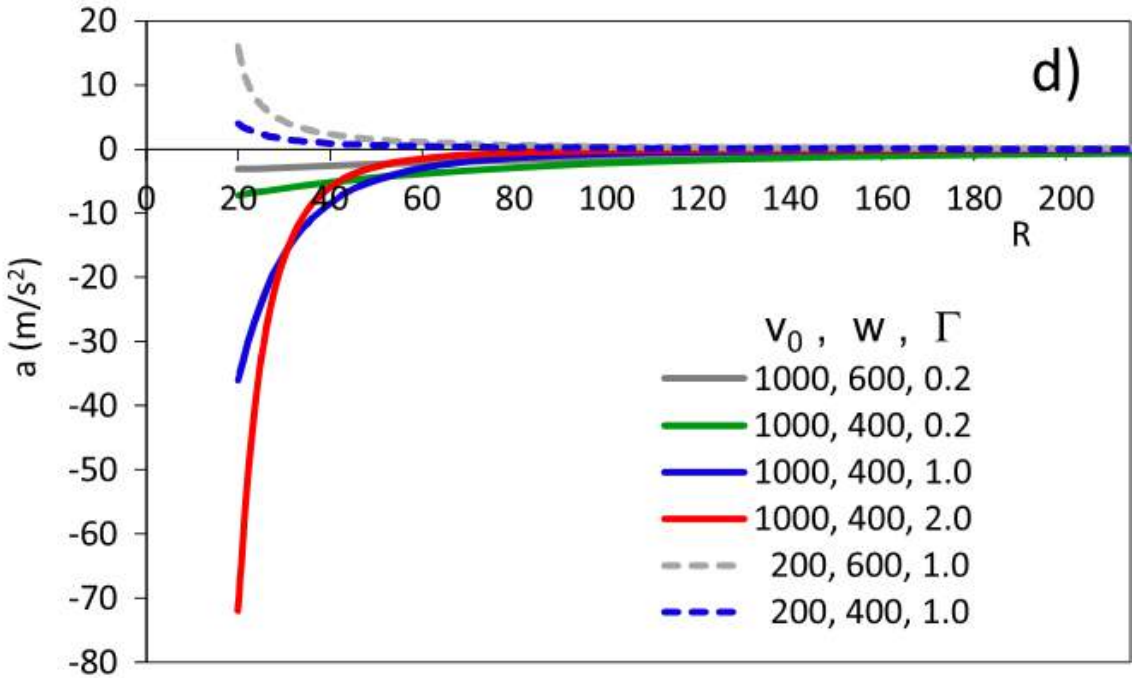

Test of the Drag-Based Model

Data samples

Schwenn et al. 2005

Manoharan 2006

LASCO CME catalog

r_0 , v_0 , t_O for 38 events

unknown γ, w and CME morphology

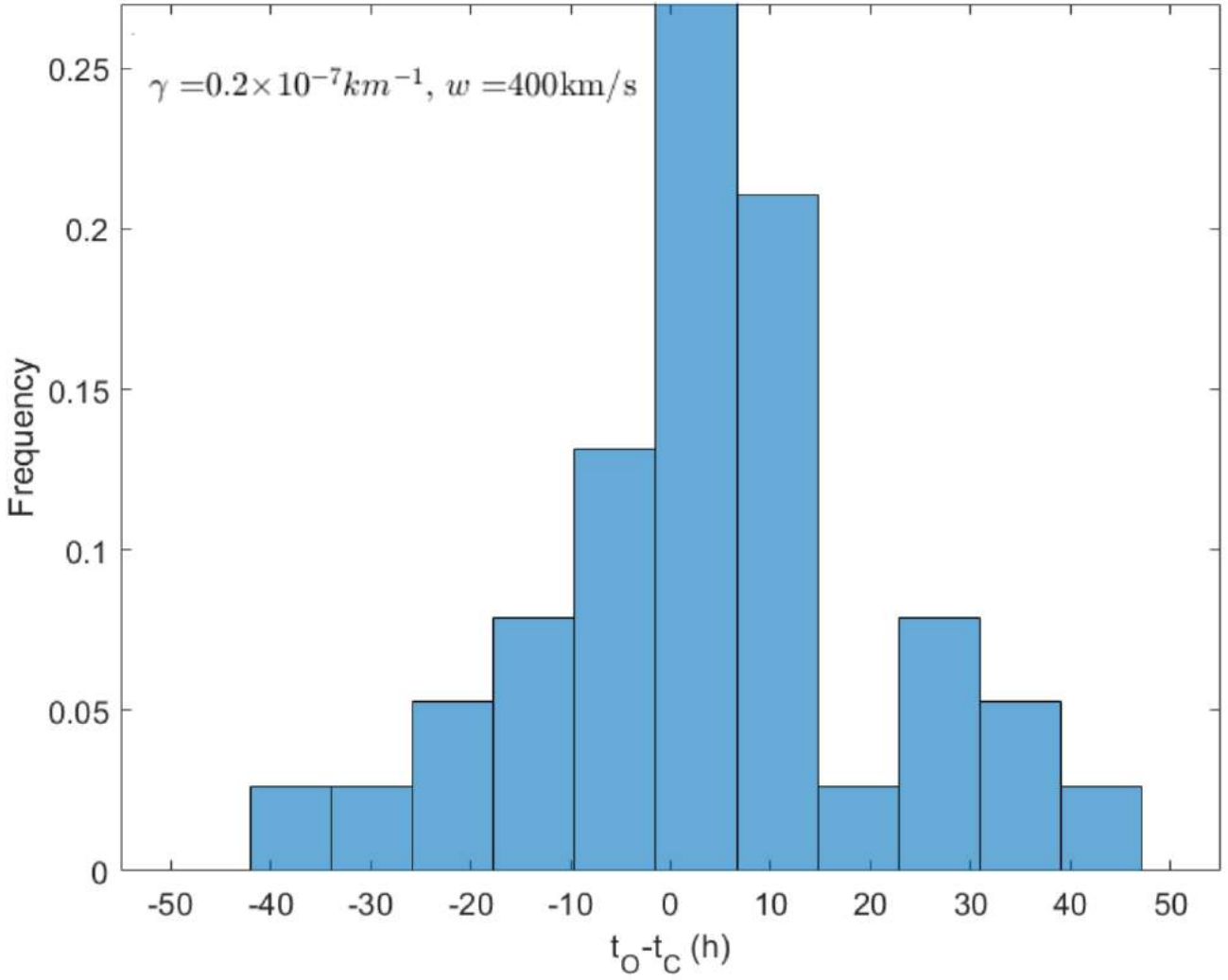

Test of the Drag-Based Model

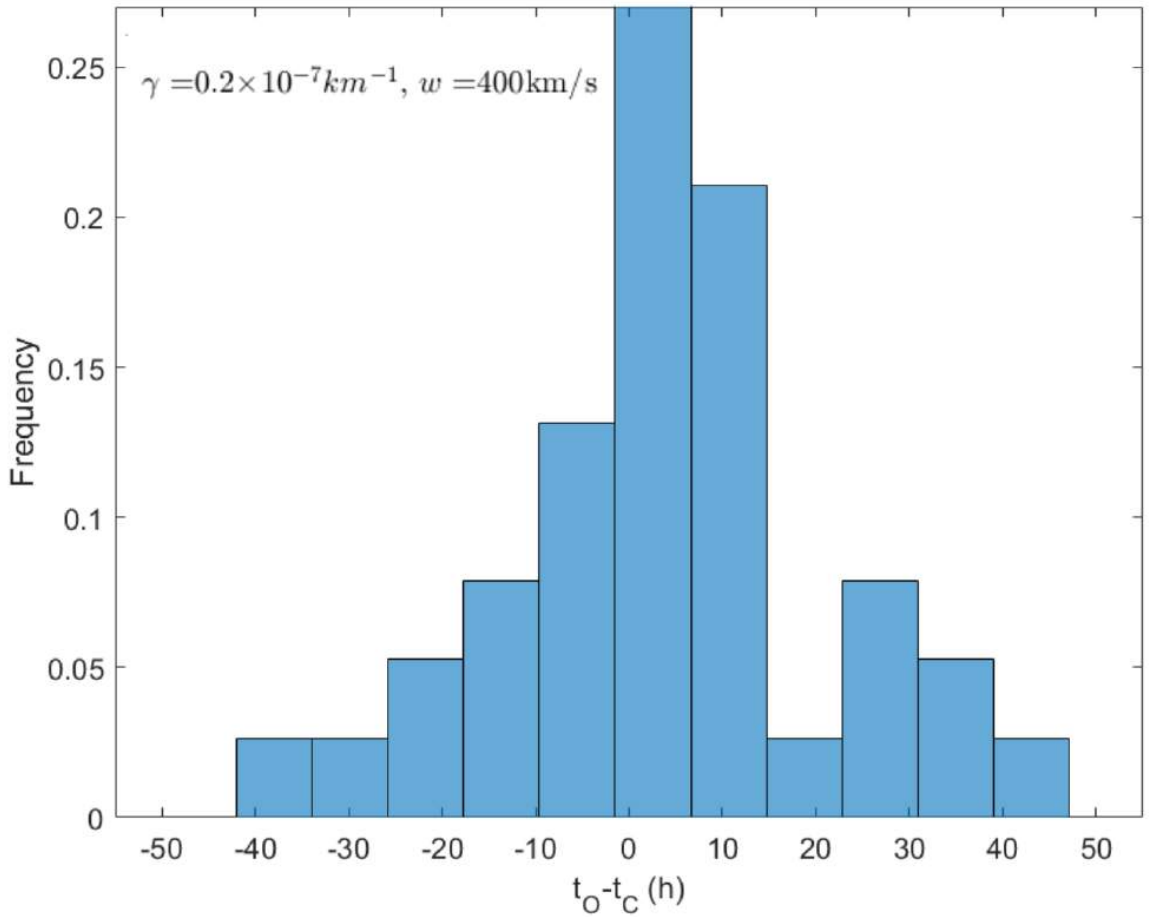

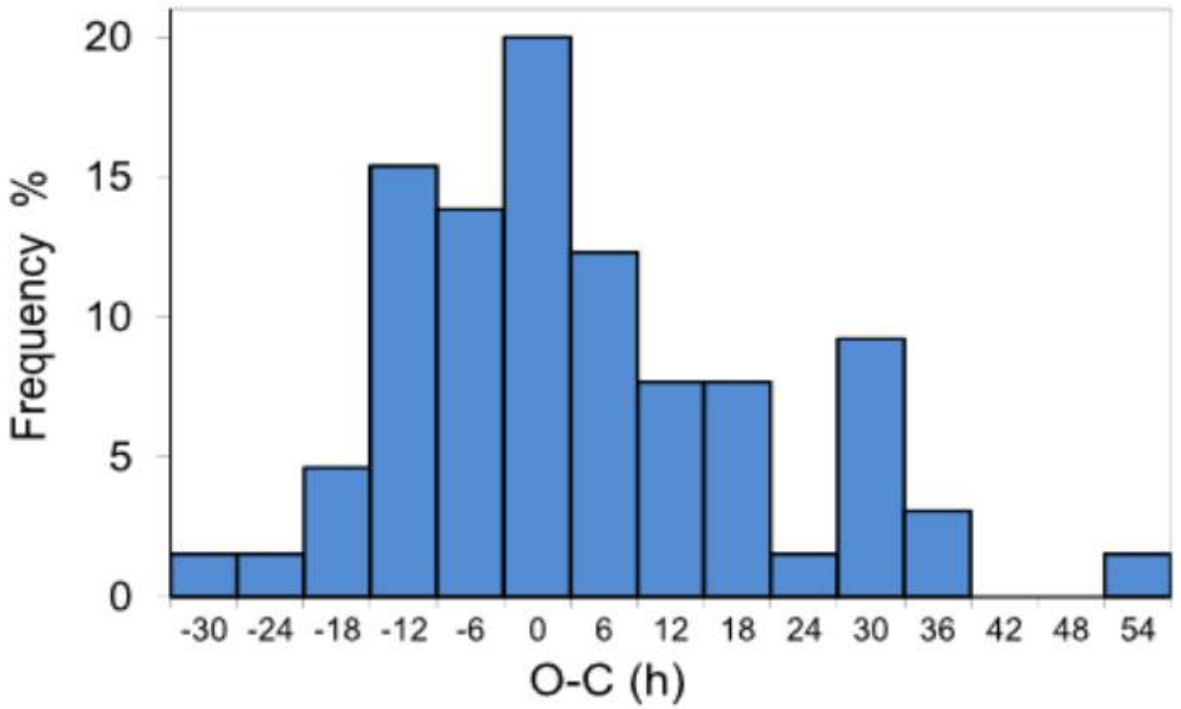

(**Vrsnak et al. 2012**)

Istogrammi stessa range

Extra Slides

Correlation between solar wind and drag parameter

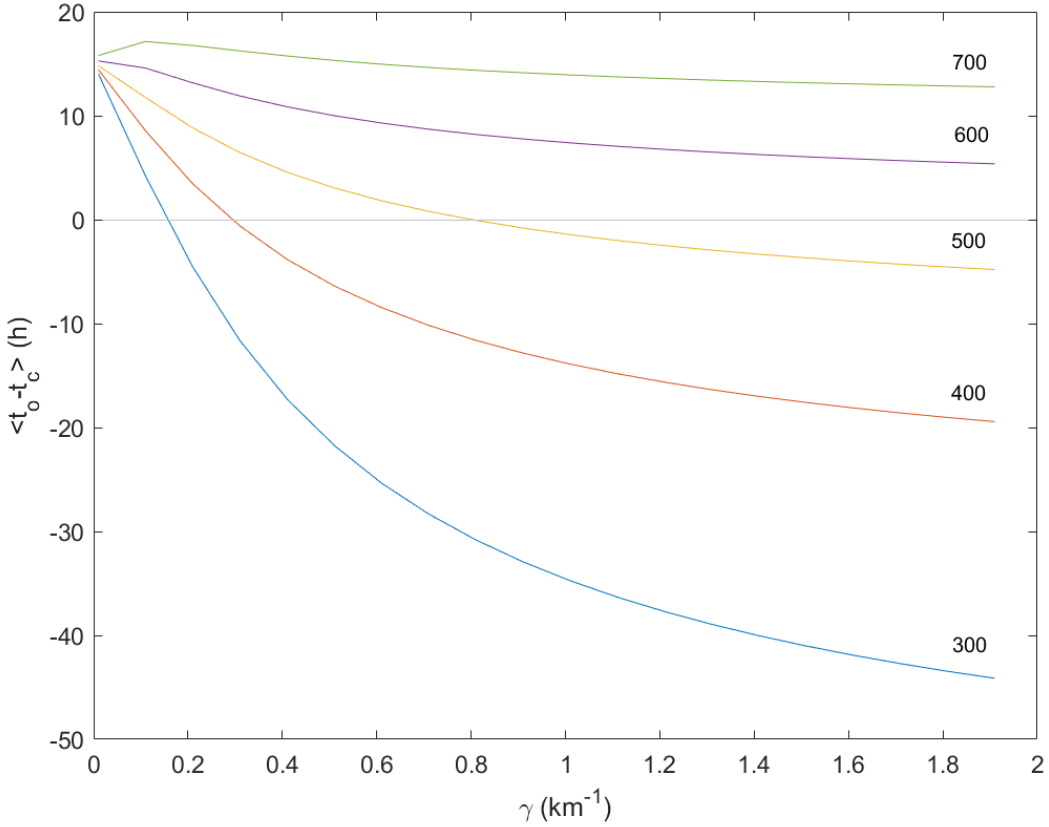

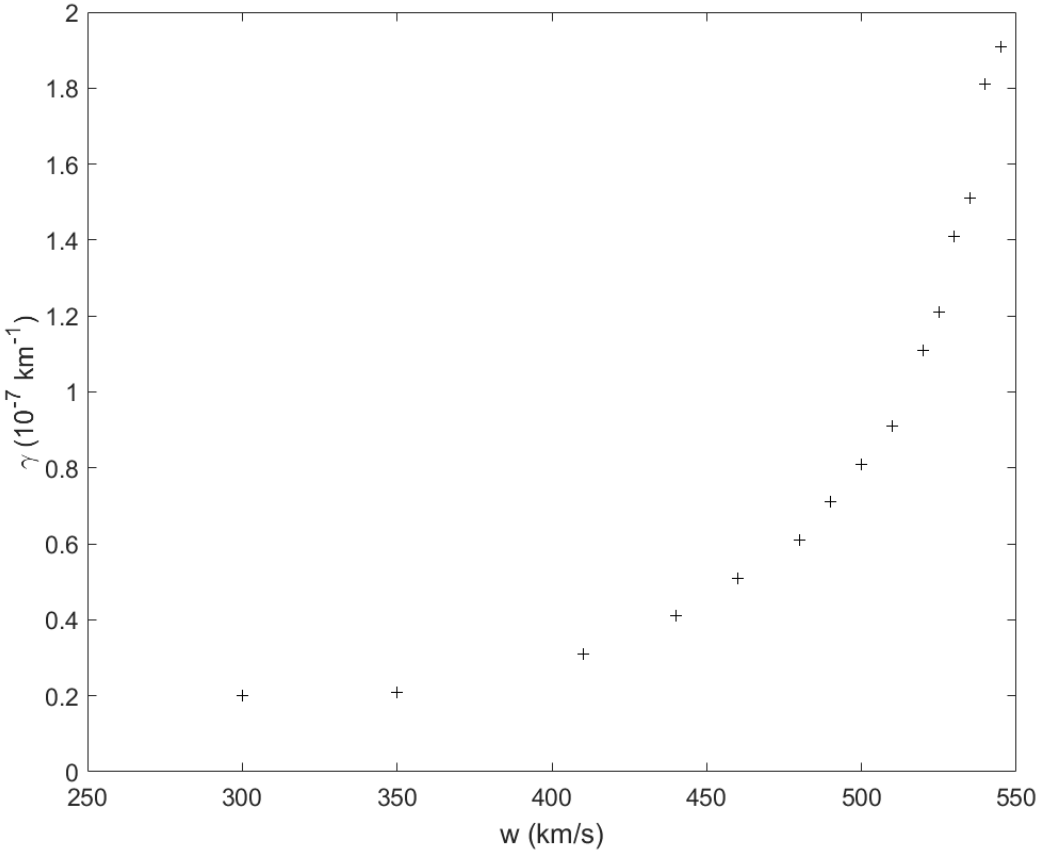

Extra Slides

Mean value and standard deviation of time difference distribution

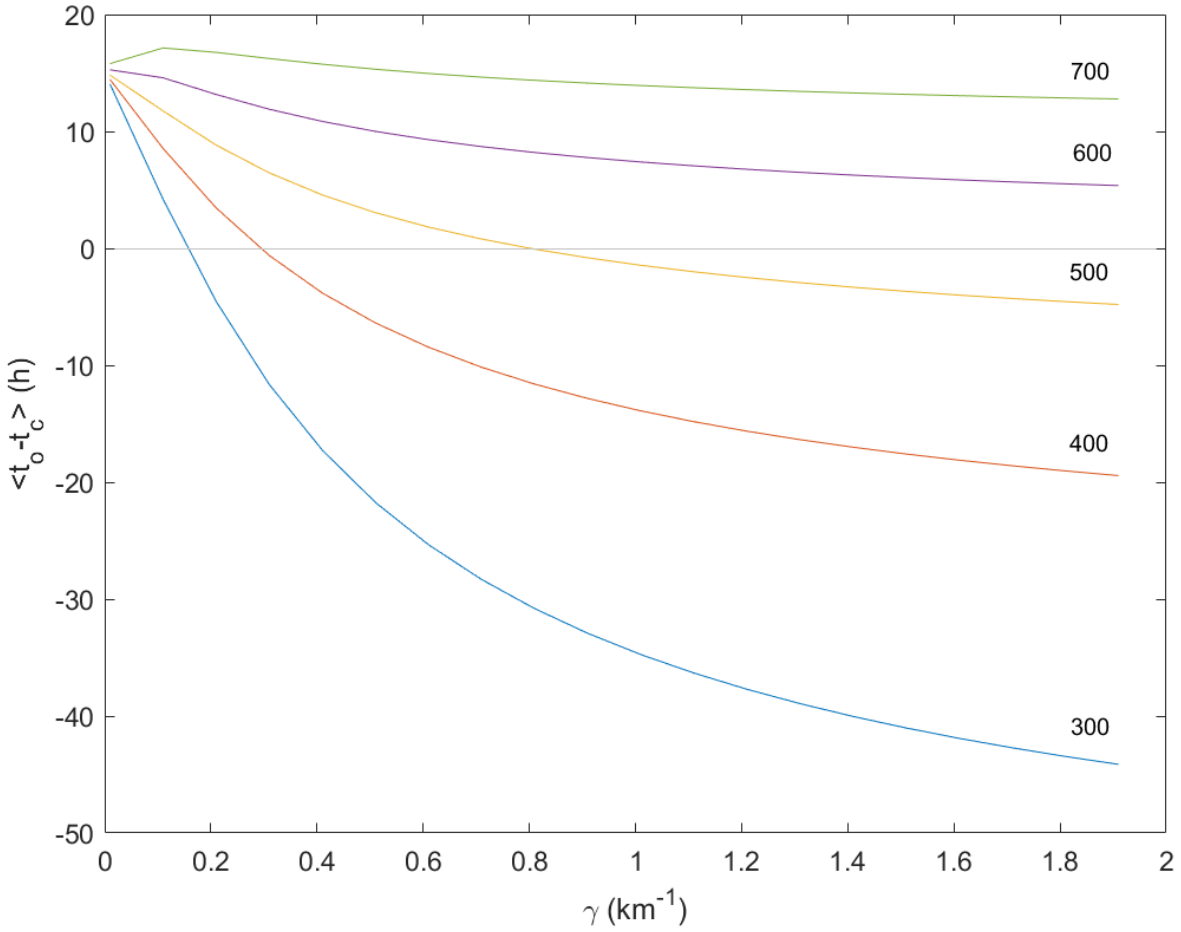

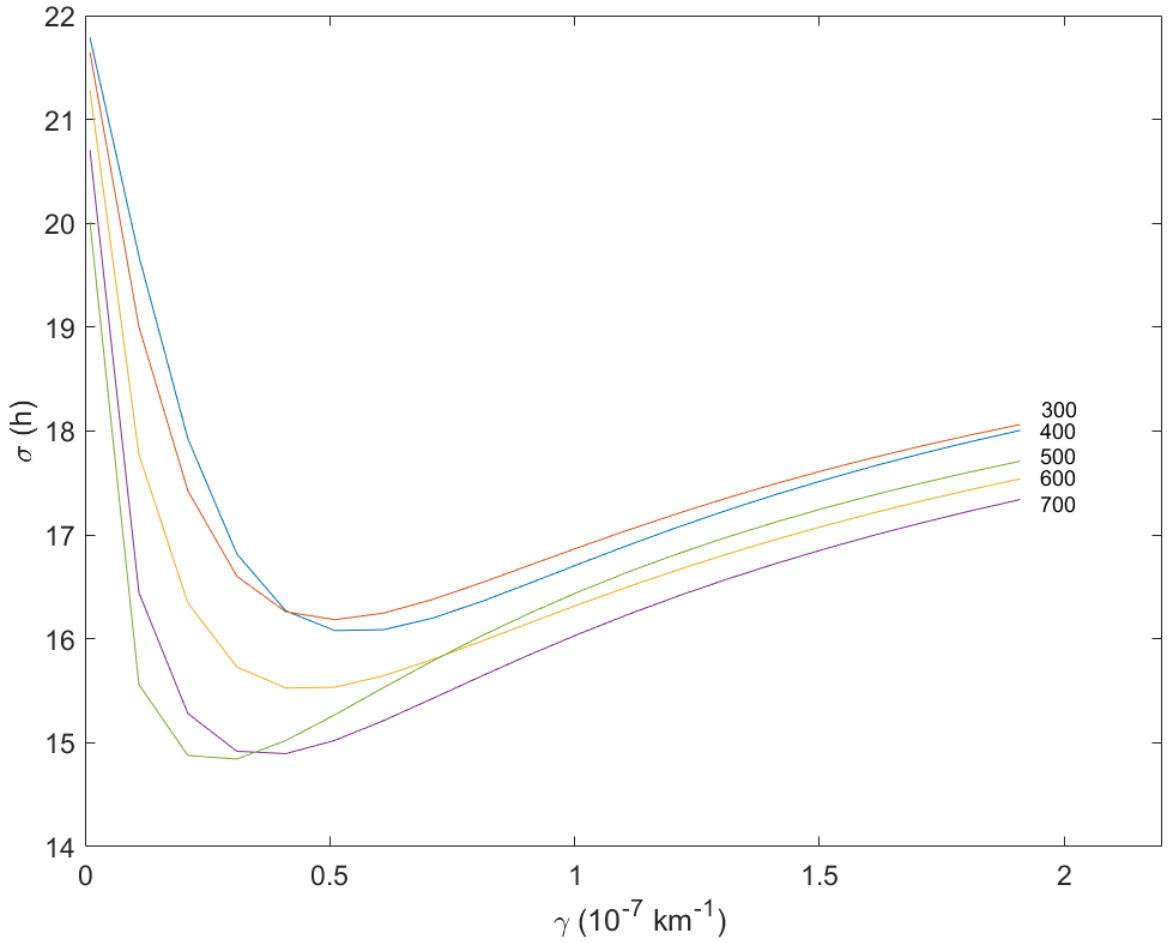

Advanced Drag-Based Model

Cone model (**Fisher & Munro 1984, Vrsnak & Zic 2005**)

a.

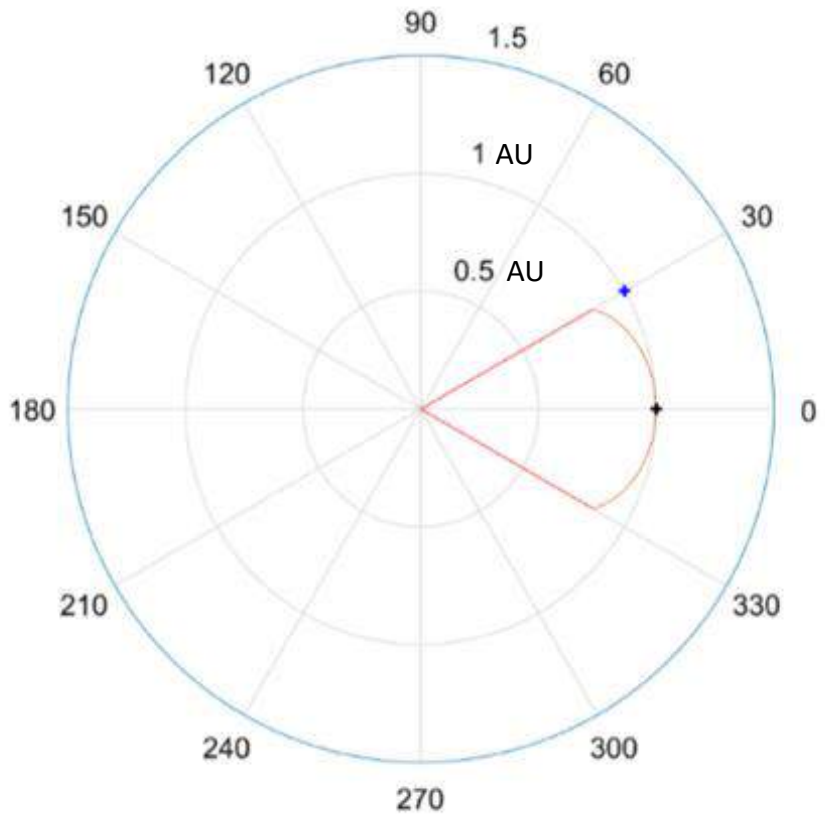

b.

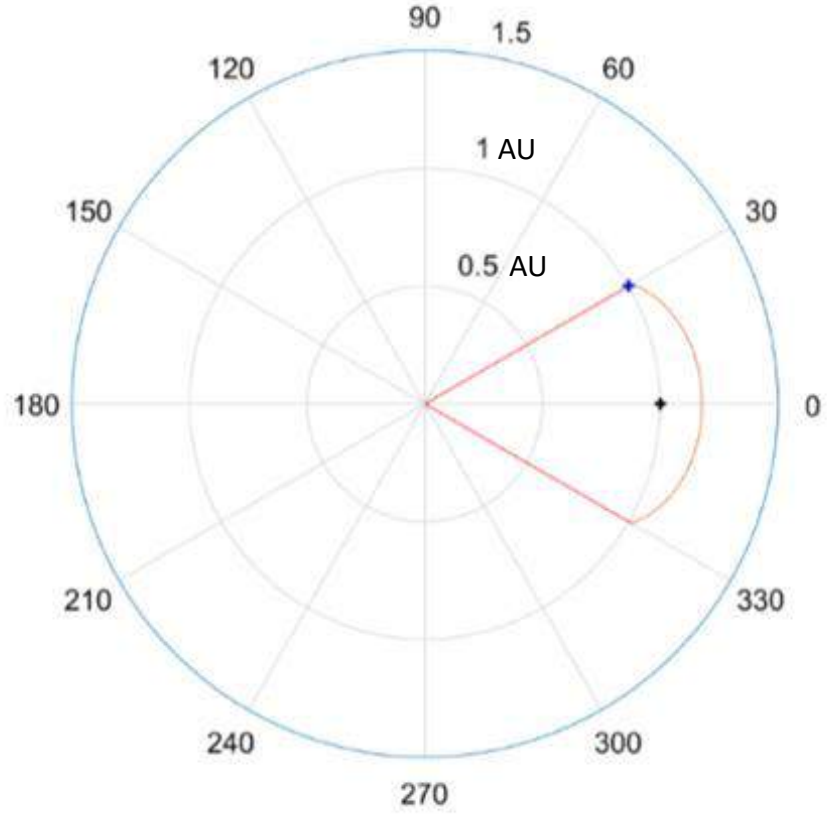

$\omega = 30°$

$v_0 = 1000 km/s$

$w = 400 km/s$

$\gamma = 0.2 \times 10^{-7} km^{-1}$

a. $\alpha = 0°$ $t_C = 53.0$h

b. $\alpha = 30°$ $t_C = 63.3$h

Test of the Drag-Based Model

Reconstruction of CME geometry through multiple point of view observations: the STEREO mission (**Kaiser et al. 2008**)

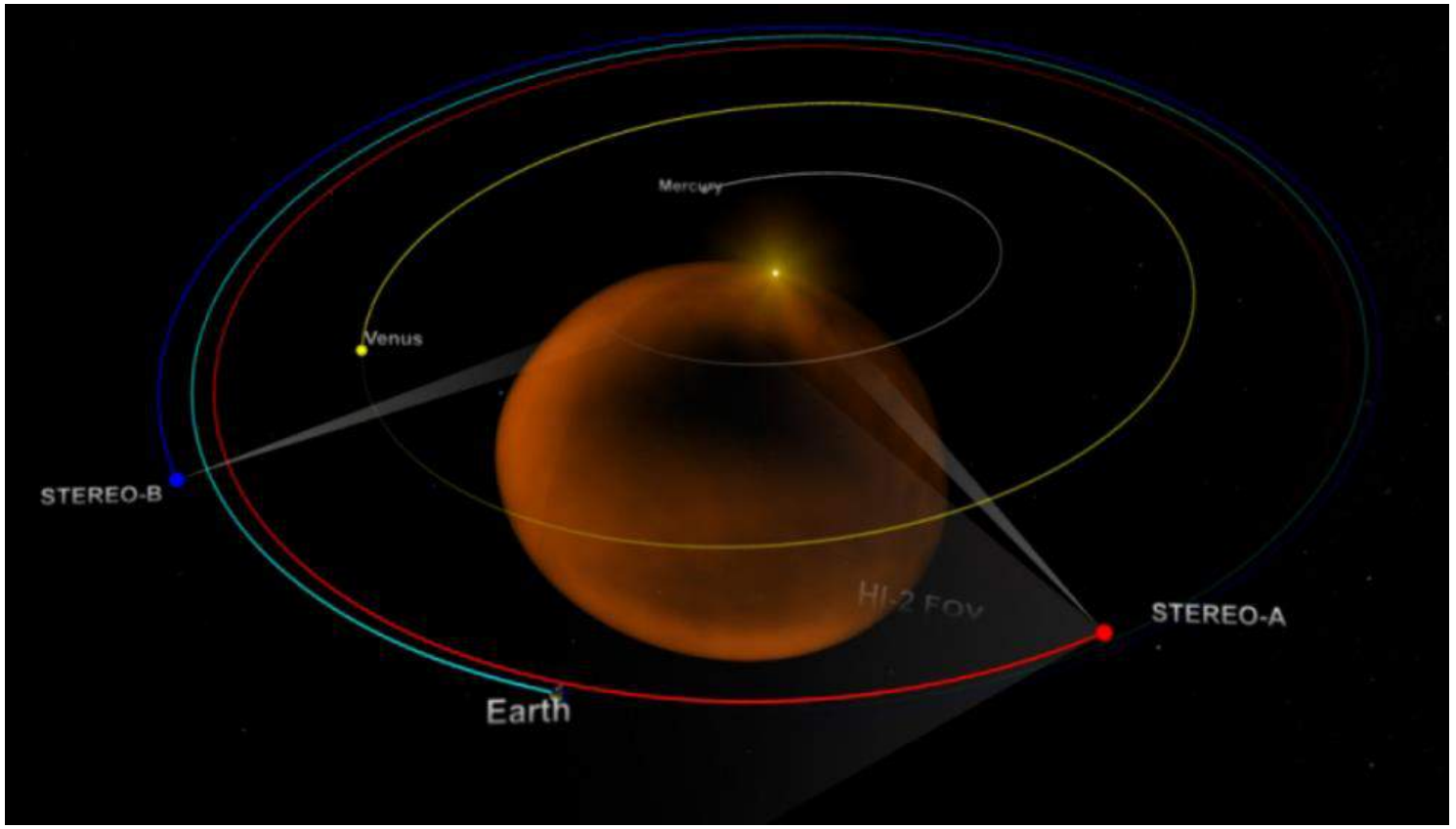

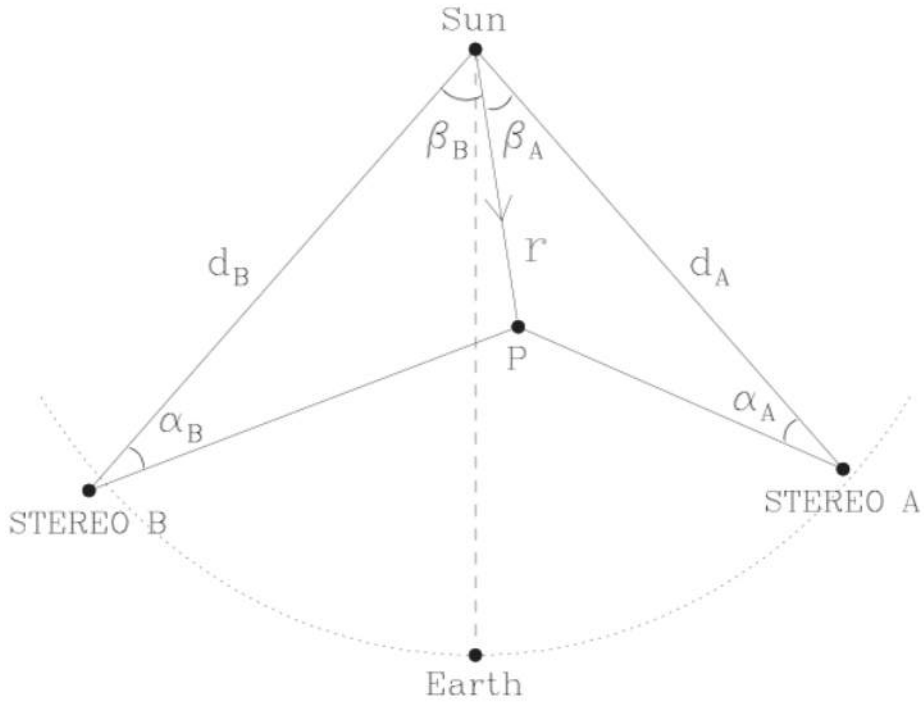

Probabilistic Advanced Drag-Based Model

Distribution of initial conditions and parameters

drag parameter distribution obtained by inversion of DBM equations by employing a sample of 91 CME events. (**Vrsnak et al. 2012**)

distribution.

Interestingly, no correlation is found between γ and w. This might be a somewhat surprising result since the solar-wind speed and density are anticorrelated, so one would expect also that w and $\gamma \propto \rho_w$ (see Equation (2)) are anticorrelated. Most likely, the $\rho_w(w)$ anticorrelation is masked by a large range of CME masses involved in the sample as well as

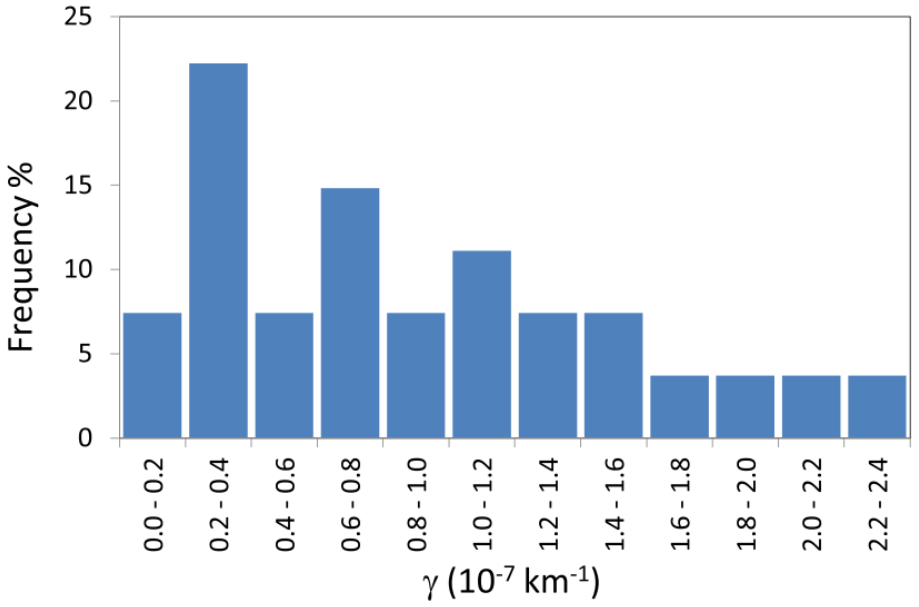

Probabilistic Advanced Drag-Based Model

Distribution of initial conditions and parameters

Lognormal distribution of CME speeds (**Yurchyshyn et al. 2005**)

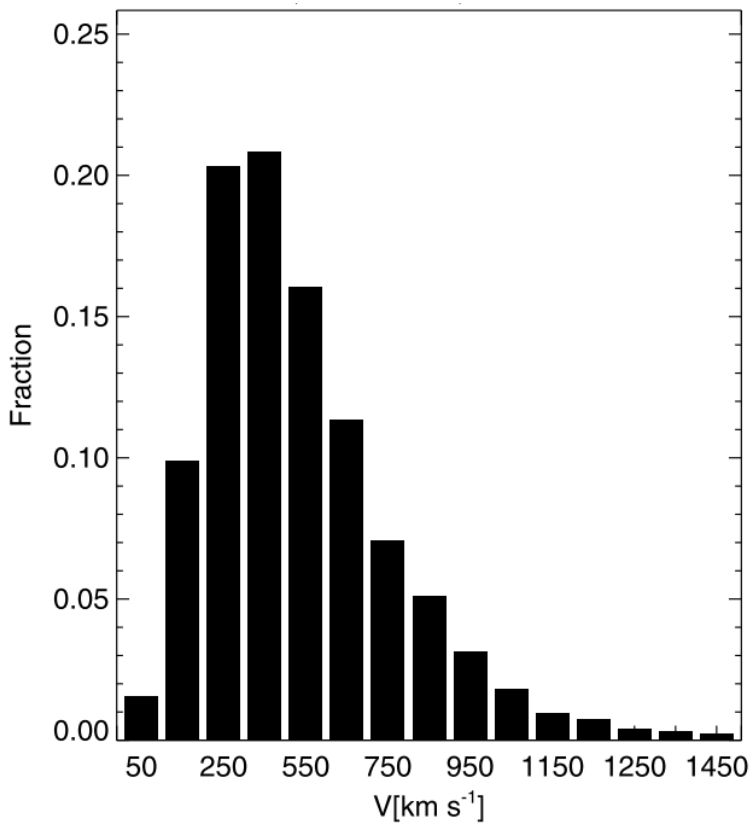

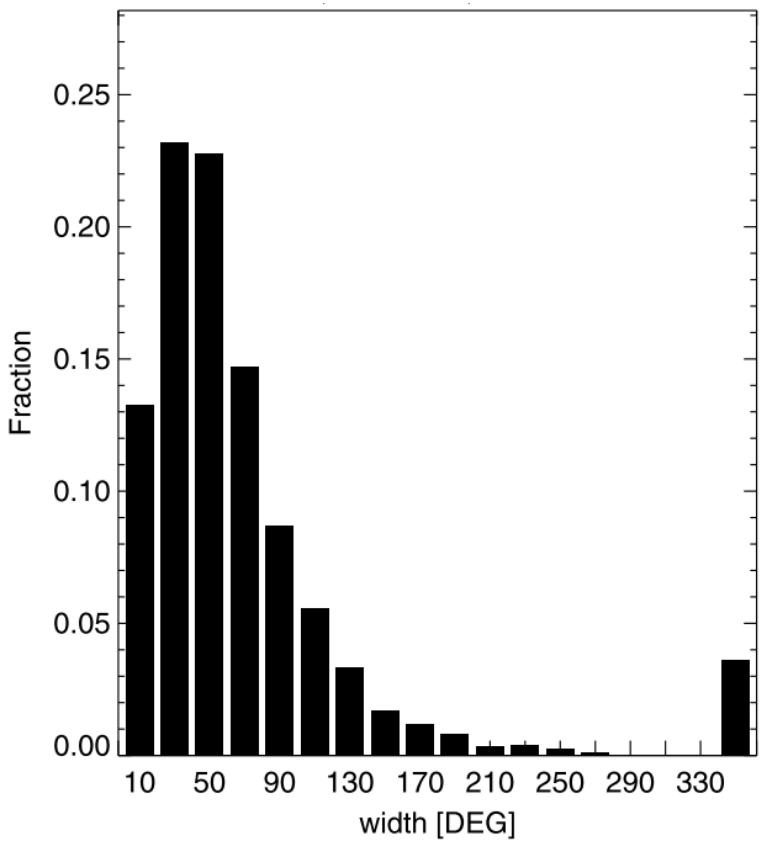

Probabilistic Advanced Drag-Based Model

Distribution of initial conditions and parameters

Lognormal distribution of CME speeds (**Yurchyshyn et al. 2005**)

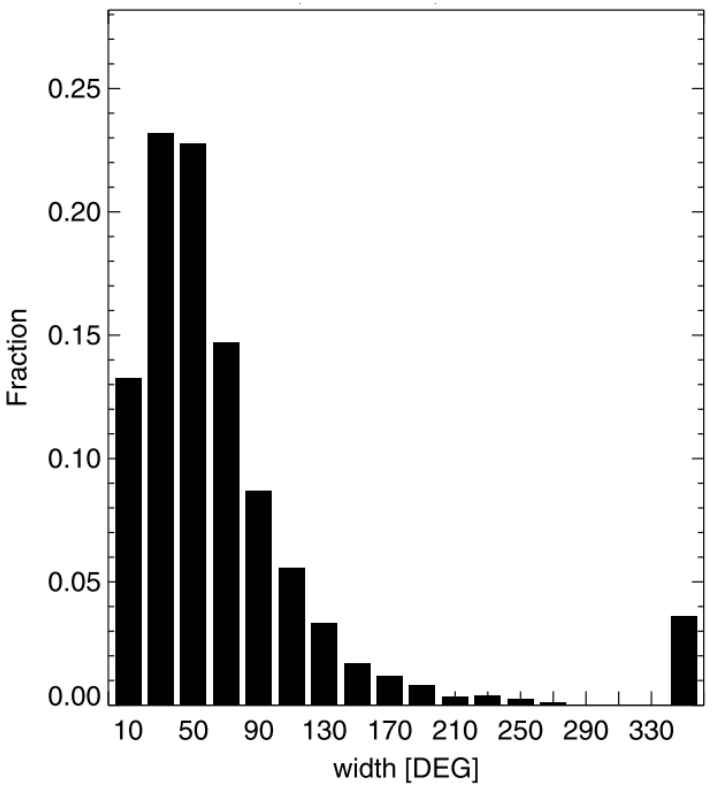

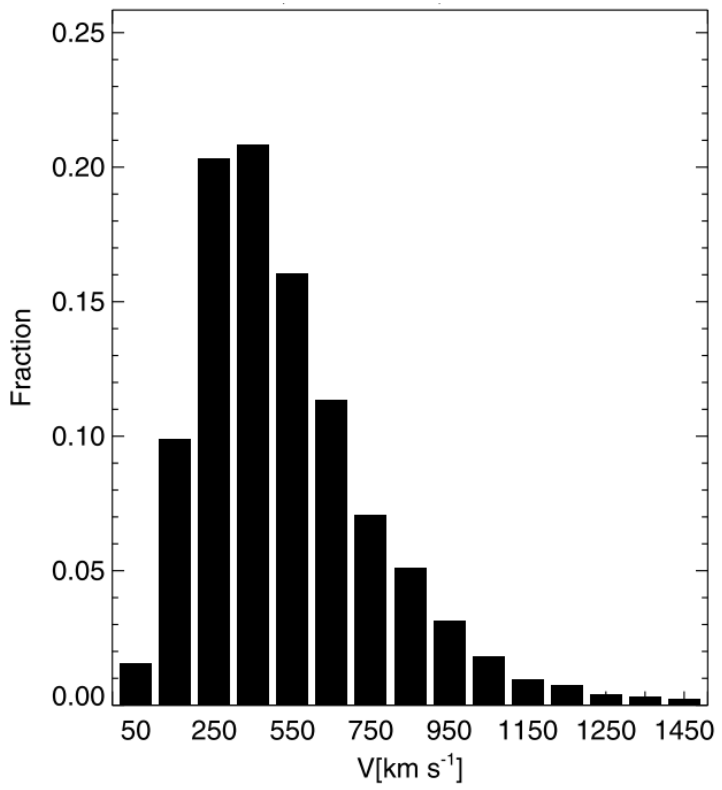

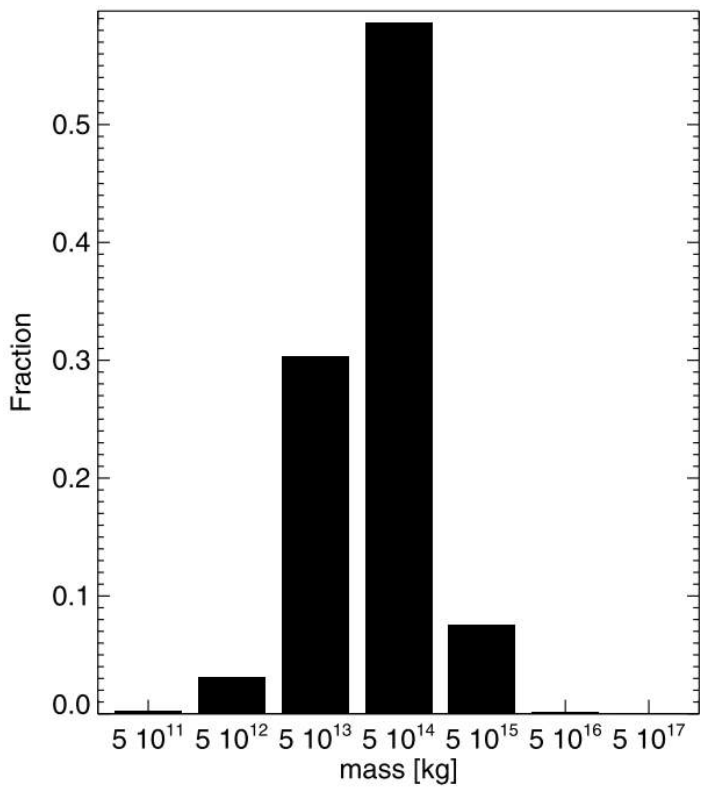

Test of the Drag-Based Model

Reconstruction of CME geometry through multiple point of view observations: the STEREO mission (**Kaiser et al. 2008**)

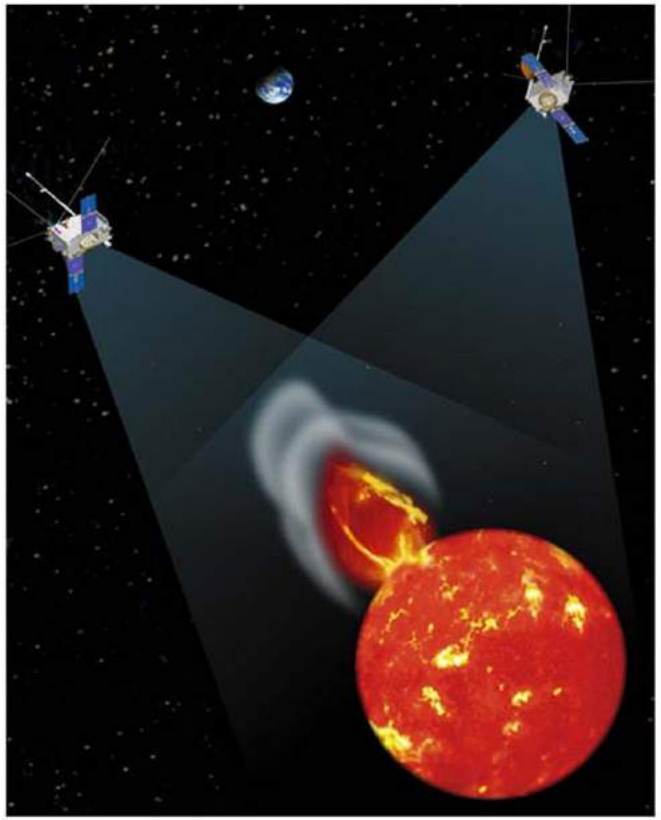

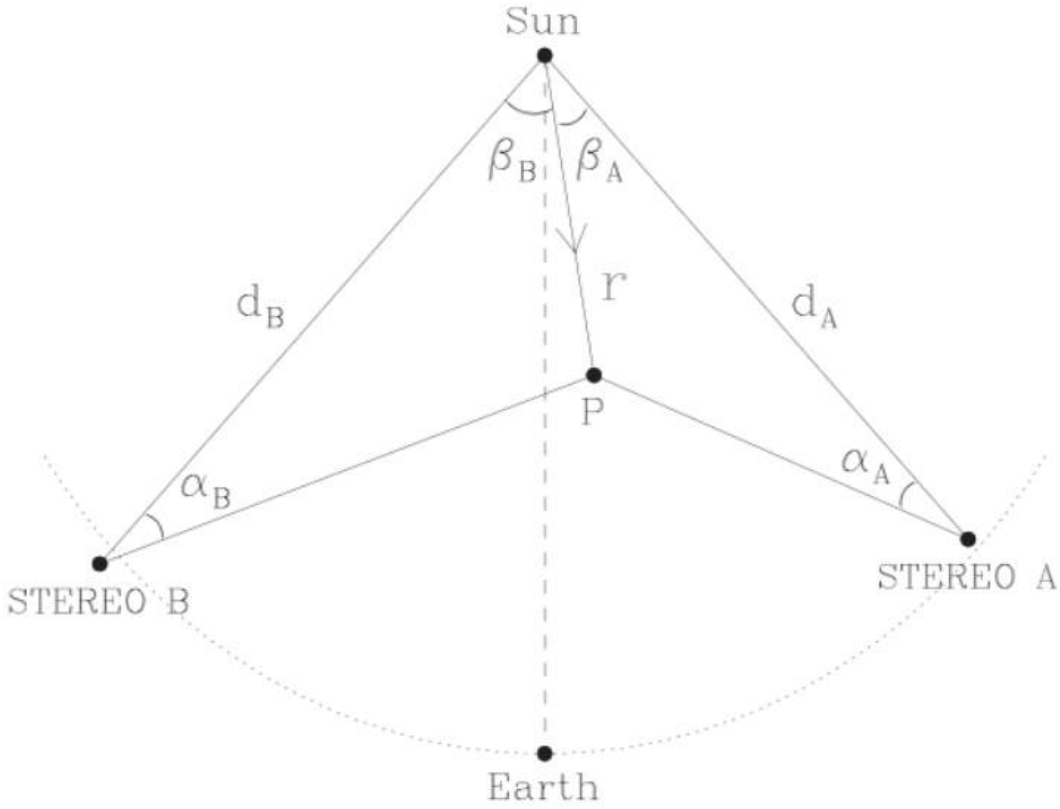

Advanced Drag-Based Model

Data sample

Tong Shi et al. 2015

- (shock or magnetic effect in WIND data) for 14 events;

- known CME morphology (Cone Model) thanks to reconstruction of ICME shape obtained by means of multiple point of view observations (STEREO);

- known errors on determination of leading edge position and speed from coronagraphic images

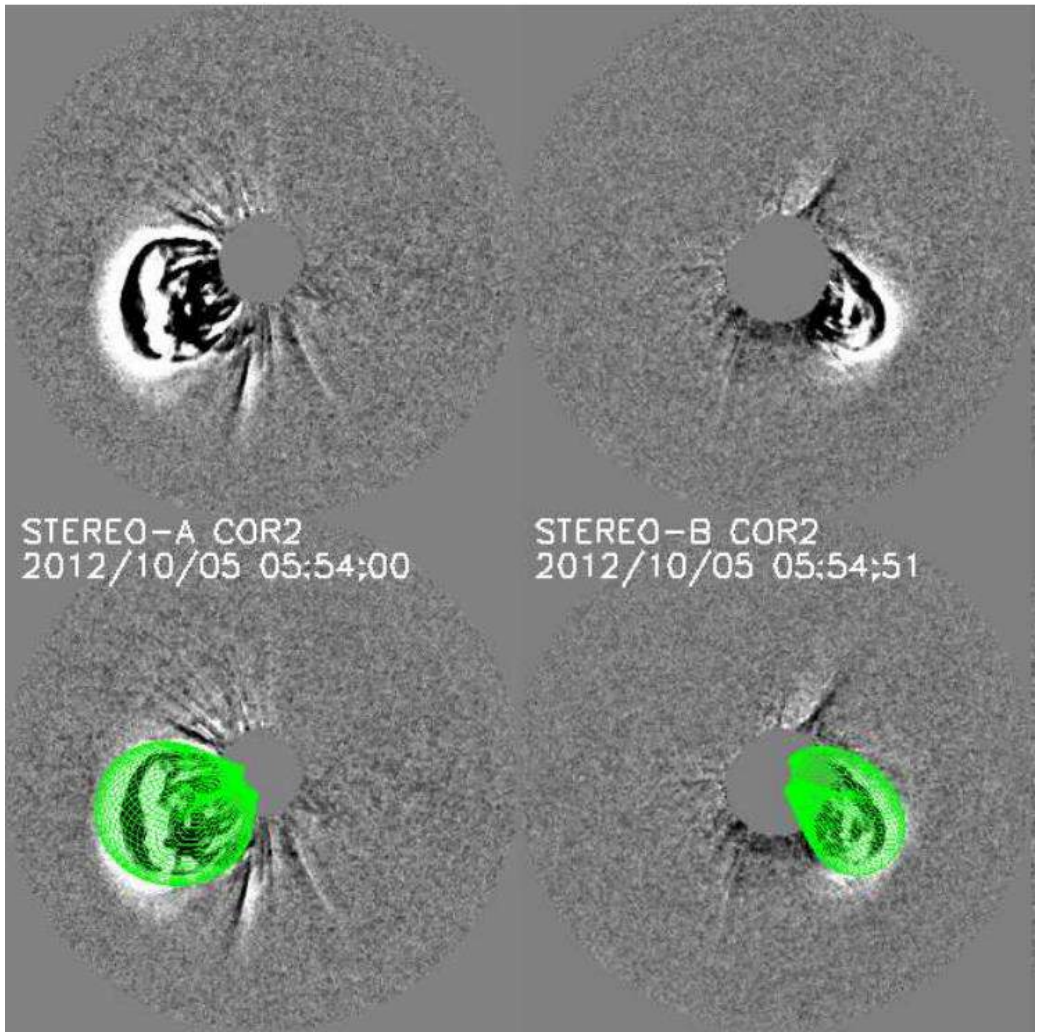

Probabilistic Advanced Drag-Based Model

Time distribution

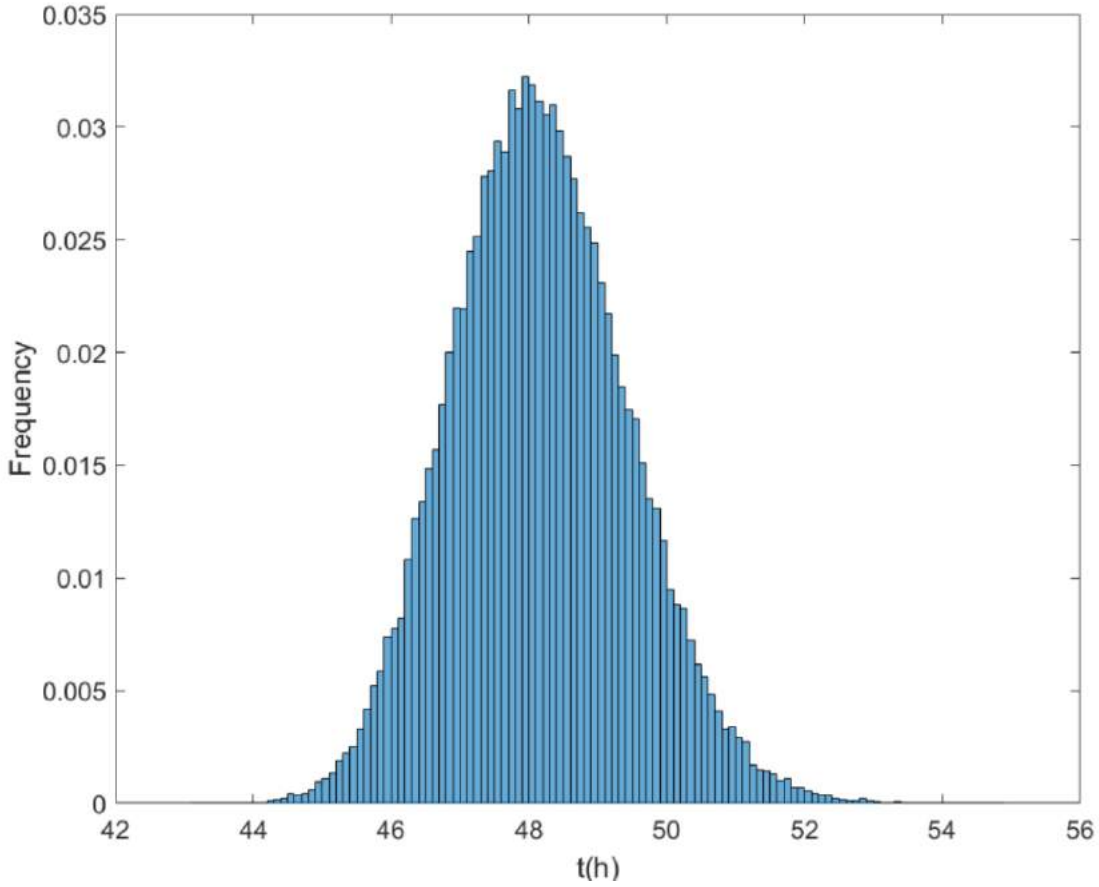

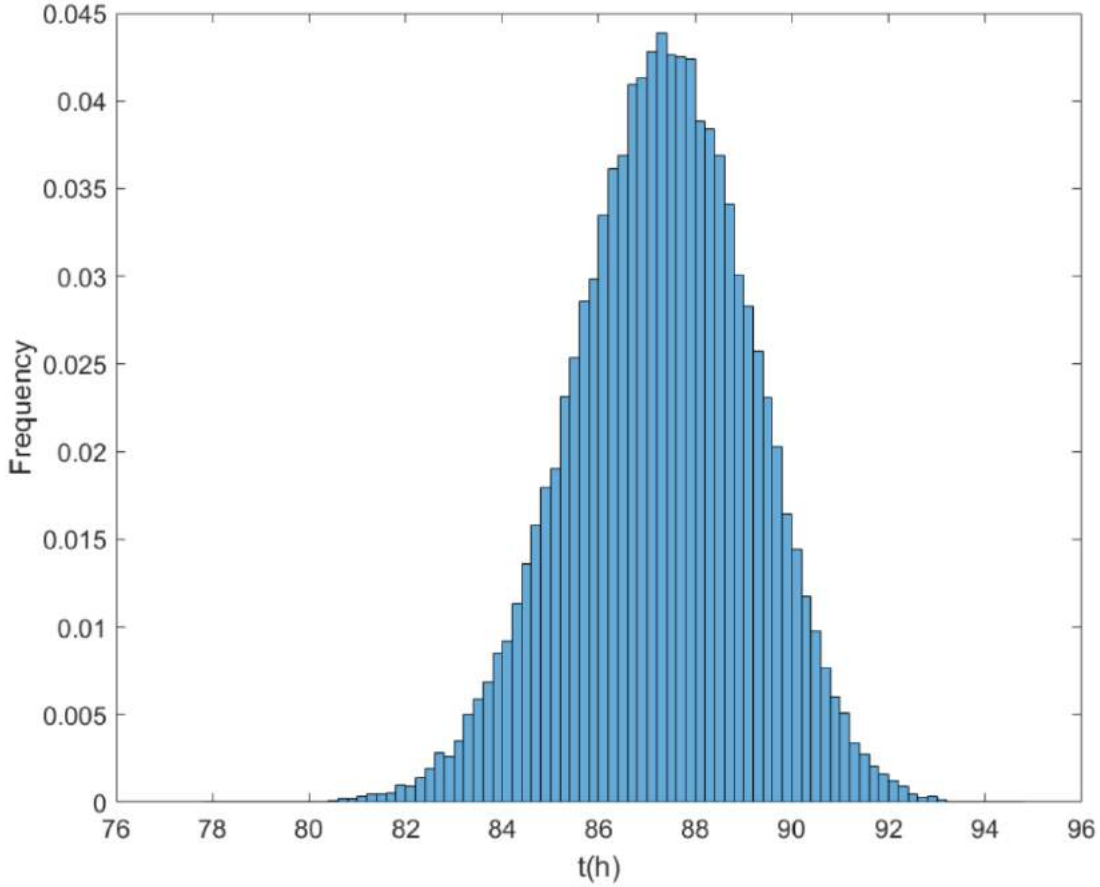

2.3. *Transit Time*

The CME transit time is the time elapsed from the occurrence of the CME to its arrival at 1AU. This parameter can be directly obtained from the in situ data by WIND (see Figure 3). In the 2012 October 5 event, a clear shock is seen at 05:00 UT on October 8 as indicated by the sudden jumps in the proton density, speed, and temperature (as denoted by the vertical dashed line in the figure). Behind the shock is a sheath region with enhanced proton density and temperature and variable magnetic field. A Magnetic Cloud (MC; Burlaga et al. 1981) is then identified by a strong magnetic field, a smooth rotation of the field, and a depressed proton temperature (marked by the shaded region). The MC ends at

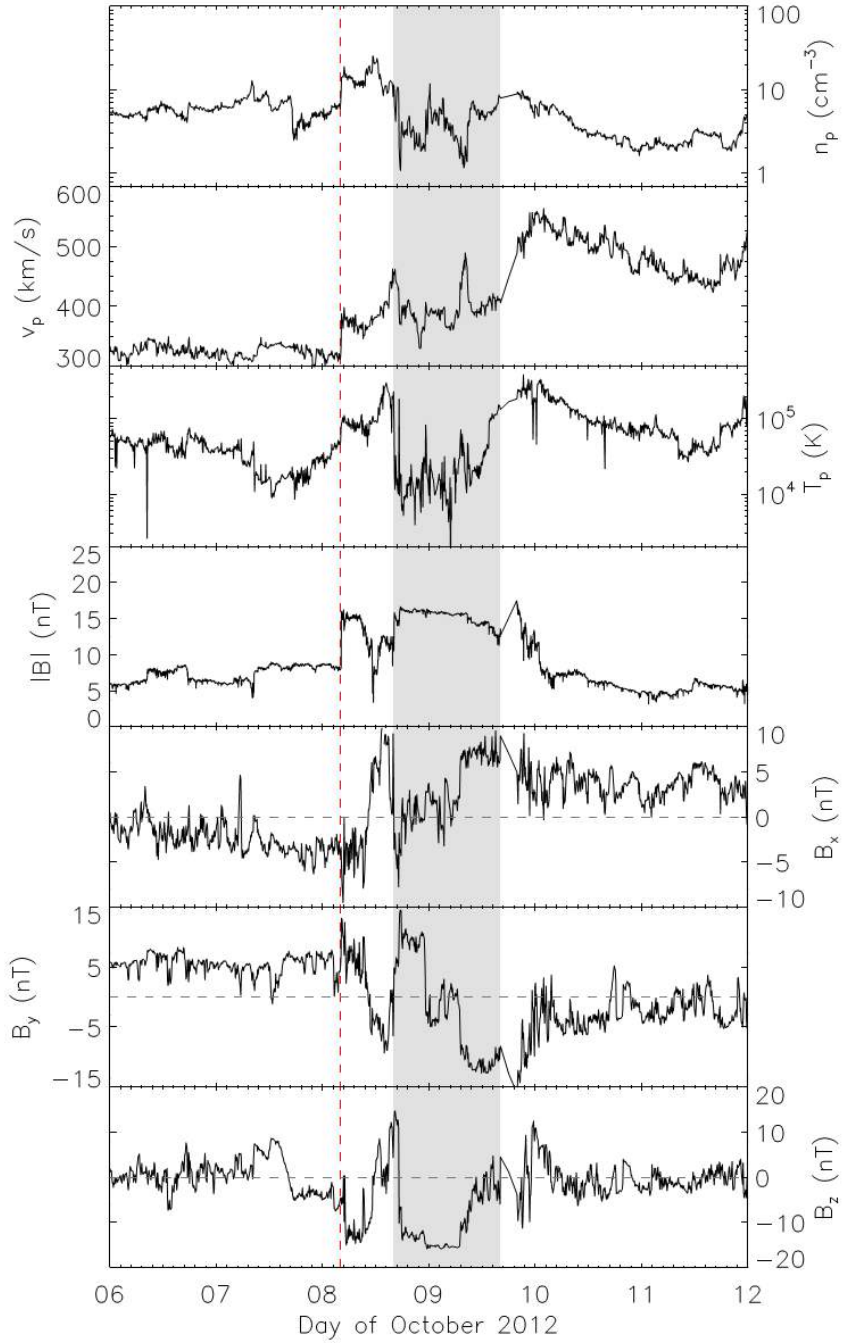

Probabilistic Advanced Drag-Based Model

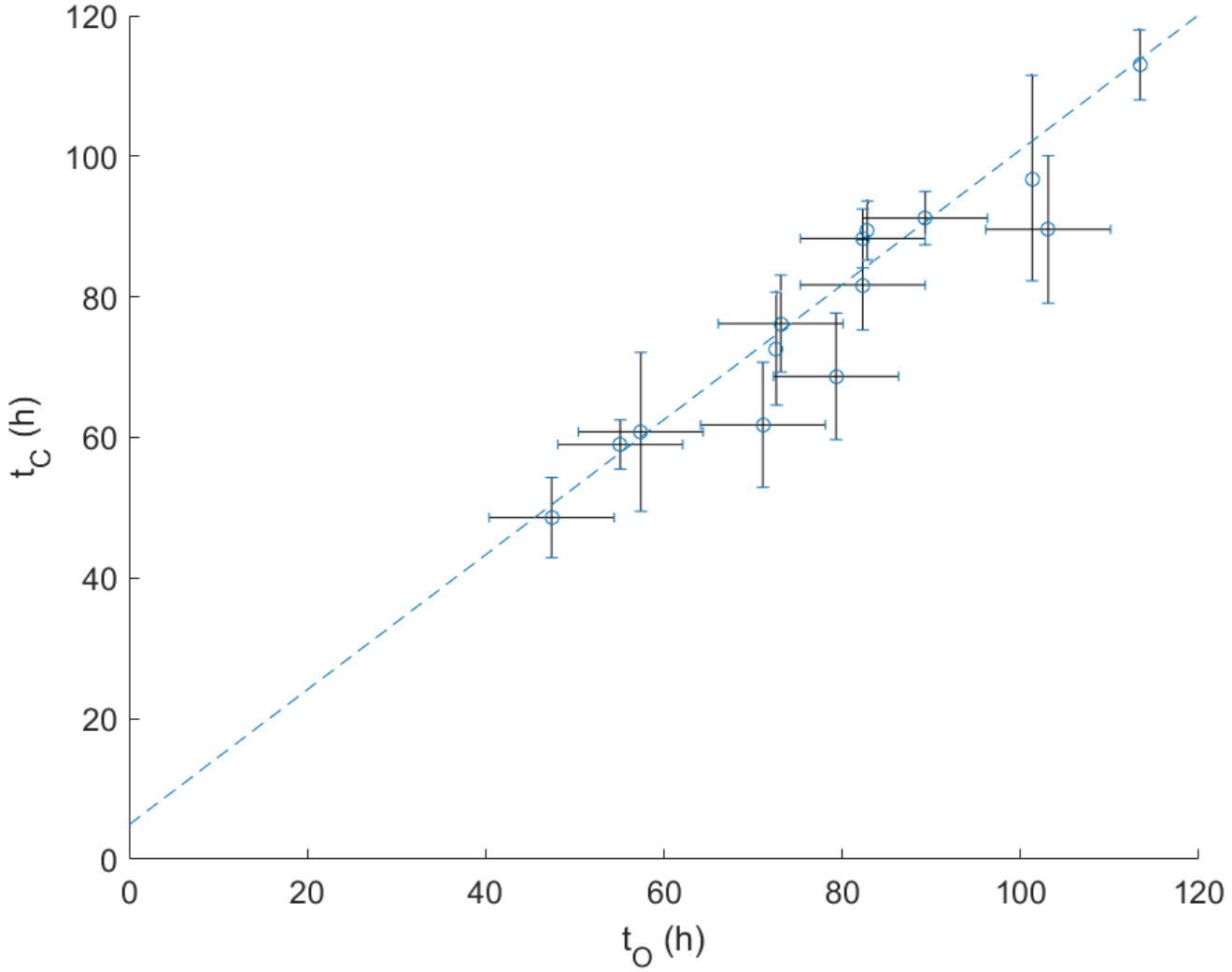

$$t_C = 4.9 \text{ h} + 0.96 \times t_O$$
$$\sigma_a = 9.3 \text{ h}$$
$$\sigma_b = 0.11$$
$$\rho_{ab} = -0.97$$

Probabilistic Advanced Drag-Based Model